Developing Procedures for Screening High Emitting Vehicles and Quantifying the Environmental Impacts of Grades

by

Sangjun Park

Thesis submitted to the Faculty of the
Virginia Polytechnic Institute and State University
in partial fulfillment of the requirements for the degree of

Master of Science
in
Civil and Environmental Engineering

Hesham Rakha, Chair

Kyoungho Ahn, Member

Antonio Trani, Member

November, 2005

Blacksburg, Virginia

Keywords: Mobile Source Emission Models, Fuel Consumption Models, High Emitting Vehicles, and Roadway Grades

Developing Procedures for Screening High Emitting Vehicles and Quantifying the Environmental Impacts of Grades

Sangjun Park

Abstract

Since the transportation sector is highly responsible for U.S. fuel consumption and emissions, assessing the environmental impacts of transportation activities is essential for air-quality improvement programs. Also, high emitting vehicles need to be considered in the modeling of mobile-source emissions, because they contribute to a large portion of the total emissions, although they comprise a small portion of the vehicle fleet. In the context of this research, the thesis quantifies the environmental impacts of roadway grades and proposes a procedure that can enhance the screening of high emitting vehicles.

First, the study quantifies the environmental impacts of roadway grades. Although roadway grades are known to affect vehicle fuel consumption and emission rates, there do not appear to be any systematic evaluations of these impacts in the literature. Consequently, this study addresses this void by offering a systematic analysis of the impact of roadway grades on vehicle fuel consumption and emission rates using the INTEGRATION microscopic traffic simulation software. The energy and emission impacts are quantified for various cruising speeds, under stop and go conditions, and for various traffic signal control scenarios. The study demonstrates that the impact of roadway grade is significant with increases in fuel consumption and emission rates in excess of 9% for a 1% increase in roadway grade. Consequently, a reduction in roadway grades in the range of 1% can offer savings that are equivalent to various forms of advanced traffic management systems.

Second, the study proposes a new procedure for estimating vehicle mass emissions from remote sensing device measurements that can be used to enhance HEV screening procedures. Remote Sensing Devices (RSDs) are used as supplementary tools for screening high emitting vehicles (HEVs) in the U.S. in order to achieve the National Ambient Air Quality Standards (NAAQS). However, tailpipe emissions in grams cannot be directly measured using RSDs because they use a concentration-based technique. Therefore, converting a concentration measurement to mass emissions is needed. The research combines the carbon balance equation with fuel consumption estimates to make the conversion. In estimating vehicle fuel consumption rates, the VT-Micro model and a Vehicle Specific Power (VSP)-based model (the PERE model) are considered and compared. The results of the comparison demonstrate that the VSP-based model under-estimates fuel consumption at 79% and produces significant errors (R^2 = 45%), while the VT-Micro model produces a minimum systematic error of 1% and a high degree of correlation (R^2 = 87%) in estimating a sample vehicle's (1993 Honda Accord with a 2.4L engine) fuel consumption. The sample vehicle was correctly identified 100%, 97%, and 89% as a normal vehicle in terms of HC, CO, NO_X emissions, respectively, using its in-laboratory measured emissions. Its estimated emissions yielded 100%, 97%, and 88% of correct detection rates in terms of HC, CO, NO_X emissions, respectively. The study clearly demonstrates that the proposed procedure works well in converting concentration measurements to mass emissions and can be applicable in the screening of HEVs and normal emitting vehicles for several vehicle types such as sedans, station wagons, full-size vans, mini vans, pickup trucks, and SUVs.

Acknowledgements

I do not think it is possible to express in one word all of my gratitude to the people who helped me both directly and indirectly to complete this thesis in a word. But I would like to express my thanks to them.

First of all, my heartful appreciation goes to my adviser, Dr. Hesham A. Rakha who generously gave me a lot of inspiration and financial support and continuously encouraged me. As he is a distinguished professor and adviser, I really respect him and confirm that I will follow the lessons learned from him. I do not in my mind know how to express my thanks to him, since I owe so many things to him. Also, I deeply thank Dr. Kyoungho Ahn who introduced me to environmental problems in the transportation field. He has given a lot of ideas to me so that I may complete my thesis. I would say that I could not complete my thesis without his help. I really appreciate his continuous support and friendship. I think there is no way to pay my debts. In addition to Dr. Rakha and Dr. Ahn, I want to give my thanks to my committee member, Dr. Antonio A. Trani, for his invaluable advice and recommendations.

I am also thankful to Dr. Linsey C. Marr who is an Assistant Professor in the environmental and water resources engineering program area of the Civil and Environmental Engineering department at Virginia Tech. She especially contributed to the study of screening high emitting vehicles.

I also would like to express my thanks to Dr. Antoine G. Hobeika, Dr. Hojong Baik and my seniors, juniors, friends, and colleagues in Virginia Tech. They always gave me invaluable help, generosity, and friendship.

Finally, I dedicate this thesis to my lovely wife, Bosle Shin, who always understands, believes, and supports me.

Table of Contents

List of Tables

List of Figures

Chapter 1: Introduction

The transportation sector is one of the dominant sources of US fuel consumption and emissions. Specifically, highway travel accounts for approximately 75 percent of the total transportation energy use and slightly more than 33 percent of the national emissions of the Environmental Protection Agency's (EPA) six criteria pollutants (carbon monoxide, carbon dioxide, oxides of nitrogen, hydrocarbons, sulfur dioxide, and particulate matter). Consequently, an accurate assessment of motor-vehicle emissions is essential for an effective air-quality improvement program.

In an attempt to reduce transportation-related emissions, the National Ambient Air Quality Standard (NAAQS) was instated. The NAAQS regulates the amount of primary pollutants (those directly emitted to the atmosphere by vehicles) and secondary pollutants (those formed through chemical reactions of primary emissions). For example, ozone, which is a secondary pollutant, is formed by chemical reactions involving volatile organic compounds (VOCs) and nitrogen oxides (NO_x) in the presence of sunlight. It is known that ozone concentrations can damage crops and other vegetation, acid can damage human artifacts, and particulates contribute to haze and poor visibility. Mobile emissions also contribute to greenhouse gas emissions of CO_2. While the adverse effect of CO and ozone are generally well known, the effects of PM and most toxics are still not well understood. Consequently, there is an urgent need to ensure that transportation projects pose minimal environmental hazards by developing tools that can assess and compare the environmental impacts of these projects prior to their implementation in the field.

1.1 Problem Definition

Estimating the effects of traffic-flow improvement projects in metropolitan areas on air quality and energy involves a lengthy chain of factors. These factors were described in detail in a report written by numerous experts in the field of transportation-related environmental modeling (NRC, 1995). The report describes how increases in the highway supply can cause changes in traffic flows on the affected roadways (e.g., changes in speed distribution and variation, and/or shifts in traffic volumes) that might result in changes in the energy consumption and emissions of vehicles traveling on those roadways. These changes can evolve over time in response to changes in the amount of travel or in-land use patterns, with corresponding effects on emissions and energy use. The study concludes that the incremental effects of all these changes on air quality and energy use must be estimated to determine the full effects of capacity changes.

The NRC report also discusses the spatial and temporal impacts of traffic-flow improvement projects by indicating, "*There is both a spatial and a temporal dimension to these analyses. A change in supply may involve adding capacity and improving traffic flow at only one location on the highway system. However, the network character of the system is likely to affect travel patterns at other locations. Traffic may be diverted from alternative routes, or travelers may shift their time of travel to preferred travel times to take advantage of the new capacity or change their mode of travel if they are encouraged to reduce auto trips by using transit or bicycle or by walking. If the addition of the new capacity is sufficiently large, it can induce new or longer trips, influence auto purchasing decisions, and cause residents or businesses to change their location to take advantage of the improved access. Similarly, emissions from these changes are not confined to the location of the project, but depending on local atmospheric conditions (e.g. heat and wind patterns), may have broader effects on the air quality of the region and beyond. Individual highway projects may not have measurable effects on regional air quality, but the cumulative impacts of many projects could. Thus, whereas a highway capacity enhancement project may be localized, its effects are unlikely to be*."

The factors that impact vehicle emissions can be broadly classified as environmental, vehicle, roadway, and traffic related factors. Environmental factors include the ambient temperature, relative humidity, wind speed, etc., while the vehicle factors include the fuel system, fuel type, engine efficiency, availability of a catalytic converter, etc. Roadway conditions include the roadway grade, while traffic conditions include the level of congestion on a roadway. A critical factor in modeling the environmental impacts of transportation systems is the issue of high-emitter or high-emitting vehicles (HEVs). HEVs are motor vehicles that produce higher emissions than the average-emitting vehicles under normal driving conditions. Studies have shown that a small fraction of HEVs contribute significantly to the total mobile source emissions (Wenzel et al., 1998; Wolf et al., 1998). For example, one study found that 7.8 percent of the fleet is responsible for 50 percent of the total emissions (Lawson et al., 1990). Other studies indicate that 5 percent of the vehicles emit 80 percent of the emissions (Wolf et al., 1998). Consequently, Screening HEVs has been a key to control the total mobile source emissions.

The evaluation of the energy and environmental impacts associated with transportation improvement projects requires a comprehensive evaluation tool that is sensitive to vehicle dynamics.

1.2 Research Objectives and Contributions

The objectives of this research effort are two-fold: Quantify the impact of roadway grades on mobile source emissions and propose an enhanced procedure for screening high emitting vehicles. These two objectives result in two major contributions:

a. The study presents a systematic analysis of the energy and environmental impacts of roadway grades.

b. The study provides an improved procedure that utilizes remote sensing emission measurements for screening of high emitting vehicles.

1.3 Thesis Layout

This thesis is organized into five chapters. The second chapter provides a review of current state-of-the-art energy and emission models. The literature review discusses the contribution of motor vehicle transportation to air pollution and energy consumption, including those factors affecting fuel consumption and emissions. Furthermore, regulations such as the air quality standards, Clean Air Act Amendments, conformity analysis, and the air-quality related planning process are discussed. Various existing fuel consumption and emission models are also described. The third chapter presents a case study analysis of the impacts of roadway grades on vehicle fuel consumption and emission rates. This case study is conducted using the INTEGRATION microscopic traffic simulation and assignment software. The forth chapter presents a proposed procedure for screening high emitting vehicles that uses remote sensing emission measurements. Finally, the fifth chapter concludes with the conclusions of the study and recommendations for further research.

Chapter 2: Literature Review

In this chapter several subjects are reviewed to construct a background for my research. First, the legislative background for the energy consumption and emissions requirements of the transportation sector are presented. Second, the factors that affect the vehicle fuel consumption and mobile-source emissions are introduced because one of these factors is studied in detail in Chapter 3. Third, given that the study is conducted using the INTEGRATION software, the INTEGRATION framework for modeling vehicle emissions is discussed in detail. Finally, the issue of grade impacts on vehicle emissions and high emitting vehicles is discussed in order to identify the need for the proposed research effort.

2.1 Transportation and Energy Consumption

In 1975, Congress passed the Energy Policy and Conservation Act (EPCA) to improve the fuel economy by establishing Corporate Average Fuel Economy (CAFE) standard for passenger cars and light trucks. Regulating CAFE forced automobile manufacturers to improve the average fuel economy of their cars. Consequently, the average fuel economy for passenger cars was improved through the advances of the technologies. The technologies included the introduction of advanced engines and transmission systems. However, the contribution of the transportation sector to the energy consumption in the U.S. steadily increased during the past decade because of the low gas price and the increases in vehicle ownership and travel. For example, the transportation sector accounted for 65% of the total gasoline consumption in the U.S. in 1992 (NRC, 1995).

2.2 Transportation and Emission Requirements

Since the Clean Air Act Amendments (CAAA) of 1970 was enacted some major legislation has been issued. The Environmental Protection Agency (EPA), which was established by the CAAA, endeavored to achieve the National Ambient Air Quality Standards (NAAQS) for six pollutants, namely: carbon monoxide (CO), lead (pb), nitrogen dioxide (NO_2), ozone (O_3), particulate matter (PM-10), and sulfur dioxide (SO_2) (NRC, 1995).

2.2.1 1990 Clean Air Act Amendments (CAAA)

In 1990, congress amended the CAA in order to improve the air quality by means of the reductions of the mobile source emissions including HC, CO, NO_X, and PM emission. Consequently, it introduced a variety of programs for the reduction of vehicle emissions such as strict emission testing procedures, expanded vehicle inspections and maintenance (I/M) programs, and clean fuel programs. This resulted in the reductions in the mobile source emissions (EPA, 1994). The amendments also required the submission of State Implementation Plans (SIP) and the EPA approval of SIPs (NRC, 1995).

2.2.2 Inter-modal Surface Transportation Efficiency Act (ISTEA)

The ISTEA of 1991 was made into law to provide a new vision for surface transportation (U.S. DOT, 1991). This act allowed highway funds to be transferred to the activities that contribute to achieving air quality standards, and it provided authorizations for highway construction, highway safety, and mass transportation expenditures. The Congestion Mitigation and Air Quality Improvement (CMAG) program was authorized by the ISTEA to provide funds for the projects that contribute to air quality improvements and reduce congestion.

2.2.3 State Implementation Plan Submissions (SIPs)

Each state is responsible for preparing and submitting a State Implementation Plan which demonstrates how the National Ambient Air Quality Standards (NAAQS) will be achieved, maintained, and enforced under the Clean Air Act. In addition, the state must obtain the EPA approval of the SIP (EPA, 2001). In SIPs, mobile source emission inventories should be projected and the impacts of transportation plans, programs, and projects on emissions should be quantified.

2.2.4 Conformity Process

Transportation conformity requires EPA, DOT, and a variety of regional agencies to incorporate the air quality and transportation planning development process under the Clean Air Act. Metropolitan Planning Organization (MPO) and DOT must demonstrate that new violations or delays in the attainment of standards will not be caused or contributed by transportation activities (NRC, 1995). Specifically, MPOs are responsible for demonstrating that higher emission levels than those of 1990 baseline year will not happen because of regional transportation improvement programs that include both federal and nonfederal projects. The construction of these projects should have emission levels lower than before (NRC, 1995).

2.3 Factors Affecting Transportation Energy Consumption and Emissions

Vehicle fuel consumption and emissions are caused by several factors that include: (a) Travel-related factors, (b) Driver-related factors, (c) Highway network characteristics, and (d) Vehicle characteristics and other factors. The following sections describe these factors in some detail.

2.3.1 Travel-Related Factors

The significant factors that affect fuel consumption rates are speed and acceleration levels. Engine friction and tire friction are also critical factors when power steering and air conditioning are working at low speeds. The aerodynamic drag is a dominant factor at high speeds (An et al., 1993). Also, vehicle fuel consumption rates are caused by the modal operation of the vehicle. For example, the cold start running causes lower fuel efficiency (Baker, 1994).

The number of trips, distance traveled, and the vehicle operating modes are factors that affect mobile source emissions. Speed, acceleration and engine load levels affect emission rates. Based on the emission rates estimated by MOBILE5a developed by the EPA and EMFAC7F developed by the California Air Resources Board (CARB), emission rates are high at low speed levels under traffic congestion. On the other hand, NO_X emission rates are high at high speed levels (NRC, 1995).

2.3.2 Driver-Related Factors

Driving behavior that includes accelerating, braking, and gear-shifting is a critical factor that affects both fuel consumption and emissions. Generally, high fuel consumption and emissions are caused by aggressive behaviors such as sharp accelerating and braking. For example, An et al reported that 15 percent increases in fuel consumption resulted from repeated braking maneuver in a congested urban area, and aggressive driving behavior with quick accelerations caused 10 percent increases in fuel consumption (An et al., 1993). On the other hand, aggressive driving behavior caused 15 times higher CO emissions and 14 times higher VOC levels than those from average driving behavior (NRC, 1995).

2.3.3 Highway-Related Factors

The geometric design of highways also affects vehicle fuel consumption and emissions. For example, roadway grades contribute to the increases in fuel consumption and emissions because a vehicle requires additional engine power to overcome grade resistance. This results in high A/F ratio that increases fuel consumption and emission rates. Rough road surfaces, which result in high rolling resistance, also induce the increases in fuel consumption. One study demonstrated that driving on rough roads at typical highway speeds increased fuel consumption by five percent when compared to normal quality roads (Baker, 1994). Also, the facilities in highways, such as intersections, lamps, toll booths, and weaving sections, result in emission increases because vehicles driven at those facilities need to accelerate and/or decelerate.

2.3.4 *Vehicle-Related and Other Factors*

Other primary factors that affect fuel consumption and emissions are vehicle characteristics such as vehicle weight, engine size, and technologies. Large size, heavy weight, automatic transmission, and the use of accessories such as power seats and windows, air conditioner, and power brakes and steering generally require more fuel (Murrell, 1980). Consequently, this results in more emissions.

Also, suitable vehicle maintenance is required to prevent the decreases in fuel economy. One study demonstrated that vehicle fuel consumption could increase up to 40 percent without suitable maintenance (Baker, 1994). The study also presented that inappropriate engine tuning and wheel misalignment could increase vehicle fuel consumption.

Weather conditions and ambient temperature also affect vehicle fuel consumption and emissions. For example, low temperature and high winds result in high fuel consumption rates. More vehicle emissions are exhausted because of cold start at low temperatures. Evaporative emissions increase as the temperature increases.

On the other hand, vehicle age is one of the critical factors that affect emissions. Generally, older vehicles emit more emissions than newer vehicles (Enns et al., 1993).

Finally, the interaction that happens in roadways can significantly affect vehicle emissions.

2.4 INTEGRATION Framework for Modeling Vehicle Emissions

Since the INTEGRATION model was developed by Michel Van Aerde, it has been enhanced over two decades. For example, the INTEGRATION model was expanded by including the VT-Micro emission models. In addition, the vehicle acceleration logic was enhanced by using vehicle dynamics models. In this section, a brief description of the INTEGRATION is presented to provide the reader with a basic understanding of the INTEGRATION prior to presenting the results in Chapter 3 and 4.

2.4.1 *Traffic Modeling*

First, the individual vehicles, which are specified in a time-varying O-D matrix, are generated and disaggregated into a sequence of individual departures. The INTEGRATIOM model uses a maximum likelihood approach for the calibration of O-D demand. Once a vehicle enters the network, the vehicle's desired speed is calculated based on the steady state car-following model that was proposed by Van Aerde and Rakha. The model merges the Pipes and Greenshields models into a single-regime model. In terms of vehicle decelerations and accelerations, the required deceleration rate is computed by dividing the speed differential, between a vehicle and the vehicle a head of it, by the deceleration time. On the other hand, the maximum vehicle acceleration is estimated by using a vehicle dynamics model to constrain vehicle acceleration, as illustrated in Equation [1] (Rakha et al., 2004).

$$a = \frac{F - R}{M} \qquad [1]$$

Where a is the vehicle acceleration (m/s^2), F is the tractive force, M is the vehicle mass, and R is the resistance force.

The INTEGRATION model has the lane changing logic that slow vehicles move to the right lane and fast vehicles move to the left lane. The lane changing logic also allows vehicles to move to lanes that offer them the longest headway (Rakha et al., 2004).

2.4.2 Modeling Vehicle Fuel Consumption and Emissions

The fuel consumption and emission rates are estimated by using the VT-Micro model together with the estimated vehicle speed and acceleration levels. In order to construct the VT-Micro model, chassis dynamometer data measured at the Oak Ridge National Laboratory (ORNL) were utilized. Specifically, nine normal emitting vehicles, six light duty vehicles and three light duty trucks, were included into the ORNL data to represent an average vehicle that had average characteristics such as engine displacement, vehicle curb weight, and vehicle type considering average vehicle sales. The ORNL data included a total of between 1,300 to 1,600 individual measurements for each vehicle with the corresponding speed and acceleration levels. In the ORNL data, the vehicle acceleration and speed ranged from -1.5 to 3.7 m/s^2 and from 0 to 33.5 m/s (0 to 121 km/h), respectively. Consequently, the VT-Micro model finally incorporated a combination of linear, quadratic, and cubic speed and acceleration terms, and was separated into two models for positive and negative accelerations, as illustrated in Equation [2] (Rakha et al., 2004).

$$MOE_e = \begin{cases} e^{\sum_{i=0}^{3}\sum_{j=0}^{3}(L_{i,j}^{e}\times u^i \times a^j)} & \text{for } a \geq 0 \\ e^{\sum_{i=0}^{3}\sum_{j=0}^{3}(M_{i,j}^{e}\times u^i \times a^j)} & \text{for } a < 0 \end{cases} \quad [2]$$

Where $L^e_{i,j}$ and $M^e_{i,j}$ represent model regression coefficients for MOE "*e*" at speed power "*i*" and acceleration power "*j*". The final VT-Micro model produced emission produced good fits to the ORNL data (R^2 in excess of 0.92 for all MOEs).

In addition, models for five light duty vehicles and two light duty trucks were constructed within the VT-Micro model framework by using data from 60 light duty vehicles and trucks. In the construction, Classification and Regression Tree Algorithms (CART) were used to group vehicles into homogenous categories (Rakha et al., 2004). Also, high emitting vehicle emission models, which had four different high emitting vehicle categories, were incorporated into the VT-Micro model. The HEV model was demonstrated that it introduced a margin of error of 10 percent when compared to in-laboratory bag measurements (Ahn et al., 2004).

2.5 Modeling of Grade Impacts on Vehicle Emissions

2.5.1 Roadway Grade Impacts

The fact that vehicles running on a steep grade exhaust more emissions is reasonable. From one past study, we can recognize its contribution partially. Pierson et al. (1996) conducted a study quantifying driving mode effects on a large, in-use vehicle fleet with remote sensors. The emission factors for 3.76% uphill and downhill grades were measured in the Fort McHenry. In the study, they concluded that uphill grade emissions were higher than downhill emissions by factors of 1.52, 1.86, and 2.19 for non-methane hydrocarbons (NMHC), CO, and NOx emissions, respectively. As can be seen in the study, grade impacts may be significant. However, grade impacts with other factors affecting emission rates were not fully captured in the study, because these factors could not be completely controlled under real road conditions. A study systematically quantifying grade impacts could hardly be found, because of the difficulties of controlling those factors.

2.5.2 Modeling of Grade Impacts using the INTEGRATION software

In order to model grade impacts using the VT-Micro model, the estimated acceleration levels should be adjusted in terms of roadway grade levels. The INTEGRATION uses the steady state car-following model proposed by Van Aerde and Rakha to simulate vehicle acceleration behaviors (Rakha et al., 2004). However, using the steady state car-following model generally produces unrealistic acceleration rates, usually high acceleration rates. In order to solve this problem, a vehicle dynamics model computing the maximum acceleration levels from the resultant forces acting on a vehicle was proposed, as illustrated in Equations [1] (Rakha et al., 2004).

The next step is to adjust the computed acceleration to the roadway grade, before it is used as an input parameter to the VT-Micro model, as illustrated in Equation [3].

$$a_{adjusted} = a + 9.81 \bullet g \quad [3]$$

Where $a_{adjusted}$ is the adjusted vehicle acceleration (m/s^2), 9.81 is the value of the acceleration of gravity (m/s^2), and g is the roadway grade (%).

2.6 High Emitting Vehicles

2.6.1 Definition of high emitting vehicles

High emitting vehicles have had much attention from researchers and regulators after the promulgation of federal regulation in the 1970s. The EPA defines high emitters as vehicles whose emissions of hydrocarbons (HCs), nitrogen oxides (NO_x) are two and/or carbon monoxide (CO) are three times higher than the national standards for new vehicles (EPA, 1999). And OBD-II equipment is programmed to identify when vehicle emissions exceed 1.5 times certification standards (NRC, 2001). As can be seen, high emitting vehicles are defined as vehicles having emissions greater than cut-points or standards.

From the 80's, several definitions to high emitters could be found. Those definitions can be categorized into three types in terms of methodologies used. The first type is using the mean and standard deviation of the sampled vehicle fleet. For example, GM researchers, Haskew and Gumbleton, suggested to define high emitters as vehicles exceeding six standard deviations from the mean of the sampled FTP data (Haskew et al., 1988). The second type is to define the dirtiest 10% of the fleet or vehicles responsible for 50% of the total emissions as high emitters. For example, Stedman, who developed a remote sensor, defined gross emitters as the proportion of vehicles responsible for 50% of the CO emissions (Stedman, 1989). The third type is to employ specific values in the unit of gram/mile or % concentration as the cut points. However, the reason that these cut points were employed was not mentioned in the literatures. In 1990, Lawson et al. provided the criteria for classifying low-emitting, high emitting, and super-emitting vehicles, in terms of CO concentration. For their study, they defined a low-emitting car as emitting 1.3% CO concentrations, a high-emitting car as emitting 8.5% CO, and a super-emitting car as emitting 17% CO (Lawson et al., 1990).

2.6.2 Impacts of High Emitting Vehicles

The fact that a small proportion of high emitting vehicles are responsible for a large amount of emissions was established by a number of studies. The utilized cut points to identify high emitters are varied depending on the objectives of studies, as demonstrated in the previous section. Thus, the magnitude of high emitters' impacts on overall vehicle emissions was different from each others. Also, the quantified impacts were varied depending on the type of employed data such as mass emission measurements or concentration measurements by remote sensors. However, in those studies, the high emitter impacts were computed in a same way. First, all measurements are sorted in the order of emission rates. Second, the ratio of high emitters to the vehicle fleets is calculated based on the cut points. Third, the aggregated contribution of high emitters is computed to find the percentage of the emissions emitted by high emitters from the total emissions.

One of the famous studies addressing high emitters' impacts is Wayne and Horie's study in 1983. They evaluated the in-use vehicle surveillance program in California. In this study, they concluded that 47% of the CO emissions were produced by only 12% of the vehicles tested (Wayne et al., 1983). Another famous study is Stedman's study in 1989. He analyzed the effectiveness of the state's oxygenated fuels program by using remote sensing measurements, and concluded that 10% of the vehicles produce more than 50% of the CO emissions (Stedman, 1989). In 1999, McClintock analyzed RSD and IM240 test data from 1997 and 1998 to develop high-emitter identification criteria. In his study, the worst-polluting 10% of vehicles for each pollutant emitted 63% of total CO, 47% of total HC, and 32% of total NO emissions (McClintock, 1999).

2.6.3 Methodology to Identify High Emitting Vehicles

This section briefly describes methodologies to identify high emitting vehicles. Inspection and Maintenance (I/M) programs are mainly discussed and other methodologies are introduced, in order to describe how high emitters are identified.

2.6.3.1 I/M program

I/M programs used in most states can be categorized into three types in terms of their implementation structures, which are the Centralized, Decentralized and Hybrid network types (NRC, 2001). These criteria are based on the scale, number and function of stations. Each state in the US has its own I/M program appropriate for its environment. The status of I/M program implementation can be found in the EPA's document (EPA, 2003).

General procedure of I/M program has several steps. First, a basic visual inspection, known as a visual anti-tampering check, is conducted by the inspector. The inspector checks the presence of emission control components such as catalytic converter, exhaust gas recirculation (EGR) valve, positive crankcase ventilation (PCV) valve, fuel inlet restrictor, air pump and vapor canisters. After the visual inspection, the inspector conducts a gas gap pressure test, which is testing whether harmful evaporative emissions are leaking from a vehicle's gas tank. Second, the vehicle is tested under the real-world simulated conditions to test whether vehicle exhaust emissions exceed cut points. Otherwise, the inspector checks the vehicle's On-Board Diagnostics (OBD).

Emission tests are divided into mass emissions and concentration measurement tests, in terms of measurement methods. Mass emission tests directly measure the mass of emitted emissions from the vehicle's tailpipe. Emission measurements are usually expressed the mass of emissions divided by the distance-traveled by the testing vehicle under a simulated road condition (NRC, 2001). The Federal Test Procedure (FTP), IM240, BAR31, IM93/CT93, and IM147 all fall into this categorization. On the other hand, concentration tests measure the relative concentrations of vehicle exhaust emissions. Idle speed and Acceleration Simulation Mode (ASM) tests fall into this categorization (NRC, 2001).

2.6.3.2 Remote sensing devices

Remote sensing devices (RSD) are tools that measure the concentration of pollutants emitted by on-road vehicles. The key technology in remote sensing is an infrared absorption principle. The amount of infrared light reflected and absorbed is translated into the concentration of exhaust pollutant. Also, RSD has the capability of capturing vehicle speeds, acceleration levels, and license plate numbers. Different tailpipe exhaust emission measurements, remote sensors are not directly used in I/M programs. But, it is considered a supplementary tool to enhance the efficiency of I/M programs. The feasibility of employing remote sensing as a complementary part of I/M programs has been evaluated in many states. A number of states are starting utilizing RSDs in their State Implementation Plans (SIPs) such as "clean screen program" and "evaluation of I/M program performance".

2.6.3.3 On-Board Diagnostic

On-Board Diagnostics is a computer-based system monitoring the performance of some of the engine's major components, including emission controls. OBD should be built into all model year 1996 and newer light-duty cars and trucks by the 1990 Clean Air Act. A large number of states have already employed OBD checks into their I/M programs, or prepare for OBD checks (EPA, 2002).

2.7 Summary of Conclusions

The contribution of transportation sector to U.S. fuel consumption and emissions is still significant, although vehicle fuel economy has improved. Thus, legislative efforts were made from the start point of the Clean Air Act Amendments (CAAA) of 1970, in order to achieve the NAAQS by means of reducing the share of transportation sector. An accurate assessment of mobile-source emissions is essential for an effective air-quality improvement program.

From the literature review, the INTEGRATION software is appropriate for quantifying the environmental impacts, because it combines car-following, vehicle dynamics, lane-changing, and a state-of-the-art microscopic energy and emission models.

Although roadway grades may be one of the major factors affecting fuel consumption and emissions, the impact of this factor has not studied systematically. Also, it is expected to contribute much to control the total mobile source emissions to screen high emitting vehicles.

Chapter 3: Energy and Environmental Impacts of Roadway Grades

Sangjun Park and Hesham Rakha, accepted for presentation in the TRB 2006

3.1 Abstract

Although roadway grades are known to affect vehicle fuel consumption and emission rates, there do not appear to be any systematic evaluations of these impacts in the literature. Consequently, this paper addresses this void by offering a systematic analysis of the impact of roadway grades on vehicle fuel consumption and emission rates using the INTEGRATION microscopic traffic simulation software. The energy and emission impacts are quantified for various cruising speeds, under stop and go conditions, and for various traffic signal control scenarios. The study demonstrates that the impact of roadway grade is significant with increases in vehicle fuel consumption and emission rates in excess of 9% for a 1% increase in roadway grade. Consequently, a reduction in roadway grades in the range of 1% can offer savings that are equivalent to various forms of advanced traffic management systems.

Keywords: mobile source emissions, vehicle fuel consumption, and roadway grades.

3.2 Introduction

Although vehicle fuel economy has improved over the years, the contribution of mobile-source fuel consumption and emissions are still significant. Consequently, an accurate assessment of fuel consumption and emissions is essential for air-quality improvement programs. Factors affecting vehicle fuel consumption and emissions can be categorized into four categories, which are travel-related factors, driver-related factors, highway network characteristics, vehicle characteristics, and weather conditions. Roadway grades are one of the highway-related factors affecting fuel consumption and emission rates.

Although it is a well accepted fact that vehicles consume more energy and emit higher emissions as they travel along roadway upgrades, limited literature have attempted to study the effect of roadway grades on vehicle fuel consumption and emission rates. Pierson et al. conducted a field study aimed at quantifying the environmental impacts of driving modes using a large in-use vehicle fleet through remote sensor measurements (Pierson et al., 1994). The emission factors for a 3.76% uphill and downhill grade were measured in the Fort McHenry area. The study demonstrated that uphill grade emissions were higher than downhill emissions by a factor of 1.52, 1.86, and 2.19 for non-methane hydrocarbons (NMHC,) CO, and NO_x emissions, respectively.

The objective of this paper is to quantify the impact of roadway grades on vehicle fuel consumption and mobile source emission rates. The paper investigates these impacts considering hot stabilized vehicle emissions of light duty gasoline vehicles and high emitter vehicles.

In terms of paper organization, initially an overview of the INTEGRATION modeling framework is presented, because the study employs the INTEGRATION software for the analysis. It should be emphasized, however, that the focus of the paper is on the results of the analysis as opposed to the modeling framework. The framework is only presented in order to provide confidence in the results and conclusions that are derived from this research effort. The following section presents the network construction and scenario development exercises. Subsequently, the simulation results are presented and described. Finally, the conclusions of the study and recommendations for further research are presented.

3.3 INTEGRATION Modeling Framework

The INTEGRATION software (Van Aerde et al., 1988; Van Aerde et al., 1988; Van Aerde et al., 1996; M. Van Aerde & Assoc., 2002; M. Van Aerde & Assoc., 2002) was employed for this study because of several reasons. First of all, the software combines car-following, vehicle dynamics, lane-changing, energy, and emission models. Thus, mobile source emissions can be directly estimated from instantaneous speed and acceleration levels. Second, the traffic and emission modeling modules have been tested and validated extensively. For example, the software, which was developed over the past two decades, has not only been validated against standard traffic flow theory (Rakha et al., 1996; Rakha et al., 2002), but has also been utilized for the evaluation of real-life applications (Rakha et al., 1998; Rakha et al., 2000). Furthermore, the INTEGRATION software offers unique capability through the explicit modeling of vehicle dynamics by computing the tractive and resistance forces on the vehicle each deci-second (Rakha et al., 2001; Rakha et al., 2002; Rakha et al., 2004). It should be noted that the procedures described in this paper are general and could be applied to other commercially available software if they combine the modeling of various resistance and tractive forces acting on a vehicle with accurate model vehicle fuel consumption and emission models.

The INTEGRATION software uses car-following models to capture the longitudinal interaction of a vehicle and its preceding vehicle in the same lane. The process of car-following is modeled as an equation of motion for steady-state conditions (also referred to as stationary conditions in some literature) plus a number of constraints that govern the behavior of vehicles while moving from one steady-state to another (decelerating and/or accelerating). The first constraint governs the vehicle acceleration behavior, which is typically a function of the vehicle dynamics (Rakha et al., 2002; Rakha et al., 2004). The second and final constraint ensures that vehicles maintain a safe position relative to the lead vehicle in order to ensure asymptotic stability within the traffic stream. A more detailed description of the longitudinal modeling of vehicle motion is provided by (Rakha et al., 2004). Alternatively, lane-changing behavior describes the lateral behavior of vehicles along a roadway segment. Lane changing behavior affects the vehicle car-following behavior especially at high intensity lane changing locations such as merge, diverge, and weaving sections.

The software also models vehicle fuel consumption and emission rates using the VT-Micro framework (Rakha et al., 2004). The VT-Micro model was developed from experimentation with numerous polynomial combinations of speed and acceleration levels. Specifically, linear, quadratic, cubic, and quadratic terms of speed and acceleration were tested using chassis dynamometer data collected at the Oak Ridge National Laboratory (ORNL). The final regression model included a combination of linear, quadratic, and cubic speed and acceleration terms because it provided the least number of terms with a relatively good fit to the original data (R^2 in excess of 0.92 for all Measures of Effectiveness (MOE)). The ORNL data consisted of nine normal emitting vehicles including six light-duty automobiles and three light duty trucks. These vehicles were selected in order to produce an average vehicle that was consistent with average vehicle sales in terms of engine displacement, vehicle curb weight, and vehicle type. The data collected at ORNL contained between 1,300 to 1,600 individual measurements for each vehicle and MOE combination depending on the envelope of operation of the vehicle, which has a significant advantage against emission data collected from few driving cycles since it is impossible to cover the entire vehicle operational regime with only a few driving cycles. Typically, vehicle acceleration values ranged from –1.5 to 3.7m/s^2 at increments of 0.3m/s^2 (-5 to 12ft/s^2 at 1 ft/s^2 increments). Vehicle speeds varied from 0 to 33.5m/s (0 to 121km/h or 0 to 110ft/s) at increments of 0.3m/s (Ahn et al., 2002; Ahn et al., 2004; Rakha et al., 2004). In addition to, the VT-Micro model was expanded by including data from 60 light duty vehicles and trucks. Statistical clustering techniques were applied to group vehicles into homogenous categories using Classification and Regression Tree algorithms. The 60 vehicles were classified into 5 LDV and 2 LDT categories. In addition, high-emitter vehicle emission models were constructed using second-by-second emission data. The HEV model was found to estimate vehicle emissions with a margin of error of 10% when compared to in-laboratory bag measurements (Rakha et al., 2003; Ahn et al., 2004).

The INTEGRATION software computes the effective tractive force as the minimum of two forces; namely: the maximum engine tractive force (F_e) and the maximum frictional force that can be sustained between the vehicle wheels and the roadway surface (F_{max}) (Rakha et al., 2001; Rakha et al., 2002; Rakha et al., 2004; Rakha et al., 2004). The aerodynamic resistance (R_a), rolling resistance (R_{rl}), and the grade resistance (R_g) are also computed each deci-second. Subsequently, the maximum vehicle acceleration is then computed as

$$a = \frac{\min(F_e, F_{\max}) - (R_a + R_{rl} + R_g)}{m}, \qquad [1]$$

where a is the vehicle acceleration (m/s^2) and m is the vehicle mass (kg).

In estimating vehicle emissions, given that the power required to overcome the aerodynamic and rolling resistance forces were accounted for in the development of the fuel consumption and emission models, the effective vehicle acceleration is adjusted to account for the component of the vehicle weight opposing the vehicle motion as

$$a_e = a + 9.8067G, \qquad [2]$$

where a_e is the effective acceleration (m/s^2), 9.8067 is the acceleration of gravity (m/s^2), and G is the roadway grade. The effective acceleration accounts for the actual engine load required to negotiate a grade in addition to moving the vehicle. The speed and acceleration levels are then input into the VT-Micro model to estimate instantaneous vehicle fuel consumption and emission rates.

3.4 Scenario Development

In developing the test scenarios, three sets of variables are considered. The first variable set is comprised of network characteristics, which include link lengths, number of lanes, lane saturation flow rates, roadway grades, and control type (stop sign or signal control). The second set of variables includes operational characteristics such as signal timing parameters (cycle lengths, phase splits, and offsets). The third set of parameters includes traffic demand loadings, traffic composition, and vehicle characteristics.

In quantifying the impact of roadway grade on vehicle fuel consumption and emission rates, three scenario sets are analyzed. For each of these three scenario sets the roadway grade is varied from 0 to 6% considering a normal light duty vehicle (the Oak Ridge National Lab composite vehicle) and a high emitter vehicle (Type 4).

3.4.1 Constant Speed Scenario

In the constant speed scenario vehicle fuel consumption (L/km) and emission rates (g/km) are compiled for different grades and cruising speeds. The cruising speeds are varied from 5 to 100 km/h at increments of 5 km/h while roadway grades are varied from -6 to +6% at increments of 1%. In addition, the analysis considers varying the length of the grade while maintaining a constant distance weighted average grade. This scenario evaluates the impact of climbing identical elevation differences considering different grade levels for the same travel distance.

The objective of the constant speed scenario is to quantify the impact of roadway grades on vehicle fuel consumption and emission rates at different cruising speeds.

3.4.2 Stop Sign Control Scenario

The objective of this scenario is to quantify the impact of roadway grades on vehicle fuel consumption and emission rates for a stop sign controlled roadway. This scenario involves vehicle deceleration and acceleration considering different acceleration levels. The scenario is executed on a 2-km single lane roadway in which a single vehicle is simulated to travel a free-flow speed of 64 km/h where a stop sign is located after 1 km. The vehicle acceleration levels are varied from 40 to 100% the maximum rate at increments of 20% in order to analyze the impact of driver aggressiveness on fuel consumption and emission rates.

3.4.3 Signal Control Scenario

The scenario quantifies the variation in MOEs as a function of traffic signal offsets and roadway uphill and downhill grades. The network used in this analysis is composed of three signalized intersections along a 2 km long roadway segment. Signalized intersections are located after 500 m, 1000 m, and 1500 m. The cycle length at each of the three intersections is set at 60 s with offsets varying from 0 to 50 s as the increment of 10 s. Each of three signals is controlled by two-phase timings with a 70:30 phase split (east/west versus north/south). Roadway grades are varied from 0 to 6% at increments of 1% with an uphill grade in the eastbound direction and a downhill grade in the westbound direction. The free-flow speed of the network is 64 km/hr (40 mi/h) with a lane saturation flow rate of 1600 veh/h. A traffic demand of 800 veh/h is loaded in the eastbound and westbound directions, respectively. Alternatively, the northbound and southbound demands are set at 320 veh/h.

3.5 Results

The results for each of the three scenarios are presented in the following sections. We start with the uniform speed scenario followed by the stop-sign scenario and conclude with the traffic signal scenario.

3.5.1 Uniform Speed Scenario

This section describes the results for the constant speed scenarios for both normal and high emitting vehicles. These runs were executed by simulating the motion of a vehicle along a 1-km section at a constant speed. Vehicle fuel consumption and emission rates were computed for the entire trip to compute a distance based fuel consumption and emission rate.

Normal Light Duty Vehicle

The results demonstrate, as would be expected, an increase in the vehicle fuel consumption and emission rate with an increase in the roadway grade, as illustrated in Figure 3-1. The results also demonstrate a bowl-shaped relationship with respect to the cruise speed with the minimum fuel consumption rate occurring at a speed of 75 km/h. Given that a vehicle traveling at lower speeds spends more time traveling the 1-km roadway section, despite the lower time-based fuel consumption and emission rate, the total fuel and emissions consumed is significantly higher at lower speed levels. As a vehicle speed increases the time-dependent rate also increases, however at a rate that less than the travel time increase rate. Consequently, the distance-based fuel consumption and emission rate decreases until the rate of increase in the time-dependent rate exceeds the rate of decrease in time spent in the system. A more detailed description of these behaviors and the reasoning for these behaviors can be found elsewhere in the literature (Rakha et al., 2003).

The variation in CO_2 emission rates as a function of cruise speed and roadway grade appears to be similar to that of fuel consumption. Specifically, the CO_2 emission rates demonstrate a bowl shaped functional form with respect to cruise speed with the highest rates occurring at low speeds. However, the minimum CO_2 emission rate, unlike the fuel consumption rate, varies as a function of the roadway grade. Specifically, the minimum CO_2 rate occurs at a cruise speed of 75 km/h for a 0 to 6% grade, as demonstrated in Table 3-1.

Alternatively, the functional form of the HC and CO emission profiles differs from the CO_2 and fuel consumption profiles. The HC and CO profiles are similar, however at low speed ranges the profiles differ. The HC and CO emission rates demonstrate a bowl shaped functional form with extremely high rates at high cruise speeds. In case of the CO emissions the increase in emissions at low speeds is minimal, this is not the case for HC emissions.

Finally, the variation in the NO_x emission rate as a function of the cruise speed exhibits a slightly different behavior when compared to other measures of effectiveness (MOEs). Specifically, the functional form has an optimum speed that fairly low (30 km/h) that decreases with an increase in cruise speeds.

The MOE behavior as a function of vehicle cruise speed and roadway grade levels varies for different MOEs. For example, fuel consumption and CO_2 emission rates are more sensitive to variations in cruise speed levels than to variations in roadway grades. Alternatively, HC, CO, NO_x emissions are more sensitive to roadway grades. Furthermore, NO_x and CO_2 emissions are more sensitive to roadway grades in the 35 to 65 km/h and the 65 to 95 km/h cruise speed range, respectively, as illustrated in Figure 3-2. Alternatively, HC and CO emissions are more sensitive to roadway grades at high cruise speeds (100 km/h).

The higher HC, CO, and NO_x emissions for 6% versus 0% grade at a speed of 100 km/h is a result of the higher engine load (combination of speed and acceleration) under these conditions. It should be noted that the scale for these emissions are much smaller and thus the figure exaggerates the impact of grades when compared to CO_2 and fuel consumption rates.

The final analysis investigates differences in vehicle fuel consumption and emission rates associated with alternative grade design scenarios considering identical overall grades. The results demonstrate that steep and short grades result in higher fuel consumption and emission rates when compared to long and mild grades for identical grade climbs considering equal segment lengths, as illustrated in **Figure 3-3**. Consequently, from a design perspective a mild long grade is more efficient than a short steep grade.

Table 3-1: Max/Min Fuel Consumption and Emission Rates (Normal LDV)

Grade		Fuel Consumption		HC		CO		NOx		CO_2	
		Speed (km/h)	Rate (l/km)	Speed (km/h)	Rate (g/km)	Speed (km/h)	Rate (g/km)	Speed (km/h)	Rate (g/km)	Speed (km/h)	Rate (g/km)
Max	0%	5	0.354	5	0.347	5	1.876	100	0.283	5	822.71
	1%	5	0.389	5	0.363	5	2.046	100	0.407	5	905.17
	2%	5	0.427	5	0.378	100	2.783	100	0.560	5	992.98
	3%	5	0.467	5	0.395	100	4.764	100	0.719	5	1086.13
	4%	5	0.509	5	0.415	100	8.645	100	0.869	5	1184.83
	5%	5	0.554	100	0.532	100	15.977	100	0.996	5	1288.84
	6%	5	0.601	100	0.872	100	28.881	95	1.102	5	1398.16
Min	0%	75	0.078	75	0.070	80	1.128	30	0.087	75	180.85
	1%	75	0.092	75	0.071	75	1.221	30	0.123	75	212.26
	2%	75	0.108	65	0.080	30	1.359	25	0.169	75	250.99
	3%	75	0.127	60	0.093	20	1.435	20	0.223	75	292.99
	4%	75	0.147	50	0.112	20	1.533	20	0.287	75	337.97
	5%	60	0.168	45	0.133	20	1.660	15	0.360	75	384.94
	6%	60	0.190	35	0.156	20	1.818	15	0.439	75	432.75

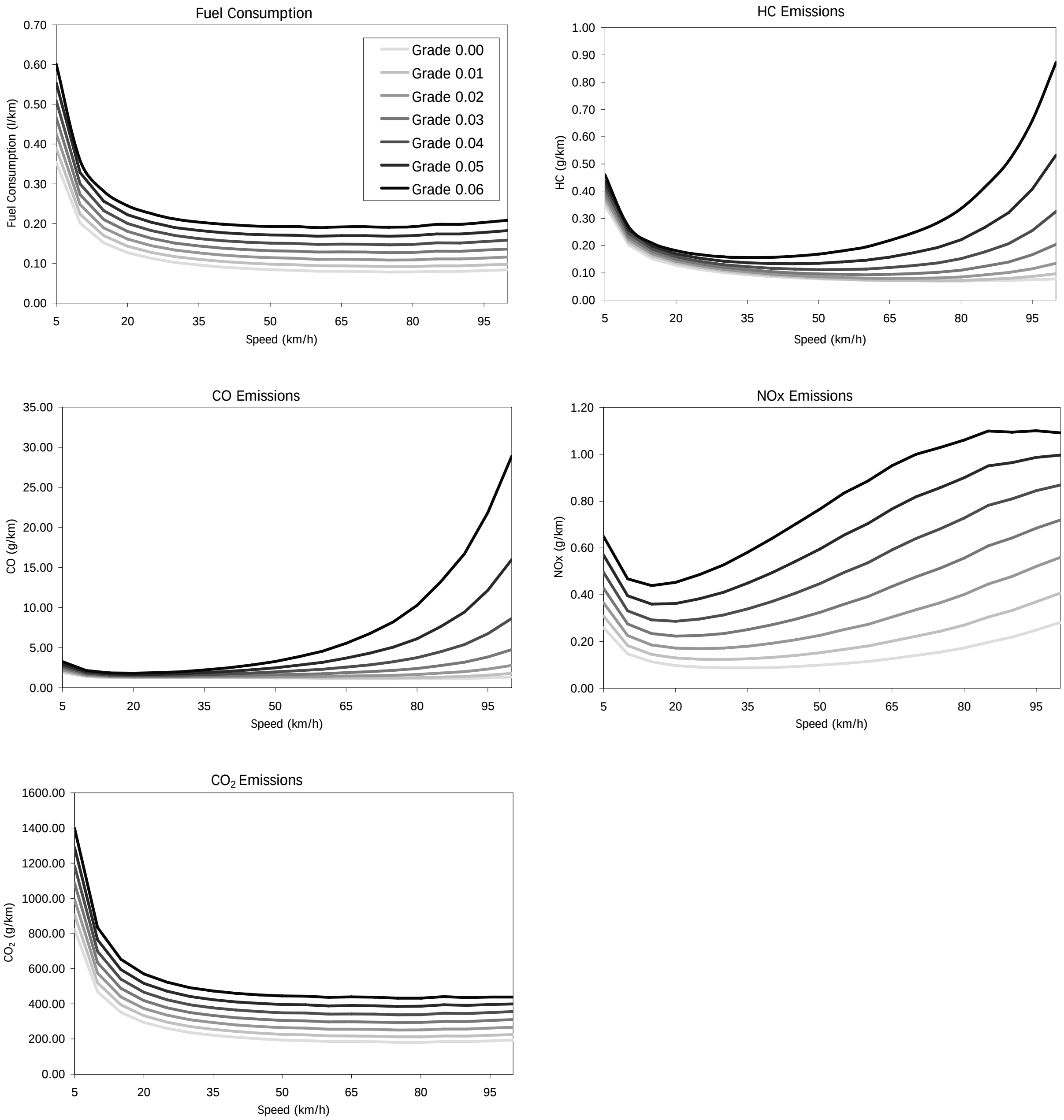

Figure 3-1: MOE profiles for Normal LDV

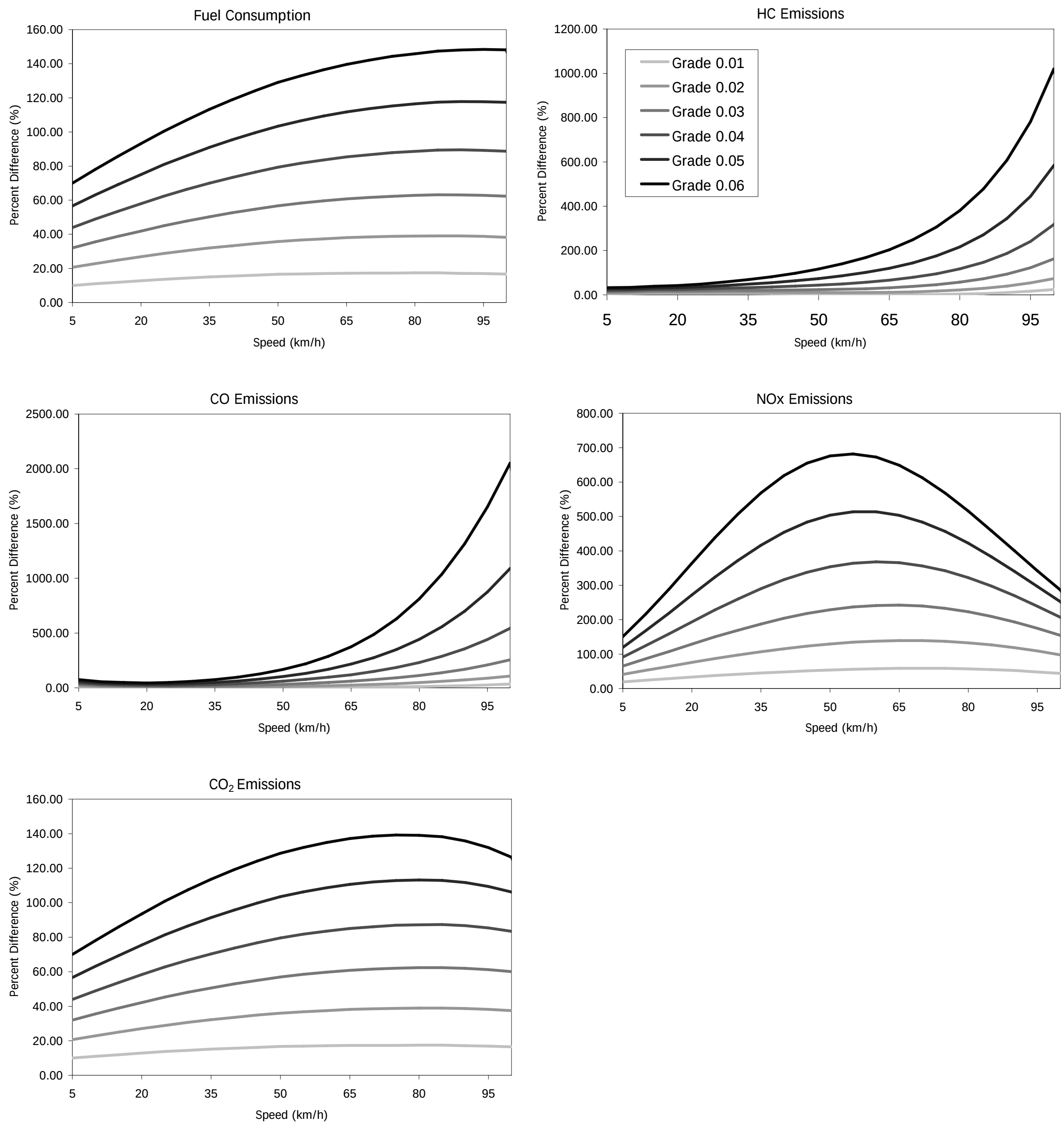

Figure 3-2: Percent change in MOEs relative to 0% grade for Normal LDV

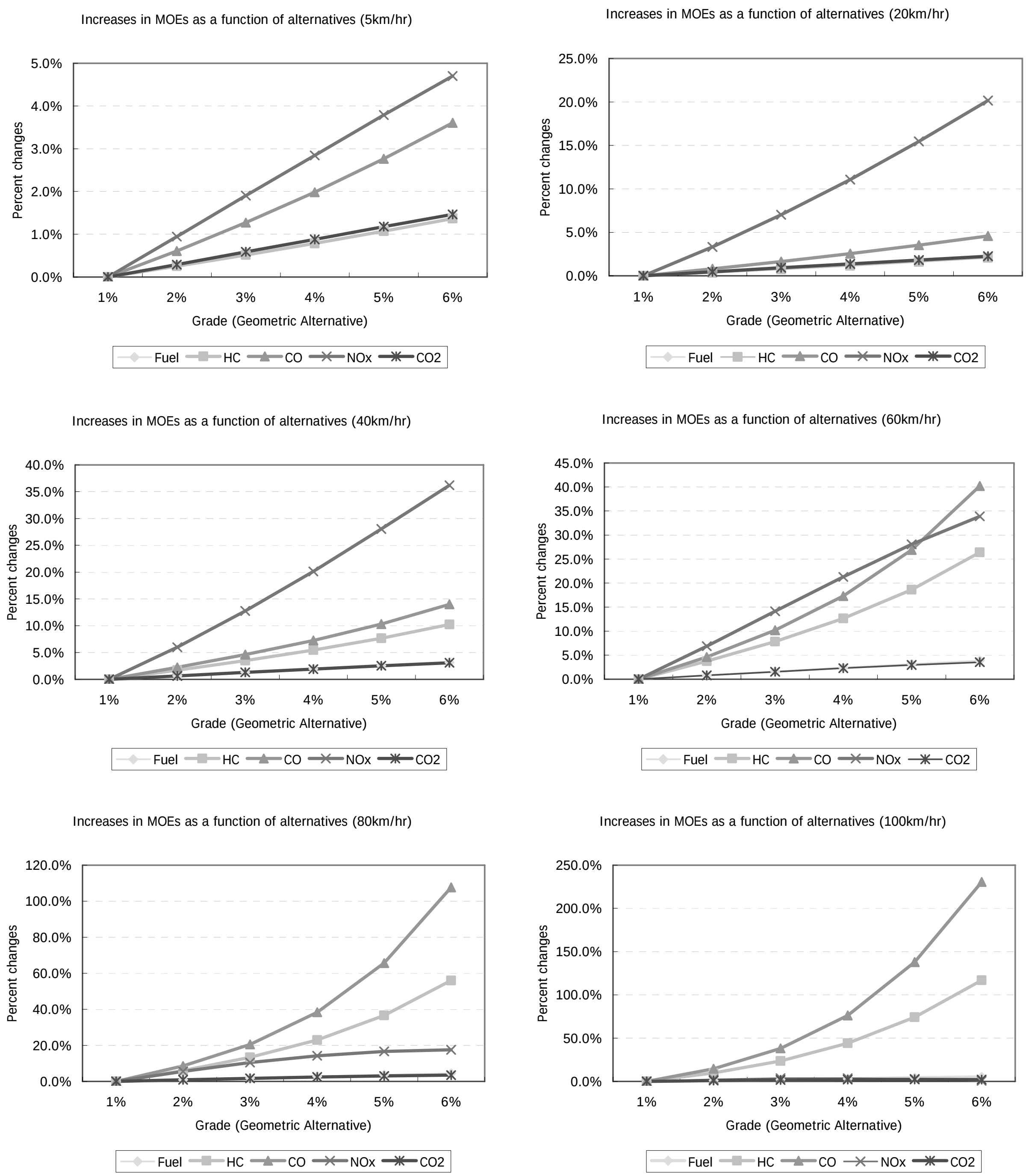

Figure 3-3: Increases in MOEs as a function of Geometric Alternatives

High Emitting Vehicle

The fuel consumption and emissions for the HEV also increase as roadway grades increase. Comparing the results of the Normal LDV with those of the HEV, the shapes of fuel consumption, CO_2, and NO_x emission behavior as a function of cruise speed and grade levels are similar. However, the absolute values of the HEV fuel consumption and CO_2 emission rates are less than those of the Normal LDV. This is because the Normal LDV utilized has a larger engine than the HEV. In case of the NOx emissions, the mass emissions for the HEV are significantly higher than those for the Normal LDV. Furthermore, the speed ranges at which the NO_x emission rates are high shift to low speed ranges relative to those for the Normal LDV. On the other hand, the shapes of HC and CO emission profiles for the HEV are different from those for the Normal LDV. Specifically, the Normal LDV produces higher emissions at high speed ranges, while the HEV produces higher emissions at low speed ranges.

The percentage change in MOEs relative to the 0% grade scenario for each of the roadway grades considering an HEV is calculated. The percentage changes in MOEs of the HEV are relatively smaller than those of the Normal LDV. This is because the mass of emissions at zero grade, denominator, is much higher than that of the Normal LDV. That is, the changes in MOEs for the HEV are higher in terms of absolute values but smaller in terms of relative values than those of the Normal LDV.

Looking into the MOE profiles as a function of speed and roadway grade levels, the impacts of the HEV are different from those for Normal LDV. That is, Fuel consumption, HC, CO, and CO_2 emissions are more sensitive to the variation in speed levels. However, NO_x emissions are more sensitive to roadway grades.

3.5.2 Stop Sign Control Scenario

The main objective of the stop sign scenario is to quantify the impact of roadway grade during stop-and-go maneuvers. This scenario is different from the uniform speed scenario in that this scenario involves vehicle deceleration and acceleration. Within this scenario an analysis of the impacts of roadway grades and acceleration levels on vehicle fuel consumption and emission rates is conducted.

As discussed earlier in the methodology section, four different acceleration levels are considered in this scenario. The acceleration levels are varied from 40% to 100% the maximum rate at increments of 20%. **Figure 3-4** illustrates the acceleration, speed, and emission profiles for two acceleration level runs. The upper-left figure illustrates the VT-Micro model validity boundary superimposed on the speed/acceleration profile of a simulated vehicle for different acceleration levels. As can be seen, two observations exceed the VT-Micro boundary when the vehicle accelerates at its maximum capacity (100% acceleration level). Otherwise all data are within the valid range of the VT-Micro model. The figure also illustrates the temporal variation in vehicle fuel consumption and emission rates as a vehicle decelerates and accelerates along different roadway grade sections. The figure demonstrates that the vehicle fuel consumption rate decreases as the vehicle decelerates and increases significantly while the vehicle accelerates. The figure also demonstrates that vehicle fuel consumption emission rates are significantly dissimilar for different grades.

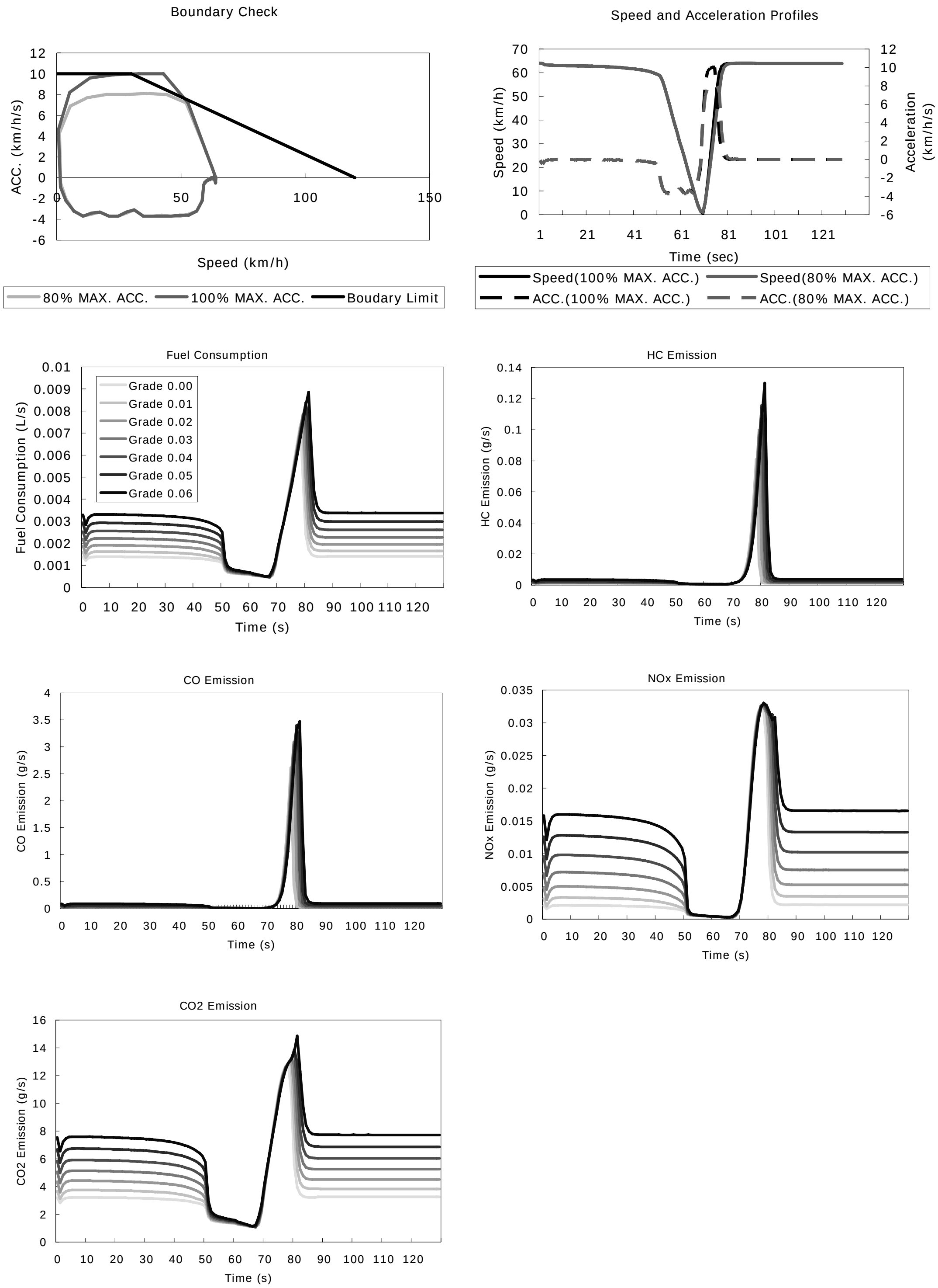

Figure 3-4: Speed, acceleration, and MOE profiles as a function of time

Normal Light Duty Vehicle

Before scrutinizing the results of the stop sign scenario, it is meaningful to compare the results of two scenarios, the uniform speed and stop sign scenarios, without any consideration of roadway grade impacts. The differences in fuel consumption and emission rates for the two scenarios considering a 0% grade are calculated. As the result of the comparison, the fuel consumption, HC, CO, NO_x, and CO_2 emission rates of the stop sign scenario are 23%, 143%, 274%, 78%, and 20% higher than those of the uniform speed scenario, respectively, considering the Normal LDV, and 13%, 18%, 20%, 4%, and 11% higher, respectively, considering the HEV. As can be seen, all MOEs of the stop-sign scenario were higher than those of the uniform speed scenario, as would be expected given that the vehicle has to stop. The additional HC and CO emissions for the Normal LDV that result from the introduction of a stop are significant. The results demonstrate that stop-and-go behavior has significant impacts on HC and CO emissions in comparison to other emissions for both normal and HEV.

Analyzing the roadway grade impact results for the stop sign scenario, the MOEs are more sensitive to roadway grades than vehicle acceleration levels. Changes in MOEs' as a function of acceleration levels, relative to the base 40% maximum acceleration level, vary from – 9% to 228%. Alternatively, the MOEs vary from 1% to 364% as a function of roadway grades, relative to the 0% grade base case.

The percentage change in MOEs as a function of the vehicle's acceleration level demonstrates a significant increase in HC and CO emissions in comparison to other MOEs. Considering the roadway grade effects, the percentage changes are more drastic at lower grade levels. The percentage change in MOEs relative to the 40% maximum acceleration level at 0% and 6% grade is calculated. Consequently, the HC and CO emission changes vary from 26% to 127% and from 32% to 228%, respectively. On the other hand, the NO_x and CO_2 emissions slightly decrease as the vehicle's acceleration level increases. The NO_x and CO_2 emission changes vary from -9% to 1% and from -3% to -1%, respectively. Finally, the fuel consumption rate is impacted slightly by the vehicle's acceleration level.

Comparing the results in terms of roadway grade impacts, the results demonstrate an increase in MOEs as roadway grades increase, as was the case for the uniform speed scenario. The percentage changes in the MOEs are not as significant as in the case with the uniform speed scenario. That is, the fuel consumption, HC, CO, NO_x, and CO_2 emissions have a maximum change of 111%, 207%, 338%, 364%, and 108%, respectively. Noteworthy is the fact that the roadway grade impacts on HC and CO emissions are relatively small, when a vehicle is operated at higher acceleration levels.

High Emitting Vehicle

Comparing the HEV results to the Normal LDV results one observes that the MOEs decrease as the vehicle's acceleration level increases. The percentage changes in MOEs relative to the 40% acceleration level along a 0% and 6% grade are calculated. As the result of the comparison, the MOEs vary from -13% to 0%.

On the other hand, the MOEs and percentage change in MOEs as a function of roadway grade and acceleration levels are calculated. As the result of the comparison, the relative changes are not higher than those of the Normal LDV. The fuel consumption, HC, CO, NO_x, and CO_2 emissions have maximum changes of 98%, 70%, 104%, 94%, and 98%, respectively. However, the absolute values for the MOEs are much higher than those of the Normal LDV, except for the fuel consumption and CO_2 emission rates. The ratio of the HEV to Normal LDV MOEs is calculated for each of a 0%~6% roadway grade. Consequently, the fuel consumption, HC, CO, NO_x, and CO_2 vary 80%~76%, 697%~558%, 308%~262%, 896%~387%, and 101%~103%, respectively. The results demonstrate that unlike the Normal LDV, the HC and CO emissions are relatively insensitive to vehicle deceleration levels.

3.5.3 Signal Control Scenario

Prior to discussing the signal control scenario results, a description of the Performance Index (PI) concept is presented given that it is utilized as an objective function in computing the optimum traffic signal offsets. The PI is computed as

*Performance Index = Number of Stops * 10 + Total Delay.*

First, the optimal offsets are computed to maximize the PI. Subsequently, the environmental impacts are computed for the identified signal timings. It should be noted that the east bound direction travels uphill while the west bound direction travels downhill.

The percentage changes in MOEs as a function of the roadway grade are calculated. The fuel consumption, HC, CO, NOx, CO_2 vary 13%~109%, 8%~121%, 12%~168%, 32%~424%, and 13%~109%, respectively, considering the east bound, and -37%~-9%, -30%~-6%, -50%~-9%, -59%~-20%, and -37%~-10%, respectively, considering the west bound. The results demonstrate an increase in MOE estimates as the roadway grade increases demonstrating that the additional MOE estimates in the east bound direction (uphill) outweigh the savings in MOEs in the west bound direction (downhill).

Normal Light Duty Vehicle

Based on the simulation results, the optimal and worst offsets for the east bound (uphill) based on the PI are 40 and 0 seconds at 0% grade, respectively. The uniform speed scenario and the signal scenario at 0% grade are compared, when the network is being controlled at optimum and worst offset. As the result of the comparison, the MOEs at the offset of 0 and 40 seconds are higher 20% ~ 59% and 41%~65% than those of the uniform speed scenario, respectively.

Of interest is whether the optimal offset varies as a function of the MOE under consideration for different roadway grades. The optimal offset for the east bound direction (uphill) based on the PI is 40 s. The optimal offset for the east bound direction using other MOEs is also 40 s. Alternatively, when considering the aggregated MOEs for the east and west bound directions, the optimal offset based on the PI is 40 s at 0, 1, 2, and 3% grade and 30 s at 4, 5, and 6% grade. The optimal offset based on fuel consumption and emissions is always 40 s regardless of the roadway grade. Also the worst offset is almost 0 s regardless of the MOE that is considered in optimizing the signal offsets. This result shows that the fuel consumption and vehicle exhaust emissions are generally low, when the network is controlled at the optimal signal offset yielded based on the PI. In summary, the PI is a good objective function in selecting traffic signal timings that enhance the environment.

Figure 3-5 illustrates the variation of MOEs as a function of roadway grades and signal offsets for the Normal LDV. The figures demonstrate that the roadway grade is critical in estimating fuel consumption and emission rates. More specifically NOx emissions are extremely sensitive to roadway grades.

High Emitting Vehicle

The variation in fuel consumption and emission rates for the HEV as a function of the roadway grade is very similar to the Normal LDV results. Similarly, the MOEs rates are close to optimal at the optimal signal offsets that are yielded by minimizing the PI. However, the differences in absolute values for the HEV are much higher than those of the Normal LDV. The ratio of the HEV to Normal LDV fuel consumption, HC, CO, NO_x, and CO_2 vary 84%~78%, 1522%~1201%, 944%~720%, 1118%~508%, and 99%~ 100%, respectively. As can be seen, the fuel consumption and CO_2 emissions are slightly lower than those of the Normal LDV. Alternatively, the HC, CO, and NO_x emissions for the HEV are much higher than those of the Normal LDV.

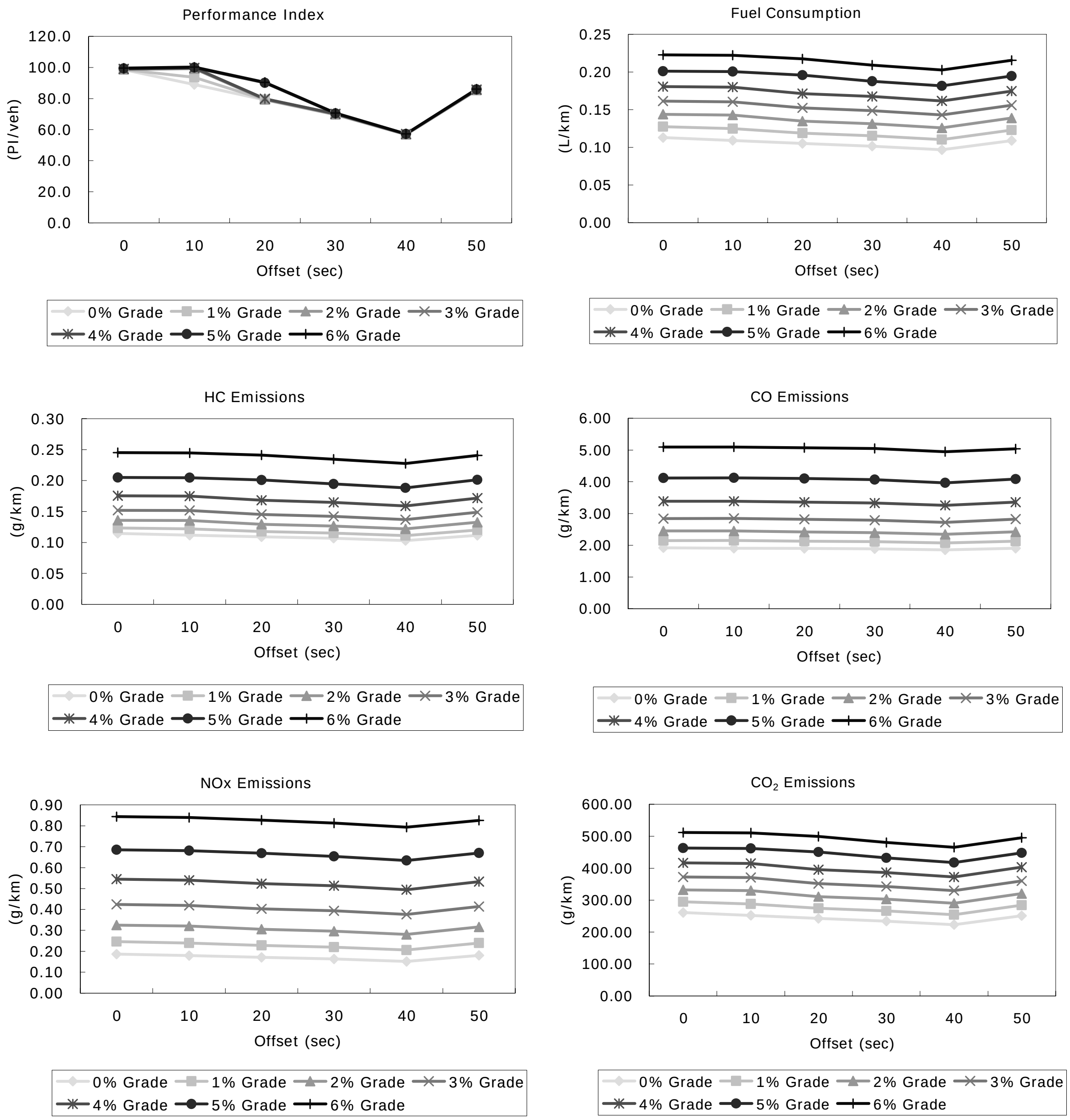

Figure 3-5: PI and MOEs as a function of signal offsets for Normal LDV

3.6 Overall Analysis of Scenarios

In this section we summarize the results of the analysis. The fuel consumption and vehicle exhaust emissions increase as roadway grade levels increase. The percentage changes in MOEs are significant, even for a 1% increase in roadway grade levels, regardless of the vehicle type (normal versus high emitter), as demonstrated in Table 3-2 and Figure 3-6 (a). For instance, the increases in MOEs for the Normal LDV range from 8% to 36% at a 1% grade relative to 0% grade under the signal control conditions. Comparing Normal LDVs with HEVs, grade impacts on HEVs are greater in terms of absolute values but lesser in terms of relative values compared to Normal LDVs.

For Normal LDVs, HC, CO, and NO_x emissions are more sensitive to roadway grades in comparison to fuel consumption and CO_2 emission rates. In terms of relative changes, HC, CO, and NO_x emissions are significantly impacted by roadway grades for cruise modes of travel. Fuel consumption, HC, CO, NO_x, and CO_2 emissions increase by 140%, 197%, 361%, 656%, and 138%, respectively, as illustrated in Figure 3-6. Alternatively, the absolute HC, CO, and NO_x emissions for the stop sign control scenario are higher than those for the other scenarios, as illustrated in Figure 3-7. The reason for the higher emissions is a result of the larger number of stops that are involved in the stop scenario compared to the other scenarios.

The MOEs for HEVs are not as sensitive as those for Normal LDVs to vehicle acceleration levels. However, the relative values for HC, CO, and NO_x emissions are also significant for cruising conditions. The fuel consumption, HC, CO, NO_x, and CO_2 emissions increase by 113%, 84%, 126%, 105%, and 112%, respectively for a 6% grade relative to a 0% grade, as illustrated in Figure 3-6. The absolute HC, CO, and NO_x emissions from the signal control scenario with the worst offset are higher than those from other scenarios. This is because HEVs are more sensitive to the increase in travel time. The fuel consumption, HC, CO, and CO_2 emissions are 33%, 57%, 53%, 29% greater than those for cruising conditions.

Figure 3-8 shows the comparison between the benefits associated with a reduction of roadway grades and the benefits of signal optimization. As can be seen in Figure 3-8 (a), the benefits yielded from signal optimization are equivalent to those from reducing roadway grades from 0% to the range of negative 1% to negative 2%. Furthermore, the benefits associated with a reduction in the roadway grade from 2% to 1% or 0% is also equivalent to the benefits obtained from signal optimization, as illustrated in Figure 3-8 (b). Finally, the results indicate that the environmental benefits associated with a reduction in roadway grade for Normal LDVs is greater than that for HEVs.

Table 3-2: Comparison of scenarios at 0%, 1%, and 6% grade (FFS = 64km/h, Max. Acc. Level = 60%)

		Uniform Speed Scenario		Stop Sign Scenario		Signal Scenario	
		Normal	High Emitter	Normal	High Emitter	Normal	High Emitter
0%	Fuel	0.0801	0.0709	0.0982	0.0802	0.0968	0.0824
	HC	0.0720	1.1581	0.1749	1.3674	0.1030	1.5501
	CO	1.1625	13.0496	4.3436	15.6208	1.8534	17.0251
	NOx	0.1247	1.8709	0.2218	1.9440	0.1514	1.7963
	CO_2	185.2292	141.7317	222.2241	157.7008	223.0919	160.9206
1%	Fuel	0.0943	0.0818	0.1109	0.0909	0.1103	0.0928
	HC	0.0728	1.2856	0.1939	1.4874	0.1111	1.6693
	CO	1.2327	14.6258	5.0308	17.0627	2.0726	18.4108
	NOx	0.1980	2.1332	0.2851	2.1803	0.2058	1.9552
	CO_2	218.3178	165.7147	250.7782	181.2075	254.2866	183.0239
6%	Fuel	0.1924	0.1511	0.2039	0.1552	0.2027	0.1596
	HC	0.2141	2.1307	0.4241	2.2850	0.2276	2.4746
	CO	5.3574	29.4986	11.8173	30.0671	4.9459	30.3239
	NOx	0.9432	3.8262	0.9400	3.6576	0.7928	3.1558
	CO_2	440.7586	299.8061	456.8297	306.4108	465.4452	317.6261

(a)

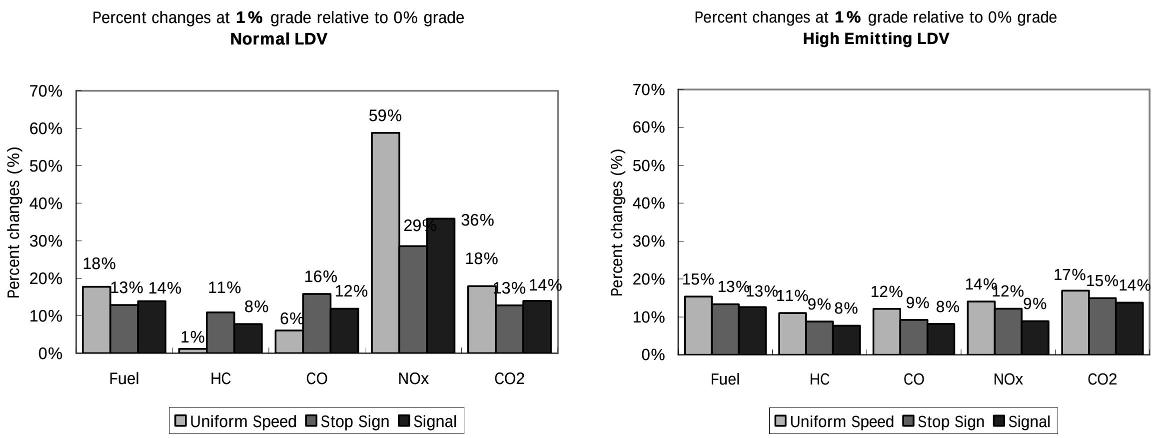

(b)

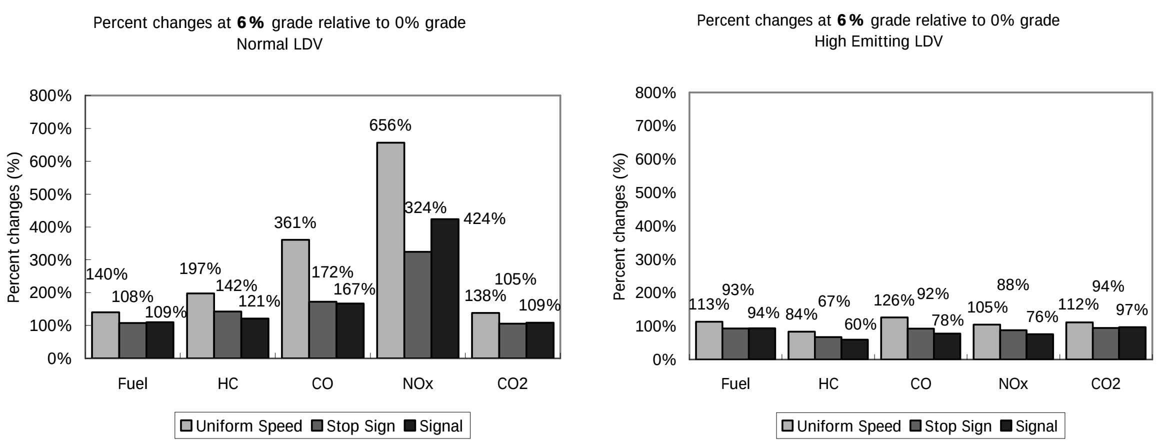

(c)

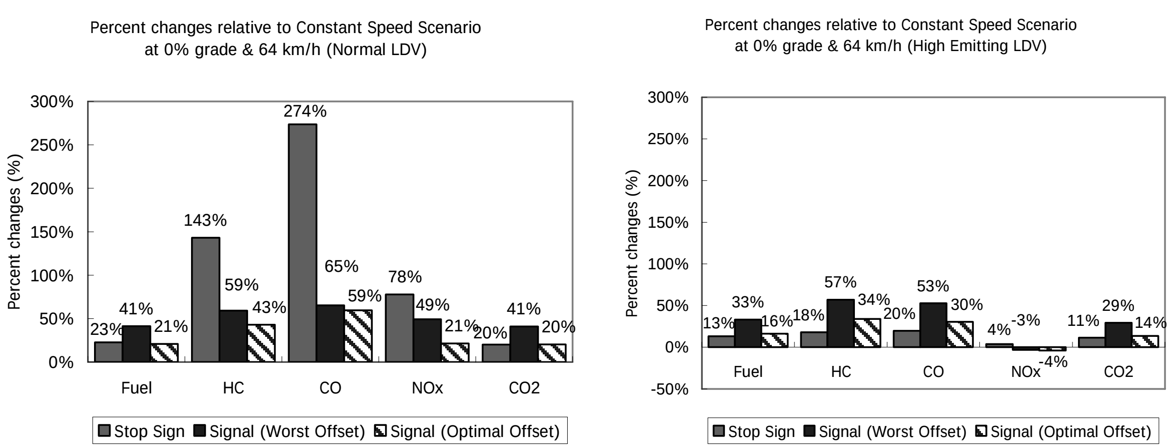

Figure 3-6: Comparison of MOE Scenarios (Percent Changes)

(a)

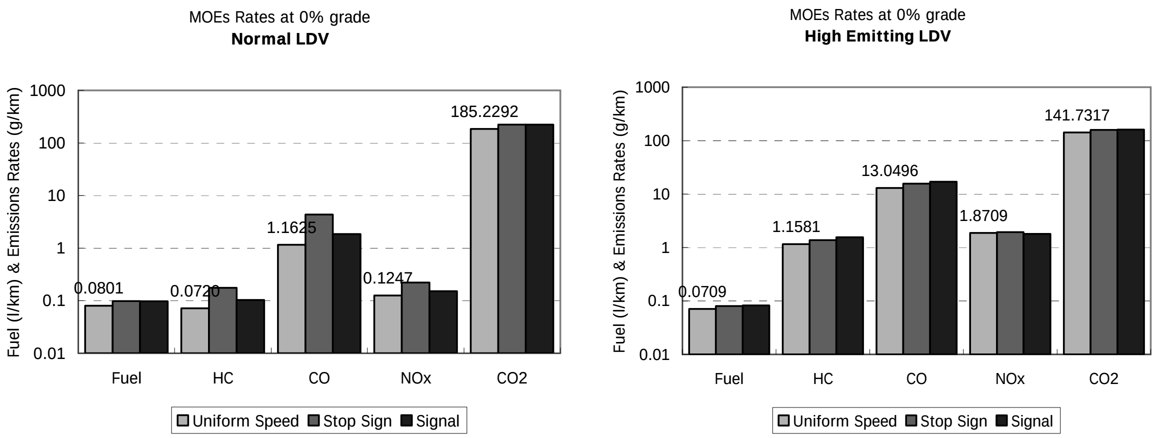

(b)

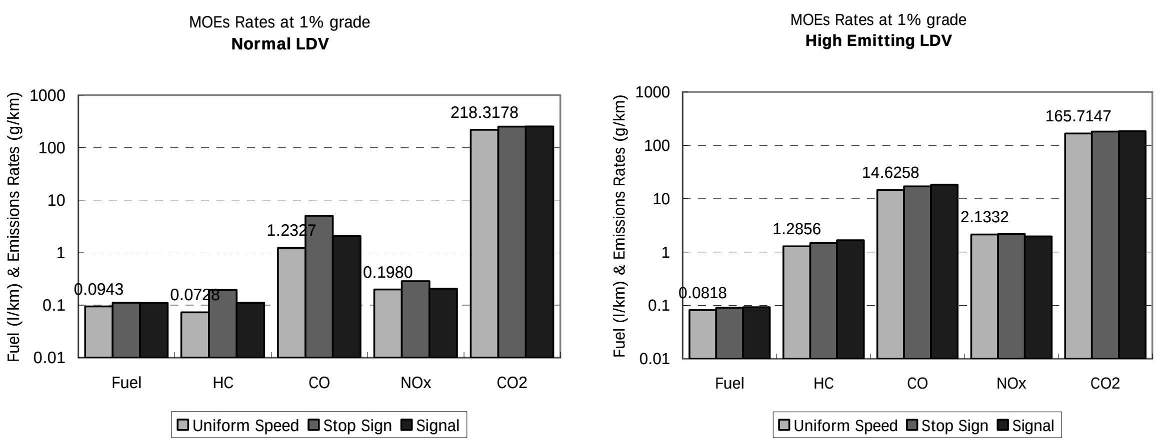

(c)

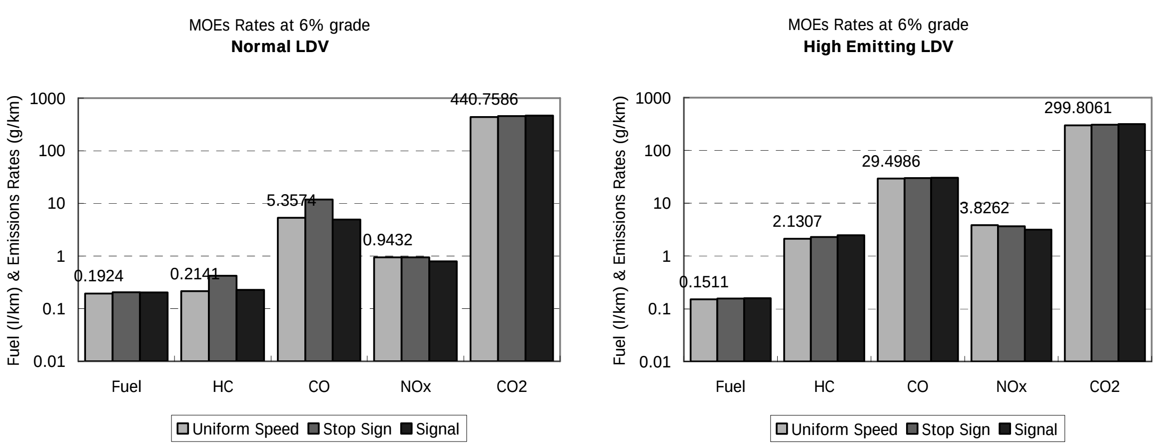

Figure 3-7: Comparison of Scenario Mass MOEs

(a)

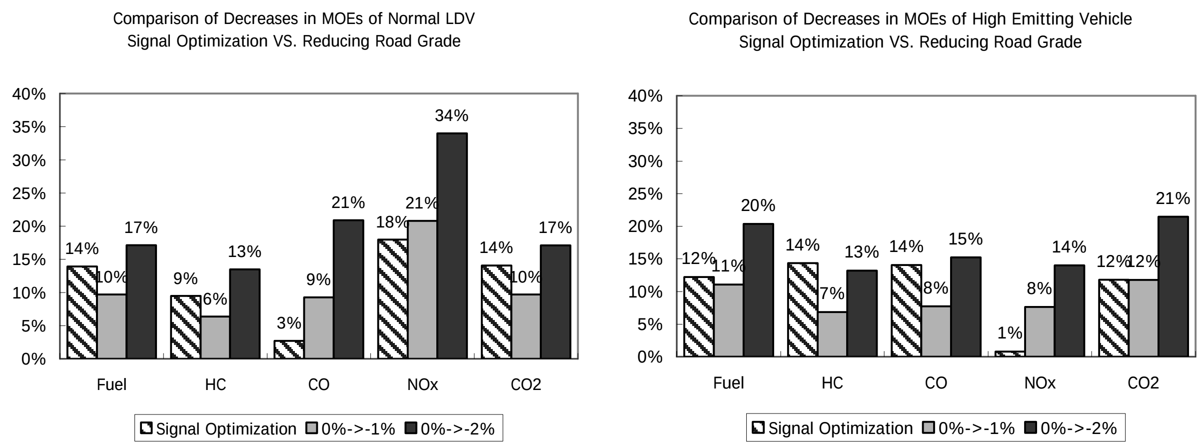

(b)

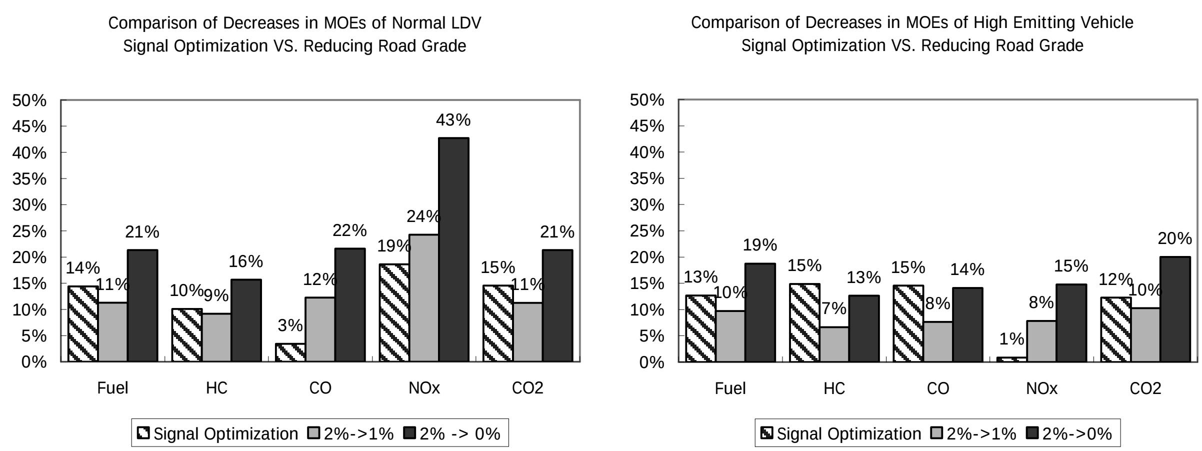

Figure 3-8: Comparison of Benefits Associated with a Reduction of Roadway Grades and Signal Optimization

3.7 Conclusions

The study quantified the impacts of roadway grades on vehicle fuel consumption and emission rates using the INTEGRATION software. Three types of traffic control scenarios were considered including cruising at a constant speed, traveling along a stop sign controlled arterial, and traveling through a network of traffic signals. The study clearly demonstrates that the impact of roadway grades on vehicle fuel consumption and exhaust emission rates should not be ignored while evaluating transportation investments. Specifically, from the uniform speed scenario to the signal control scenario, the impacts of roadway grades on fuel consumption and emission rates increases significantly even for a 1% increase in roadway grades. Specifically, the fuel consumption, HC, CO, NO_x, and CO_2 emissions for a Normal LDV increases by 148%, 1,020%, 2,051%, 682%, and 139%, respectively, for cruising conditions as a result of a 6% increase in roadway grade. When considering the stop sign control scenario, the MOEs for the Normal LDV increase by 111%, 207%, 338%, 364%, and 108%, respectively. In the case of the traffic signal control scenario, the MOEs for the Normal LDV increase by 109%, 121%, 168%, 424%, and 109%, respectively. Alternatively, the changes in MOEs for the HEV are higher in terms of absolute values, but are smaller, in terms of relative values, than those for the Normal LDV.

The study also demonstrated that by minimizing the commonly known performance index function (a weighted combination of vehicle stops and delays) in computing the optimum offset, the environmental impacts associated with the signal timings are also minimized.

Chapter 4: Screening High Emitting Vehicles

Hesham Rakha[1], Sangjun Park[2], and Linsey C. Marr[3]

4.1 Abstract

Remote Sensing Devices (RSDs) are used as supplementary tools for screening high emitting vehicles (HEVs) in the U.S. in order to achieve the National Ambient Air Quality Standards (NAAQS). However, tailpipe emissions in grams cannot be directly measured using RSDs because they are a concentration-based technique. Therefore, converting a concentration measurement to mass of emissions is needed. The research combines the carbon balance equation with fuel consumption estimates to make the conversion. In estimating vehicle fuel consumption rates, the VT-Micro model and a Vehicle Specific Power (VSP)-based model (the PERE model) are considered and compared. The results of the comparison demonstrate that the VSP-based model under-estimates fuel consumption at 79% and produces significant errors (R^2 = 45%), while the VT-Micro model produces a minimum systematic error of 1% and a high degree of correlation (R^2 = 87%) in estimating a sample vehicle's (1993 Honda Accord with a 2.4L engine) fuel consumption. The sample vehicle was correctly identified 100%, 97%, and 89% as a normal vehicle in terms of HC, CO, NO_X emissions, respectively, using its in-laboratory measured emissions. Its estimated emissions yielded 100%, 97%, and 88% of correct detection rates in terms of HC, CO, NO_X emissions, respectively. The study clearly demonstrates that the proposed procedure works well in converting concentration measurements to mass emissions and can be applicable in the screening of HEVs and normal emitting vehicles for several vehicle types such as sedans, station wagons, full-size vans, mini vans, pickup trucks, and SUVs.

Keywords: mobile source emissions, vehicle fuel consumption estimates, and high emitting vehicles.

4.2 Introduction

In an attempt to reduce air pollutant emissions to meet the National Ambient Air Quality Standards (NAAQS), many state environmental agencies are focusing their efforts on identifying high emitting vehicles (HEVs). HEVs are vehicles whose emissions of hydrocarbons (HCs), nitrogen oxides (NO_x) are two and/or carbon monoxide (CO) are three times higher than the national standards for new vehicles (EPA, 1999). Although HEVs comprise only a small fraction of the vehicle fleet, they contribute to a large fraction of total emissions. For example, one study found that 7.8 percent of the fleet is responsible for 50 percent of the total emissions (Lawson et al., 1990). Another study found that 5 percent of the vehicles emitted 80 percent of the emissions (Wolf et al., 1998).

Each of the states in the U.S. operates its own Inspection and Maintenance (I/M) Program, in order to identify and repair HEVs. In addition, other supplementary devices, such as RSDs (remote sensing devices), and OBD (On-Board Diagnostic) are used to identify HEVs. Several states are now using RSDs because they can collect on-road emission data from the in-use vehicle fleet. In contrast to traditional I/M tests that quantify emissions on a mass per time basis over a driving cycle that often lasts at least one minute. RSDs report mole fractions, or concentrations, of pollutants in exhaust at a single point in time. The advantage of RSDs is that they are able to capture measurements under real-world conditions as vehicles are driven on-road. However, several issues remain in screening HEVs and normal emitting

[1] Charles Via Jr. Department of Civil and Environmental Engineering, Virginia Tech, Blacksburg, VA. E-mail: rakha@vt.edu.

[2] Charles Via Jr. Department of Civil and Environmental Engineering, Virginia Tech, Blacksburg, VA. E-mail: Sangjun@vt.edu

[3] Charles Via Jr. Department of Civil and Environmental Engineering, Virginia Tech, Blacksburg, VA. E-mail: lmarr@vt.edu.

vehicles using RSDs, including the conversion from concentrations to mass emission rates and setting RSD-based standards to identify HEVs.

The objectives of this paper are to validate the use of RSD measurements to predict mass emission rates, to compare and contrast different methods for estimating fuel consumption rates, and to evaluate the accuracy with which RSDs can be used to screen HEVs using the proposed methods.

In terms of the paper layout, the paper first presents the validation of the procedure developed to estimate mass emissions. Secondly, the Physical Emission Rate Estimator (PERE) model that is based on vehicle specific power (VSP) and the VT-Micro model are compared, because these models can be used to estimate fuel consumption rates. The following section presents the estimation of mass emission and the comparison of emission estimates against field measurements. Subsequently, the proposed procedure is applied for screening HEVs and normal emitting vehicles. Finally, the conclusions of the study and recommendations for further research are presented.

4.3 Validation of Mass Emission Procedure

4.3.1 Conversion of Concentration Measurements to Mass Emissions

As measurement of emissions is the first step in managing vehicle exhaust, they play a very important role, since they are used in many air-quality improvement activities such as I/M programs and the development of emission models and inventories. Practically, two test methods are widely used in quantifying vehicle exhaust emissions: mass emission tests and concentration tests. Mass emission tests directly measure the mass of several pollutants emitted from a vehicle running a simulated driving cycle. In these tests, exhaust emissions are measured in units of grams per unit time or grams per unit distance. A group of tests that are named based on the underlying drive cycle fall into this category. The Federal Test Procedure (FTP) is one well known mass emission test. Others include the IM240, BAR31, IM93 (CT93), and IM147.

Concentration tests measure the pollutants in vehicle exhaust emissions and report results in units of percentage or parts per million (PPM) of total exhaust volume. Idle and ASM tests fall into this category and are used in I/M programs in several states. Additionally, RSDs measure the concentrations of emissions from on-road vehicles. RSDs are considered a supplemental tool for I/M programs, due to their ability to capture on-road emissions. Consequently, many states in the U.S. are trying to improve their I/M programs using RSDs. However, in order to estimate the actual emissions based on results from concentration tests, the relationship between concentrations and mass emission rates needs to be developed.

The literature describes two approaches for developing conversion equations. The first approach is based on regression models. For instance, Austin et al. (1989) proposed a new emission test procedure, the *Acceleration Simulation Mode* (ASM) test, that can correctly and economically identify 90% of vehicles that emit excessive nitrogen oxide (NO_x) emissions for I/M programs. In the study, they concluded that the ASM 5015 test is best for identifying high NO_X emitting vehicles and the 2500 rpm test could most correctly identify high CO and/or HC emitting vehicles. In addition, formulae were developed for the estimation of carbon monoxide (CO), hydrocarbon (HC), and nitrogen dioxide (NO_2) emissions using regression methods. In estimating CO and HC mass emissions, the concentration of CO and HC emissions are measured from the 2500 rpm test based on the engine size and used as the regressors for CO and HC mass emissions. And the engine displacement is also used as a regressor for CO and HC mass emissions. On the other hand, the NO_X mass emissions are regressed from the concentration of NO_X emissions measured by the ASM 5015 test and the emission test weight (vehicle weight plus 300 lbs for light duty vehicles) rather than the engine size. For another example, DeFries et al. (2002) constructed models for simulating Virginia IM240 emissions from concentration measurements taken from ASM 5015 and ASM 2525 test procedures, because Virginia must report emission reductions in terms of mass emissions to the EPA. In this project, the models for the conversion were constructed by utilizing full ASM tests, not fast pass ASM tests. First, raw emission concentration measurements are corrected in terms of dilution and humidity. Given that the corrected measurements, the intermediate predictor variables, HC, CO, and NO_X terms, are computed for the input variables. Finally, the IM240 mass emissions are regressed from HC, CO, NO_X terms, vehicle engine displacement, vehicle age, vehicle type, and carbureted-or-fuel injected vehicle. Specifically, HC term, NO_X term, engine displacement and vehicle age are used as regressors for IM240 HC emissions. The model for IM240 CO emissions includes CO term, engine displacement, and vehicle age as the input variables. Lastly, the model for IM240 NO_X emissions utilizes HC term, CO term, NO_X term, engine displacement, vehicle age, vehicle type, and carbureted-or-fuel injected vehicle.

The second approach is to use carbon balance for converting concentrations to mass emission rates per unit of fuel burned (NRC, 2001). For example, Stedman, who is the developer of the FEAT system (an RSD for on-road vehicle emissions), and his colleagues derived the equations for the conversions. At the time when they developed the first version of their RSD, they developed only one equation for CO emissions. This equation was then extended to HC and NO_x emissions when the system was updated to measure these pollutants (Bishop et al., 2003). In addition, Singer and Harley (1996) proposed a fuel-based methodology for computing motor vehicle emission inventories. In this study, the inventory was estimated as the product of mass-based emission factors with fuel consumption rates. In the process of calculating emission factors, the concentrations of on-road vehicle emissions are converted into mass emissions in units of grams of emissions per fuel consumed. Since the equation that they used is also based on carbon balance, it has the same structure as the equations that Stedman used. Specifically, mass emissions per fuel burned are computed by multiplying the number of moles for HC, CO, NO_X emissions per fuel burned and the molecular weight of HC, CO, and NO_X. In order to compute the number of moles for pollutant, the ratio of pollutant to the sum of CO_2, CO, and HC are multiplied to the number of moles for carbon per fuel burned.

4.3.2 Data Description

The study utilizes a dataset of second-by-second IM240 emission measurements that were taken by TESTCOM. As previously described, DeFries et el. (2002) constructed models for simulating Virginia IM240 emissions from ASM measurements. In the project, a dataset of 1702 paired ASM and IM240 emissions were utilized for the modeling purpose. The measurements were taken between September 2001 and April 2002. The vehicle model years ranged from 1981 to 2001, and body types included sedans, station wagons, full size vans, mini vans, pickup trucks, and sport utility vehicles.

A second-by-second IM240 emission test reports the vehicle's speed profile, HC, CO, and NO_x emission rates as a function of time, as illustrated in Figure 4-1. The tested vehicle in Figure 4-1 is a 1993 Honda Accord with a 2.4L engine.

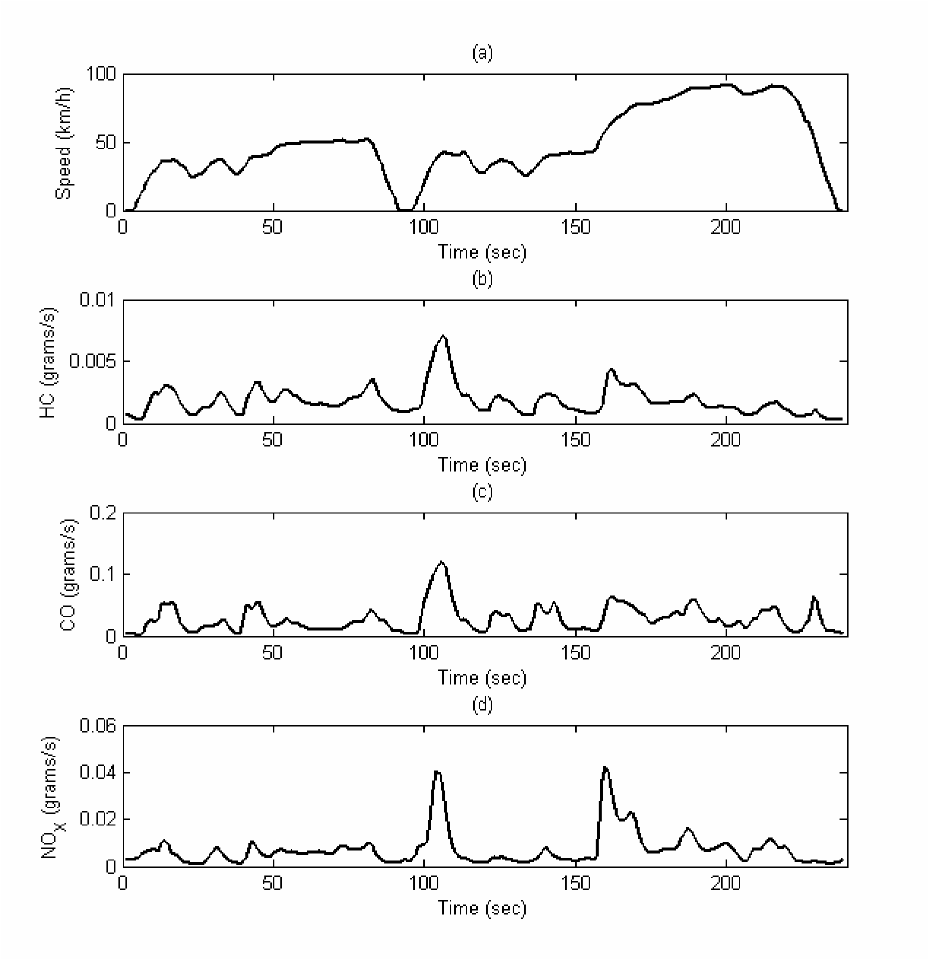

Figure 4-1: Second-by-Second IM240 emission test

4.3.3 Validation Procedure

The mass emission equations that are presented in the literature were validated by first applying them to calculate pollutant concentrations from mass emission rates measured during a sample IM240 test run. The calculated concentrations were then used together with fuel properties and the rate of fuel consumption to predict mass emission rates. Finally, predicted mass emission rates were compared to the original mass emission rates. The fuel consumption rate was computed using the carbon balance equation, and exhaust concentrations were estimated from the mass emissions using the combustion equation.

All that carbon enters the engine as fuel leaves in the form of HC (g/s), CO (g/s), CO_2 (g/s), and a typically negligible amount of particulate matter that will be ignored here. Given that the molecular weight of carbon and oxygen are 12 and 16 g/mole, respectively, the molecular weight of CO_2 can be calculated to be 44 g/mole (12+16x2). Therefore, CO_2 contains 27.3 percent (12/44) carbon. Similarly, the molecular weight of CO is 28 g/mole (12+16) and there is 42.9 percent carbon in CO. Also, according to the Code of Federal Regulations Title 40 Part 86 (40 CFR 86), HC emissions contain 86.6 percent carbon by weight. Consequently, the instantaneous carbon emission rate in units of g/s can computed as

$$C = 0.866\,HC + 0.429\,CO + 0.273\,CO_2\,. \qquad [1]$$

Recognizing that average gasoline sold in the US contains 86.4 percent of carbon, and has a density of 738.8 g/L (or 2800 g/gallon), there are 638.31 (0.864x738.8) grams of carbon in a liter of gasoline. Consequently, the fuel consumption rate (L/s) can be computed as

$$F = \frac{0.866\,HC + 0.429\,CO + 0.273\,CO_2}{638.31}. \quad [2]$$

Given that mass emissions of HC, CO, NO_x, and CO_2 were available for IM240 test runs, the emission concentrations were computed by first estimating the mass emissions of N_2 through the use of the combustion equation, which can be cast as

$$CH_{1.8} + 1.45\left(O_2 + 3.78N_2\right) \rightarrow CO_2 + 0.9H_2O + 5.48N_2, \quad [3]$$

where $CH_{1.8}$ represents gasoline; O_2 + 3.78 N_2 represents air composed of 20% O_2 and 79% N_2; combustion is assumed to be complete with an equivalence ratio of one; and formation of minor species such as NO and CO can be neglected relative to the amount of major species such as N_2 and CO_2 emitted in the exhaust.

Consequently, the mass ratio of N_2 to CO_2 can be computed as

$$\frac{5.48\,\text{mol N}_2}{1\ \text{mol CO}_2} \times \left(\frac{28\ \text{g N}_2}{\text{mol N}_2}\right) \times \left(\frac{\text{mol CO}_2}{44\ \text{g CO}_2}\right) = 3.49\frac{\text{g N}_2}{\text{g CO}_2}. \quad [4]$$

The N_2 emissions in g/s are then computed as

$$N_2 = 3.49 \times CO_2. \quad [5]$$

The volumetric concentrations of HC, CO, NO_x, and CO_2 can be computed as

$$\%HC = \frac{\frac{HC}{44}}{\frac{HC}{44} + \frac{CO}{28} + \frac{NO_x}{30} + \frac{CO_2}{44} + \frac{N_2}{28}} \times 100, \quad [6]$$

$$\%CO = \frac{\frac{CO}{28}}{\frac{HC}{44} + \frac{CO}{28} + \frac{NO_x}{30} + \frac{CO_2}{44} + \frac{N_2}{28}} \times 100, \quad [7]$$

$$\%NO_x = \frac{\frac{NO_x}{30}}{\frac{HC}{44} + \frac{CO}{28} + \frac{NO_x}{30} + \frac{CO_2}{44} + \frac{N_2}{28}} \times 100, \text{ and} \quad [8]$$

$$\%CO_2 = \frac{\frac{CO_2}{44}}{\frac{HC}{44} + \frac{CO}{28} + \frac{NO_x}{30} + \frac{CO_2}{44} + \frac{N_2}{28}} \times 100. \quad [9]$$

The estimated mass emissions of HC, CO, NO_x, and CO_2 (HC', CO', NO_x', and CO_2') are then computed as

$$HC' = 44 \times \frac{\%HC}{\%CO_2} \times \frac{0.864 \times 738.8 \times F}{12\left(1 + \frac{\%CO}{\%CO_2} + 6\frac{\%HC}{\%CO_2}\right)} \quad [10]$$

$$CO' = 28 \times \frac{\%CO}{\%CO_2} \times \frac{0.864 \times 738.8 \times F}{12\left(1 + \frac{\%CO}{\%CO_2} + 6\frac{\%HC}{\%CO_2}\right)} \quad [11]$$

$$NO_x' = 30 \times \frac{\%NO_x}{\%CO_2} \times \frac{0.864 \times 738.8 \times F}{12\left(1 + \frac{\%CO}{\%CO_2} + 6\frac{\%HC}{\%CO_2}\right)} \quad [12]$$

$$CO_2' = 44 \times \frac{0.864 \times 738.8 \times F}{12\left(1 + \frac{\%CO}{\%CO_2} + 6\frac{\%HC}{\%CO_2}\right)} \quad [13]$$

The mass emission estimates HC', CO', NO_x', and CO_2' for a sample vehicle (1993 Honda Accord equipped with a 2.4L engine) were found to be consistent with the field measurements, as clearly demonstrated in Figure 4-2. Specifically, the slope of the line ranges from 0.9988 to 0.9996 with an R^2 of 1.0 for all model estimates. This exercise demonstrates that the mass emission equations that are proposed are valid and thus can be used to estimate mass emissions.

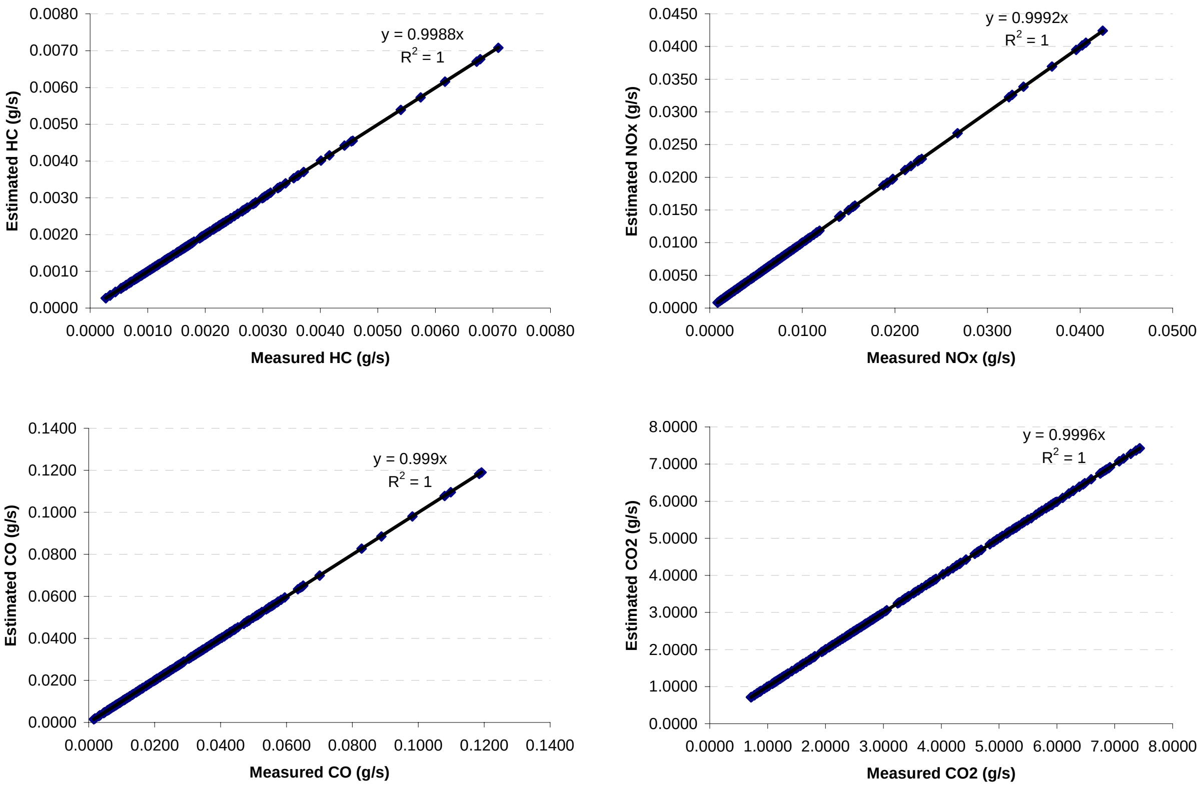

Figure 4-2: Model Validation Results

4.4 Estimation of Mass Emissions

4.4.1 Comparison of VSP and the VT-Micro Model Fuel Consumption Estimates

Having demonstrated the validity of the mass emission equations, it is clear that the accuracy of the mass emission estimates hinges on the accuracy of the fuel consumption rates that are used to compute the mass emissions. For purposes of this study we investigated two approaches for estimating a vehicle's instantaneous fuel consumption rate, namely: an approach based on the vehicle specific power (VSP) and the use of the VT-Micro model. Each of these approaches is described in some detail in this section.

VSP is a measure of engine load that has been proposed as a primary causal variable in emissions formation for modeling purposes and has been implemented in the Environmental Protection Agency's Physical Emission Rate Estimator (PERE). PERE is meant to supplement the data driven portion of MOVES and fill in gaps where necessary. The model is essentially an effort to simplify, improve, and implement the Comprehensive Modal Emissions Model (CMEM) developed at the University of California, Riverside. PERE is based on the premise that for a given vehicle, (engine out) running emissions formation is dependent on the amount of fuel consumed. As such, it models the vehicle fuel rate as well as CO_2 generation with some degree of accuracy. Being a physically based model, it has the potential (with some modification) to model new technologies (vehicles meeting new emissions standards), deterioration, off-road sources, I/M programs, as well as being able to easily extrapolate to areas where data are sparse.

The VSP approach to emissions characterization was developed by Jimenez-Palacios (1999). VSP is a measure of the road load on a vehicle; it is defined as the power per unit mass to overcome road grade, rolling, and aerodynamic resistance in addition to the inertial acceleration. VSP is computed as

$$VSP = v[a(1+\varepsilon) + gG + gC_r] + \frac{0.5\rho C_D A v^3}{m} \quad [14]$$

where v is vehicle speed (assuming no headwind) in m/s, a is the vehicle acceleration in m/s^2, ϵ is a mass factor accounting for the rotational masses (~4%), g is the acceleration due to gravity, G is the roadway grade, C_r is rolling resistance coefficient (~0.0135), C_D is aerodynamic drag coefficient, A is the frontal area, and m is vehicle mass in metric tones.

The equation can also have an added vehicle accessory loading term (air conditioner being the most significant) added to it. Moreover, higher order terms in rolling resistance can be added to increase the accuracy of the model (Gillespie, 1992). Using typical values for coefficients, in SI units the equation and assuming $C_D A/m$ ~ 0.0005, the equation can be written as

$$VSP(\text{kW/metric Ton}) = (1.04a + 9.81G + 0.132)v + 0.00121v^3 \quad [15]$$

The introduction of future technologies such as low rolling resistance tires and more aerodynamic forms can be reflected by adjusting the coefficients in the equation. It should be noted that the while it may be reasonable to assume typical values for rolling and aerodynamic resistance constants, it may pose a problem to assume a single mass for all cars (or vehicle types). There is approximately a factor of 2 difference in $C_D A/m$ between an empty compact car and a full large passenger car (J.L. Jimenez, 1999). Using a single value for all LDVs (for example) can result in a significant error (in VSP) at high speeds when the aerodynamic resistance term dominates and when feed gas emissions are relatively high.

The fuel rate in L/s can be computed as

$$F = \frac{\varphi\left[K(N) \times N(v) \times V_d + \dfrac{VSP \times m}{\eta} + \dfrac{P_{acc}(T,N)}{\eta}\right]}{LHV} \quad [16]$$

where φ is the fuel air equivalence ratio (mostly = 1), $K(N)$ is the power independent portion of engine friction (dependent on engine speed), $N(v)$ is the vehicle engine speed, V_d is the engine displacement volume, η is a measure of the engine efficiency (~0.4), $P_{acc}(T,N)$ is the power drag of accessories such as air conditioning (AC), which is a function of the ambient temperature and the humidity level. Without an AC it is some nominal value (~1 kW), and LHV is the factor lower heating value of fuel (~11.6 kJ/L).

The fuel rate is relatively insensitive to K; consequently VSP remains the primary driver of vehicle fuel consumption. The model of [16] represents the Physical Emission Rate Estimator (PERE), which is implemented within EPA's Multi-scale mOtor Vehicle and equipment Emission System (MOVES) (EPA, 2003). This model was used to estimate the fuel consumption for the same sample vehicle that was described earlier. The parameters of a 1993 Honda Accord were input to the model and the fuel consumption estimates were compared to the in-laboratory measurements over the entire IM240 drive cycle, as illustrated in Figure 4-3. The figure clearly demonstrates that the PERE model tends to under estimate the fuel consumption rate (slope of line 0.7862) and that the estimates also have a significant amount of noise (R^2 = 0.4569).

Using the fuel consumption rates that were estimated by the PERE model, the vehicle emissions were computed and compared to in-laboratory measurements, as demonstrated in Figure 4-4. As was the case with the fuel consumption estimates, the figure clearly demonstrates that the model tends to under-estimate vehicle emissions and has a significant amount of prediction error (R^2 ranges from a minimum of 32% to a maximum of 70%).

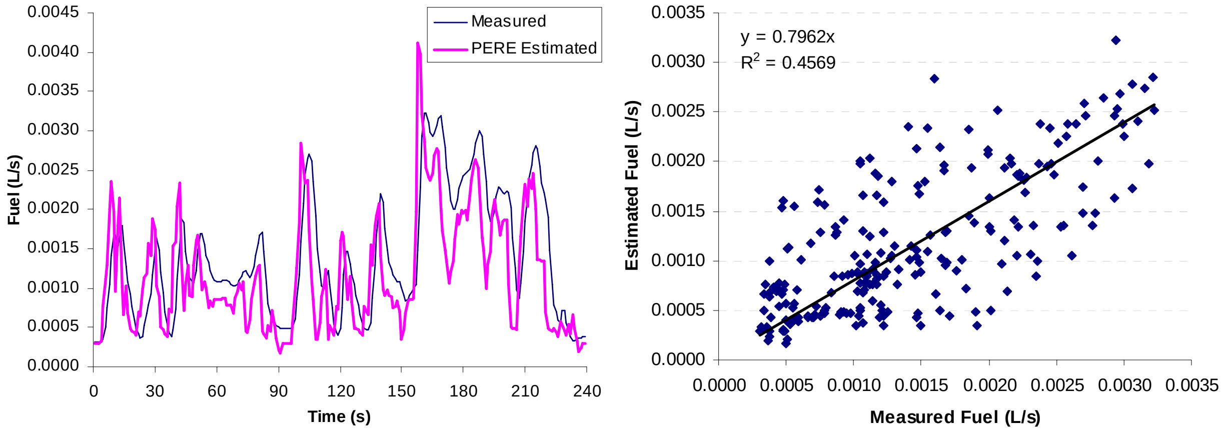

Figure 4-3: PERE Estimated vs. In-laboratory Measured Fuel Consumption Rates

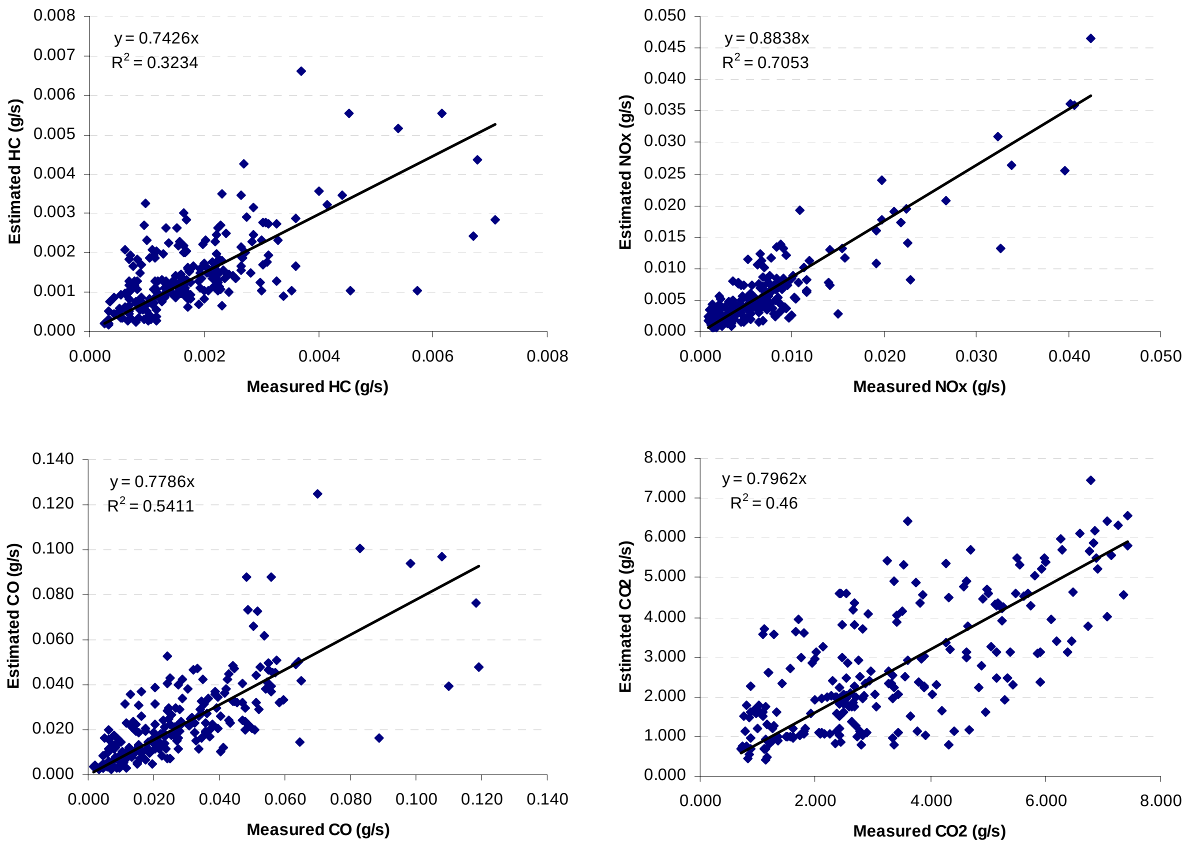

Figure 4-4: PERE Estimated vs. In-laboratory Measured Emission Rates

Given the relatively high prediction errors associated with PERE, the VT-Micro model was tested as an alternative tool for predicting the vehicle fuel consumption rate. The VT-Micro model, unlike the PERE model, is a statistical as opposed to a physical model. The model estimates vehicle fuel consumption and emission rates using a combination of speed and acceleration levels by means of a dual-regime model as

$$MOE_e = \begin{cases} e^{\sum_{i=0}^{3}\sum_{j=0}^{3} L_{i,j}^{e} \times u^i \times a^j} & \text{for a} \geq 0 \\ e^{\sum_{i=0}^{3}\sum_{j=0}^{3} M_{i,j}^{e} \times u^i \times a^j} & \text{for a} < 0 \end{cases}, \quad [17]$$

where $L^e_{i,j}$ and $M^e_{i,j}$ represent model regression coefficients for MOE e at speed exponent i and acceleration exponent j (Ahn et al., 2002; Rakha et al., 2004; Rakha et al., 2004). The model was developed using a sample of 101 light duty vehicles (LDVs). The data were gathered by EPA on a chassis dynamometer at the Automotive Testing Laboratories, Inc. (ATL), in Ohio and EPA's National Vehicle and Fuels Emission Laboratory (NVREL), in Ann Arbor, Michigan in the spring of 1997. All vehicles at ATL were drafted as a stratified random sample at Inspection and Maintenance lanes utilized by the State of Ohio. The vehicles tested at the EPA laboratory were recruited randomly. All vehicles were tested under as-received condition (without repairs). Of the total 101 vehicles 62 vehicles were tested at ATL and 39 vehicles were tested at NVREL. Of the 101 vehicles 96 vehicles had complete datasets. Furthermore, of these 96 vehicles 60 vehicles were classified as normal vehicles. These 60 normal vehicles were grouped into homogenous groups using a Classification and Regression Tree (CART) algorithm. The CART algorithm is a data-mining technique that uses a regression tree method that automatically searches for important patterns and relationships and quickly finds hidden structures in highly complex data. Tree structured classifiers or binary tree structured classifiers are built by repeating splits at active nodes. An active node is divided into two sub-nodes based on a split criterion and a split value. The splitting process is generally continued until (a) the number of observations in a child node has met a minimum population criteria or (b) a minimum deviance criteria at a node is met, where the deviance criteria D is defined as the Sum of Squared Error (SSE).

The CART algorithm was utilized to classify the 60 normal test vehicles into a number of categories that were similar in emission behavior. The dependent variable (Y) was a 60-by-4 matrix that included 4 dependent variables for 60 normal vehicles. The dependent variables included HC, CO, CO_2, and NO_x emissions averaged over 15 drive cycles. Similarly, the independent variable (X) was a 60-by-n matrix that included a number of vehicle attributes, including the vehicle model year, engine technology, engine size, and vehicle mileage. Alternatively, the X matrix can be thought of as a set of vectors X_k, each composed of 60 elements, where k is the vehicle attribute index under consideration in the CART algorithm.

The vehicles were classified into 5 LDV and 2 LDT categories, as demonstrated in Table 4-1. The Honda Accord vehicle would fit in categories LDV2, however LDV5 was selected for comparison purposes because the vehicle was closest to LDV5 in terms of fuel consumption.

Table 4-1: CART Algorithm Vehicle Classification (Rakha et al., 2004)

Vehicle Category	Number of Vehicles
Category for Light Duty Vehicles	
LDV1: Model Year < 1990	6
LDV2: 1990<=Model Year<1995, Engine Size < 3.2 liters, Mileage < 83653,	15
LDV3: Model Year >= 1995, Engine Size < 3.2 liters, Mileage < 83653,	8
LDV4: Model Year >=1990, Engine Size < 3.2 liters, Mileage >= 83653	8
LDV5: Model Year >=1990, Engine Size >= 3.2 liters	6
LDV High Emitters	24
Category for Light Duty Trucks	
LDT1: Model Year >= 1993	11
LDT2: Model Year < 1993	6
LDT High Emitters	12
Total Vehicles	96

The results of the analysis demonstrate a high degree of correlation between the estimated instantaneous fuel consumption rate and the measured rate, as demonstrated in Figure 4-5. It should be noted that a moving average (MA) of size 5 was used to smooth some of the peaks in the model estimates. The estimated VT-Micro model fuel consumption rates in conjunction with the emission concentrations were then utilized to estimate the vehicle emissions of HC, CO, NO_x, and CO_2. The results clearly demonstrate a minimum systematic error (slope of line close to 1) and a high degree of correlation (R^2 in excess of 90%).

Comparing Figure 4-3 to Figure 4-5, it appears that the VT-Micro model framework provides better estimates of vehicle fuel consumption rates and thus the vehicle emission estimates based on the fuel consumption rates and carbon balance equation are more accurate. Consequently, the VT-Micro model fuel consumption estimates were utilized for the remainder of the analysis.

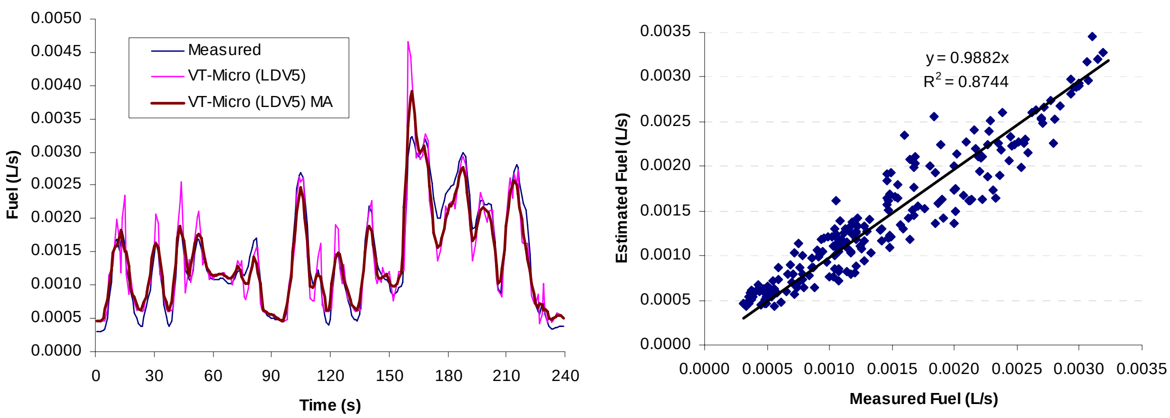

Figure 4-5: VT-Micro Estimated vs. In-laboratory Measured Fuel Consumption Rates

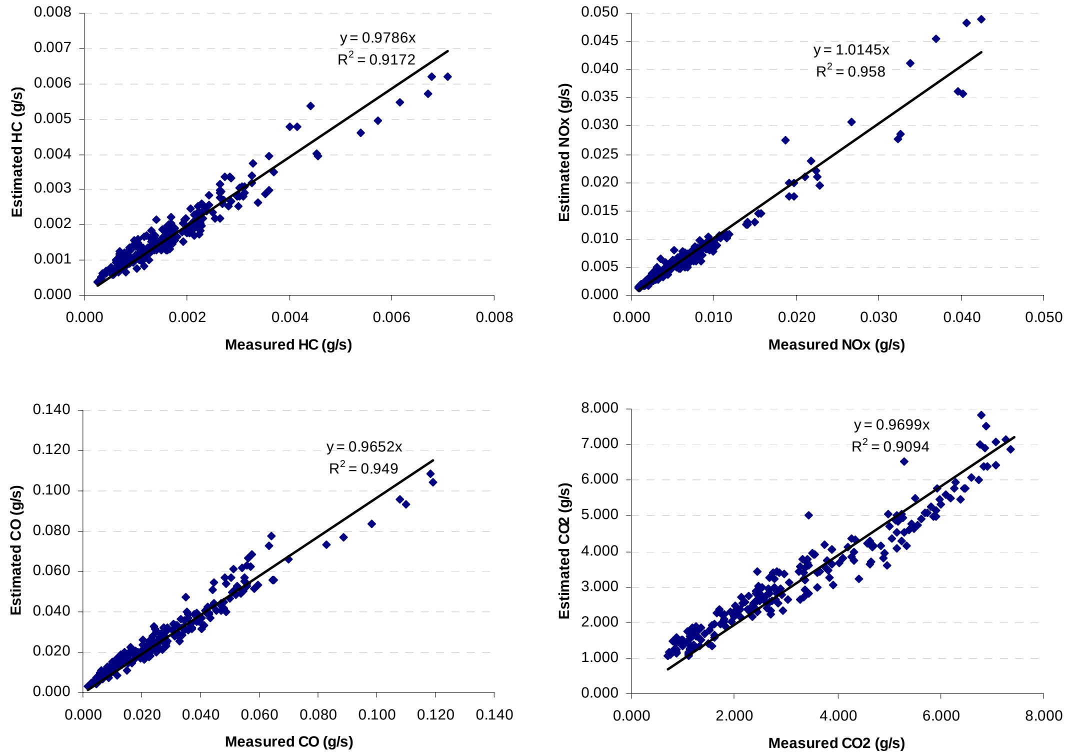

Figure 4-6: VT-Micro Estimated vs. In-laboratory Measured Emission Rates

4.4.2 Different Vehicle Type Analysis

As was demonstrated in the previous section, the VT-Micro approach provided reliable estimates of vehicle fuel consumption and mass emission estimates for the sample Honda vehicle. This section expands the analysis by considering different vehicle types including station wagons, full size vans, mini vans, pickup trucks, and sport utility vehicles, as summarized in Table 4-2.

The classification of the sample vehicles was achieved using two methods. The first method involved selecting the vehicle category based on the vehicle parameters and matching these parameters with the CART classifications that were demonstrated earlier in Table 4-1. The second approach categorized vehicles based on their fuel consumption rates by comparing each sample vehicle to the VT-Micro model vehicle classifications in terms of fuel consumption rates using the IM240 test cycle. The second approach was utilized because it provided better results in terms of systematic errors and degree of correlation.

Table 4-2: Specification of Tested Vehicles

Make	Model	Model Year	ETW (lb)	Odometer (mi)	Tr.	Engine Size	Vehicle Type	Cylinder
Ford	Escort	1993	2750	111,471	A	1.9	Station wagon	4
Ford	E150 Econoline	1988	4000	169,231	A	5	Full size	8
Mazda	MPV	1991	4000	124,733	A	3	Minivan	6
Geo	Tracker	1991	2750	5,014	M	1.6	Pickup	4
Ford	Explorer 2-DR.	1993	4500	127,928	A	4	SUV	6

Using the second-by-second IM240 emission measurements for the five sample vehicles a comparison of the VT-Micro and PERE estimates was conducted, as summarized in Table 4-3. The results summarize the slope and R^2 of the regression line for each of the vehicle types. The results of the analysis demonstrate that, in general, the VT-Micro model provides more reliable estimates of vehicle fuel consumption and emission rates, with lower systematic errors and higher degrees of correlation. As can be seen in Table 4-3, the slope of the regression line ranges from 0.73 to 1.60 and 0.67 to 1.58 for the VT-Micro and PERE models, respectively. Alternatively, the R^2 ranges from 0.51 to 0.99 and 0.00 to 0.94, for the VT-Micro and PERE models, respectively. Consequently, the proposed method utilizing the VT-Micro fuel consumption estimates is recommended for estimating mass vehicle emissions.

Table 4-3: Slope and R^2 of Trend Line

	Vehicle Type	VT-Micro Model					VSP				
		HC	CO	NO_X	CO_2	Fuel	HC	CO	NO_X	CO_2	Fuel
Slope	Station Wagon	1.02	0.96	1.05	0.97	0.99	1.02	0.84	1.20	0.91	0.90
	Full Size Van	0.81	0.81	0.99	0.82	0.83	1.01	0.98	1.47	1.03	1.02
	Mini Van	0.85	0.86	0.85	0.86	0.87	0.85	0.94	0.92	0.90	0.90
	Pickup Truck	1.28	1.16	1.60	1.13	1.15	1.07	0.67	1.58	0.81	0.81
	SUV	0.78	0.83	0.73	0.75	0.76	0.89	0.93	0.80	0.85	0.85
R^2	Station Wagon	0.51	0.84	0.89	0.86	0.86	0.00	0.17	0.59	0.28	0.26
	Full Size Van	0.94	0.99	0.88	0.81	0.77	0.66	0.94	0.57	0.04	0.12
	Mini Van	0.97	0.98	0.98	0.95	0.92	0.63	0.71	0.79	0.51	0.51
	Pickup Truck	0.91	0.96	0.88	0.76	0.65	0.62	0.67	0.60	0.24	0.26
	SUV	0.94	0.93	0.96	0.82	0.62	0.64	0.60	0.76	0.23	0.23

4.5 Screening High Emitting Vehicles

In this section, the proposed method is applied for the screening of high emitting vehicles. Unfortunately, HEV emission thresholds for a single point in time in units of grams per second as a function of vehicle speed and acceleration levels are not available in the literature. Consequently, as part of this research effort second-by-second HEV thresholds are derived for the screening of HEVs. Using the proposed thresholds the efficiency of HEV screening is evaluated using the proposed approach.

4.5.1 Emission Standards for High Emitting Vehicles

Quantitative criteria, or cut points, based on measured emission rates are desired to identify high emitting vehicles. The EPA (1999) recommends a cutoff that is two times the emission standard for HC and NO_X emissions and three times the standard for CO emissions. These thresholds are developed for an entire cycle as opposed to second-by-second data. In addition, given that vehicle base emission rates differ from one vehicle to another, scaling factors are computed from the entire trip as

$$\text{Scale Factor} = \frac{\text{IM240 Standard}}{\text{LDV's IM240 Emissions}}. \qquad [18]$$

The second-by-second cut points are then computed as

$$\text{Cutpoint} = \text{Scale Factor} \times \text{LDV Emission Rate}. \qquad [19]$$

In computing the emission cut points, the IM240 emissions for the VT-Micro normal emitting vehicle classes are computed as the ratio of vehicle emission rates (Table 4-4) to the HEV thresholds (Table 4-5) to compute vehicle-class specific scale factors using Equation [18], as summarized in Table 4-6. The results of Table 4-6 clearly demonstrate that apart from LDV1, the required scale factors are much higher that what is recommended in the literature.

Table 4-4: IM240 Emissions for Normal Emitting LDVs and LDTs using VT-Micro Model (grams/mile)

Category	HC	CO	NO_x
LDV 1	0.321	4.878	0.880
LDV 2	0.084	1.794	0.480
LDV 3	0.031	0.690	0.176
LDV 4	0.255	4.470	0.510
LDV 5	0.180	4.422	0.991
LDT 1	0.109	2.365	0.510
LDT 2	0.222	6.099	0.920

Table 4-5: IM240 Composite Emission Standards for LDVs and LDTs (grams/mile) (EPA, 1996)

Category	Model Year	HC	CO	NO_x
LDV	1996+	0.6	10	1.5
	1983-1995	0.8	15	2
LDT (GVWR<6000)	1996+			
	(<= 3750)	0.6	10	1.5
	(>3750)	0.8	13	1.8
	1988-1995	1.6	40	2.5

Table 4-6: Vehicle Specific HEV Scale Factors

Category	HC	CO	NO_X
LDV 1	2.49	3.07	2.27
LDV 2	9.49	8.36	4.17
LDV 3	25.98	21.74	11.39
LDV 4	3.13	3.36	3.92
LDV 5	4.45	3.39	2.02
LDT 1	14.64	16.91	4.90
LDT 2	7.20	6.56	2.72

4.5.2 Screening High Emitting Vehicles

Having computed the HEV cut points, the next step was to validate the proposed procedure using the carbon balance equation in conjunction with the VT-Micro fuel consumption estimates for the screening of HEVs. Because an IM240 test includes second-by-second emission rates for HC, CO, and NO_X over 240 seconds (239 measurements), 239 tests are conducted. Using the proposed procedures for estimating mass emissions from emission concentrations, the estimated mass emissions are compared against the proposed HEV cut points and the percentage of observations that are below the HEV thresholds are recorded. The objective of this exercise is to quantify efficiency of the proposed procedure in the screening of HEVs.

Figure 4-7 shows emission measurements and estimates for the Honda Accord sample vehicle that were presented earlier (Honda Accord, MY 1993, 2.4L engine) along with the proposed cut points. The sample vehicle is classified as a normal vehicle because it emits 0.22 g/mi of HC, 3.36 g/mi of CO, and 0.86 g/mi of NO_X over the entire IM240 test, which is less than the thresholds identified in Table 4-5. Consequently, it is anticipated that most of the second-by-second emission measurements will not exceed the proposed cut points. As can be seen in Figure 4-7, most emission measurements and estimates do not exceed the HEV cut points. However, there are few measurements and estimates that do exceed the cut points, which means that if a remote sensing test happened to catch this vehicle during these measurements, the vehicle would be erroneously identified as an HEV.

In validating the proposed method for screening HEVs, the percentage of correct identifications using the proposed approach are compared to direct measurement comparisons, as summarized in Table 4-7. The results are very encouraging demonstrating the use of the proposed procedure does not degrade the performance of the HEV screening procedure. For example, the Honda Accord (sedan) was correctly identified 100%, 97%, and 89% of the time as a normal emitting vehicle using in-laboratory measured emissions for HC, CO, NO_X emissions, respectively. Alternatively, 100%, 97%, and 88% of the observations were correctly identified as normal in terms of HC, CO, NO_X emissions using the estimated emissions based on the proposed approach. These results demonstrate the validity of the proposed approach. The results of identification for other vehicle types that were described earlier in Table 4-2 are also shown in Table 4-7. As can be seen in Table 4-7, the correct identification of normal emitting vehicles is consistent with in-laboratory measured emissions. Therefore, it is clearly demonstrated that the proposed methods can be applicable for the screening HEVs and normal emitting vehicles.

Table 4-7: Correct Detection Rates of both Measured and Estimated Emissions

Category	HC		CO		NO_X	
	Measured	Estimated	Measured	Estimated	Measured	Estimated
Sedan	100%	100%	97%	97%	89%	88%
Station Wagon	96%	93%	92%	90%	72%	70%
Fullsize	94%	97%	97%	98%	73%	76%
Minivan	100%	100%	100%	100%	88%	91%
Pickup	98%	98%	99%	99%	97%	96%
SUV	100%	100%	99%	99%	68%	82%

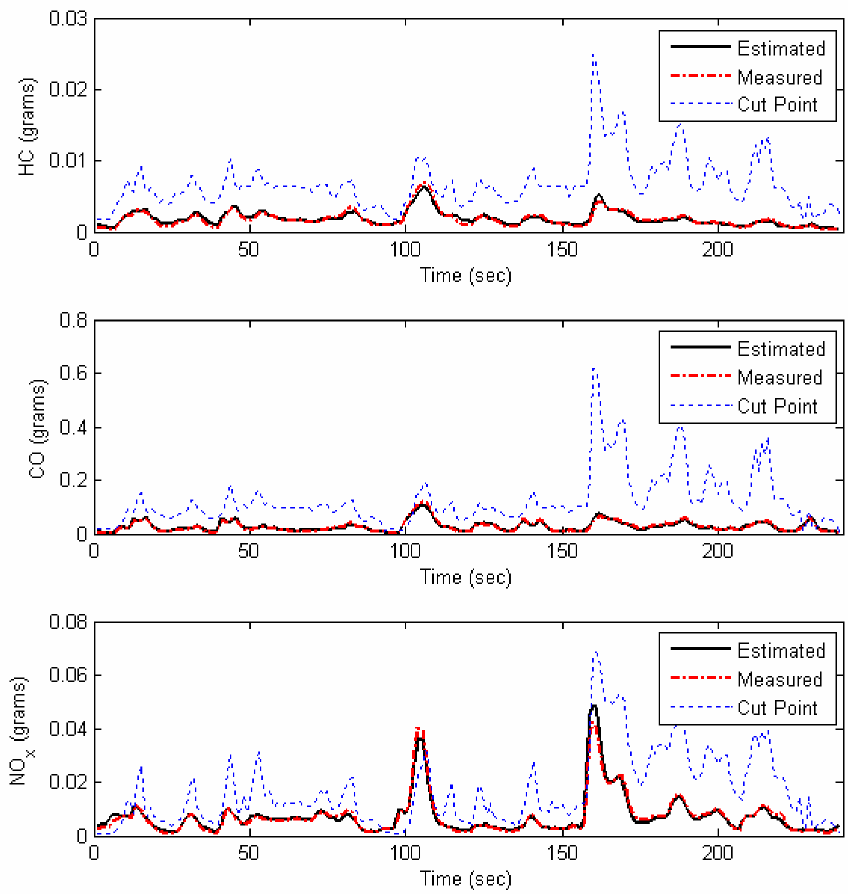

Figure 4-7: In-Laboratory Measured IM240 Emission and Estimated Emission

4.6 Conclusions

The study presents a new approach for estimating vehicle mass emissions from concentration emission measurements using the carbon balance equation in conjunction with the VT-Micro fuel consumption framework. The study demonstrates that the proposed approach produces reliable mass emission estimates for different vehicle types including sedans, station wagons, full size vans, mini vans, pickup trucks, and SUVs. The study also demonstrates that the VT-Micro fuel consumption estimates are more reliable than VSP-based fuel consumption estimates. The study demonstrates that the proposed procedure can be used to enhance current state-of-the-art HEV screening procedures using RSD technology.

As is the case with any research effort, this study demonstrates the need for further research to identify the engine load conditions that provide optimum HEV screening. Any screening procedure can produce erroneous vehicle screening depending on the vehicle speed and acceleration levels. Consequently, further research is required to identify the engine loads that are required to minimize false alarms (erroneous identification of normal vehicles as HEVs) and detection errors (erroneous identification of an HEV as a normal vehicle).

4.7 Acknowledgements

The authors are greatly indebted to the financial support provided by the Virginia Department of Environmental Quality and the ITS Implementation Center to conduct the research presented in this paper. In addition, the authors acknowledge the input received by Richard Olin of the Virginia DEQ in conducting the proposed research.

Chapter 5: Conclusions and Recommendations for Further Research

5.1 Conclusions

This thesis quantified the environmental impacts of roadway grades and proposed a new approach for estimating vehicle mass emissions that can be used to enhance current state-of-the-art HEV screening procedures using RSD technology. In conducting the analysis, the INTEGRATION and the VT-Micro fuel consumption and emission models were used in the context of traffic simulation, energy consumption, and mobile-source emission estimation. Through the analysis, it was clearly demonstrated that the environmental impacts induced due to the changes in the factors that affect transportation energy consumption and emission, such as travel-related factors, driver-related factors, highway network characteristics, and vehicle characteristics, can be quantified within a microscopic modeling tool. In addition, it was shown that the VT-Micro framework can be used to enhance HEV screening procedures since the energy consumption and emission models for several different vehicle types, including high emitting vehicles, are included in the VT-Micro model. The following sections describe the conclusions in some detail.

5.1.1 Environmental Impacts of roadway grades

The study quantified the impacts of roadway grades on vehicle fuel consumption and emission rates using the INTEGRATION software. Three types of traffic control scenarios were considered including cruising at a constant speed, traveling along a stop sign controlled arterial, and traveling through a network of traffic signals. The study clearly demonstrated that the impact of roadway grades on vehicle fuel consumption and exhaust emission rates should not be ignored while evaluating transportation investments. Specifically, from the uniform speed scenario to the signal control scenario, the impacts of roadway grades on fuel consumption and emission rates increases significantly even for a 1% increase in roadway grades. The fuel consumption, HC, CO, NO_x, and CO_2 emissions for a Normal LDV increases by 148%, 1,020%, 2,051%, 682%, and 139%, respectively, for cruising conditions as a result of a 6% increase in roadway grade. When considering the stop sign control scenario, the MOEs for the Normal LDV increase by 111%, 207%, 338%, 364%, and 108%, respectively. In the case of the traffic signal control scenario, the MOEs for the Normal LDV increase by 109%, 121%, 168%, 424%, and 109%, respectively. Alternatively, the changes in MOEs for the HEV are higher in terms of absolute values, but are smaller, in terms of relative values, than those for the Normal LDV.

The study also demonstrated that by minimizing the commonly known performance index function (a weighted combination of vehicle stops and delays) in computing the optimum offset, the environmental impacts associated with the signal timings are also minimized.

5.1.2 Screening High Emitting Vehicles

The study presented a new approach for estimating vehicle mass emissions from concentration emission measurements using the carbon balance equation in conjunction with the VT-Micro fuel consumption framework. The study demonstrated that the proposed approach produces reliable mass emission estimates for different vehicle types including sedans, station wagons, full-size vans, mini vans, pickup trucks, and SUVs. The study also demonstrated that the VT-Micro fuel consumption estimates are more reliable than VSP-based fuel consumption estimates. The study demonstrated that the proposed procedure can be used to enhance current state-of-the-art HEV screening procedures using RSD technology.

As is the case with any research effort, this study demonstrated the need for further research to identify the engine load conditions that provide optimum HEV screening. Any screening procedure can produce erroneous vehicle screening depending on the vehicle speed and acceleration levels. Consequently, further research is required to identify the engine loads that are needed to minimize false alarms (erroneous identification of normal vehicles as HEVs) and detection errors (erroneous identification of an HEV as a normal vehicle).

5. 2 Recommendations

Since high emitting vehicles contribute to a large portion of the total mobile-source emissions, even though they comprise only a small portion of the vehicle fleet, much research efforts are focused on accessing the HEVs' impacts and identifying them. From this point of view, further research efforts will be focused on quantifying the impacts of HEVs in network-wide levels and identifying the engine load conditions that result in high HEVs emissions.

First, further research efforts will be placed on quantifying the impacts of high emitting vehicles. Although some studies have demonstrated that HEVs are responsible for a large amount of total emissions, their conclusions were based on spot measurements. Consequently, there is a need to investigate the network-wide impacts of HEVs on the environment.

Second, it is recommended to analyze the engine load conditions that result in high HEV emissions. As can be seen in screening high emitting vehicles, there can happen to be some erroneous detections that identify normal vehicles as HEVs under specific vehicle speed and acceleration levels. This means that emission measurements should not be taken under those engine load conditions and should be taken under the conditions that result in high emissions for HEVs rather than normal vehicles.

Bibliography

Ahn, K., H. Rakha, et al. (2004). "Microframework for modeling of high-emitting vehicles." Transportation Research Record. n 1880 2004: 39-49.

Ahn, K., H. Rakha, et al. (2002). "Estimating vehicle fuel consumption and emissions based on instantaneous speed and acceleration levels." Journal of Transportation Engineering 128(2): 182-190.

An, F. and M. Ross (1993). Model of fuel economy and driving patterns. International Congress and Exposition, Detroit, MI, USA, Future Fuels and Emission Systems SAE Special Publications. Publ by SAE, Warrendale, PA, USA. n 949 1993.

An, F. and M. Ross (1993). Model of Fuel Economy with applications to Driving Cycles & Traffic Management. Presented at 72nd Annual Meeting of the Transportation Research Board, Washington, D.C.

Austin, T. C. and L. Sherwood (1989). "Development of Improved Loaded-Mode Test Procedures for Inspection and Maintenance Programs." SAE Technical Paper 891120.

Baker, M. (1994). Fuel Consumption and Emission Models for Evaluating Traffic Control and Route Guidance Strategies. Kingston, Ontario, Canada, Queen's University.

Bishop, G. A., D. A. Burgard, et al. (2003). "On-Road Remote Sensing of Automobile Emissions in the La Brea Area: Year 3, October 2003." Prepared for: Coordinating Research Council, Inc. Contract No. E-23-4.

DeFries, T. H., B. Limsakul, et al. (2002). "Models for Estimating Virginia IM240 Emissions from ASM Measurements." Report prepared for the Virginia Department of Environmental Quality.

Enns, P., J. German, et al. (1993). EPA's Survey of In-Use Driving Patterns: Implications for Mobile Source Emission Inventories, Office of Mobile Sources, US EPA.

EPA (1994). Milestones in Auto Emissions Control. Ann Arbor, Michigan.

EPA (1996). "High-Tech I/M Test Procedures, Emission Standard, Quality Control Requirements, and Equipment Specifications: IM240 and Functional Evaporative Systems Tests, Revised Technical Guidance (Draft)."

EPA (1999). "MOBILE6 Inspection/Maintenance Benefits Methodology for 1981 through 1993 Model Year Light Vehicles (Draft)."

EPA (2001). National Air Quality and Emissions Trends Report, 1999. Research Triangle Park, NC.

EPA (2002). "OBD: Frequently Asked Questions." Office of Transportation and Air Quality, EPA420-F-02-014.

EPA (2003). "Major Elements of Operating I/M Programs." Office of Transportation and Air Quality, EPA420-B-03-012.

EPA (2003). Proof of Concept Investigation for the Physical Emission Rate Estimator (PERE) to be Used in MOVES (EPA420-R-03-005). Ann Arbor, Michigan.

Gillespie, T. (1992). "Fundamentals of Vehicle Dynamics." Society of Automotive Engineers.

Haskew, H. and J. Gumbleton (1988). "International Fuels and Lubricants Meeting and Exposition." SAE Technical Paper 881682, Society of Automotive Engineers, Warrendale, PA.

J.L. Jimenez, P. M., G.J. McRae, D.D. Nelson and M.S. Zahniser (1999). "Vehicle Specific Power: A Useful Parameter for Remote Sensing and Emission Studies." Proceedings of the 9th CRC On-Road Vehicle Emissions Workshop, San Diego CA.

Lawson, D., P. Groblichki, et al. (1990). "Emissions from In-Use Motor Vehicles in Los Angeles: A Pilot Study of Remote Sensing and the Inspection and Maintenance Program." Journal of Air and Waste Management Vol. 40: 1096-1105.

M. Van Aerde & Assoc., L. (2002). INTEGRATION release 2.30 for windows: user's guide - volume I: fundamental features.

M. Van Aerde & Assoc., L. (2002). "INTEGRATION release 2.30 for windows: user's guide - volume II: advanced features."

McClintock, P. (1999). "Remote Sensing Measurements of Real World High Exhaust Emitters." CRC Project No. E-23-Interim Report, Prepared for the Coordinating Research Council.
Murrell, J. D. (1980). Passenger Car Fuel Economy: EPA and Road, EPA 460/3-80-010
Environmental Protection Agency, Ann Arbor, Michigan, September.
National Research Council (2001). Evaluating Vehicle Emissions Inspection and Maintenance Programs, National Academy Press, Washington DC.
National Research Council (U.S.). Transportation Research Board. Committee for Study of Impacts of Highway Capacity Improvements on Air Quality and Energy Consumption. (1995). Expanding metropolitan highways : implications for air quality and energy use. Washington, D.C., Transportation Research Board National Research Council.
NRC (2001). Evaluating Vehicle Emissions Inspection and Maintenance Programs, National Academy Press, Washington DC.
Pierson, W. R., A. W. Gertler, et al. (1994). Summary of recent tunnel studies in the Fort McHenry and Tuscarora Mountain tunnels. Forth CRC On-Road Vehicle Emissions Workshop, San Diego.
Rakha, H. and K. Ahn (2004). "Integration modeling framework for estimating mobile source emissions." Journal of Transportation Engineering 130(2): 183-193.
Rakha, H., K. Ahn, et al. (2003). "Comparison of MOBILE5a, MOBILE6, VT-MICRO, and CMEM models for estimating hot-stabilized light-duty gasoline vehicle emissions." Canadian Journal of Civil Engineering 30(6): 1010-1021.
Rakha, H., K. Ahn, et al. (2004). "Development of VT-Micro model for estimating hot stabilized light duty vehicle and truck emissions." Transportation Research, Part D: Transport & Environment 9(1): 49-74.
Rakha, H. and B. Crowther (2002). "Comparison of Greenshields, Pipes, and Van Aerde car-following and traffic stream models." Transportation Research Record. n 1802 2002: 248-262 02-2143.
Rakha, H. and Y. Ding (2003). "Impact of stops on vehicle fuel consumption and emissions." Journal of Transportation Engineering 129(1): 23-32.
Rakha, H. and I. Lucic (2002). "Variable power vehicle dynamics model for estimating maximum truck acceleration levels." Journal of Transportation Engineering 128(5): 412-419.
Rakha, H., I. Lucic, et al. (2001). "Vehicle dynamics model for predicting maximum truck acceleration levels." Journal of Transportation Engineering 127(5): 418-425.
Rakha, H., A. Medina, et al. (2000). "Traffic signal coordination across jurisdictional boundaries: Field evaluation of efficiency, energy, environmental, and safety impacts." Transportation Research Record. n 1727 2000: 42-51 00-1560.
Rakha, H., P. Pasumarthy, et al. (2004). Modeling longitudinal vehicle motion: issues and proposed solutions. Transport Science and Technology Congress, Athens, Greece.
Rakha, H., M. Snare, et al. (2004). "Vehicle dynamics model for estimating maximum light-duty vehicle acceleration levels." Transportation Research Record. n 1883 2004: 40-49.
Rakha, H., M. Van Aerde, et al. (1998). "Construction and calibration of a large-scale microsimulation model of the Salt Lake area." Transportation Research Record(1644): 93-102.
Rakha, H. A. and M. W. Van Aerde (1996). "Comparison of simulation modules of TRANSYT and integration models." Transportation Research Record(1566): 1-7.
Singer, B. C. and R. A. Harley (1996). "Fuel-based motor vehicle emission inventory." Journal of the Air & Waste Management Association 46(6): 581-593.
Stedman, D. (1989). "Automobile Carbon Monoxide Emission." Environmental Science & technology Vol. 23, No. 2: 147-149.
U.S. DOT (1991). "Intermodal Surface Transportation Efficiency Act of 1991 - Summary."
Van Aerde, M., B. Hellinga, et al. (1996). INTEGRATION: an overview of traffic simulation features. 75th Transportation Research Board Annual Meeting, Washington, DC.
Van Aerde, M. and S. Yagar (1988). "Dynamic integrated freeway/traffic signal networks: a routing-based modeling approach." Transportation Research 22A(6): 445-453.
Van Aerde, M. and S. Yagar (1988). "Dynamic integrated freeway/traffic signal networks: problems and proposed solutions." Transportation Research 22A(6): 435-443.

Wayne, L. and Y. Horie (1983). "Evaluation of CARB's In-Use Vehicle Surveillance Program." CARB Contact No. A2-043-32, Prepared by Pacific Environmental Services, Inc., Prepared for the California Air Resources Board, Sacramento, CA.

Wenzel, T. and M. Ross (1998). Characterization of recent-model high-emitting automobiles. Proceedings of the 1998 SAE International Spring Fuel & Lubricants Meeting & Exposition, Dearborn, MI, USA, Advances in General Emissions SAE Special Publications. v 1367 May 1997. SAE, Warrendale, PA, USA.

Wolf, J., R. Guensler, et al. (1998). "High-emitting vehicle characterization using regression tree analysis." Transportation Research Record(1641): 58-65.

Appendix

Appendix A: Utilized Networks

Uniform Speed Scenario

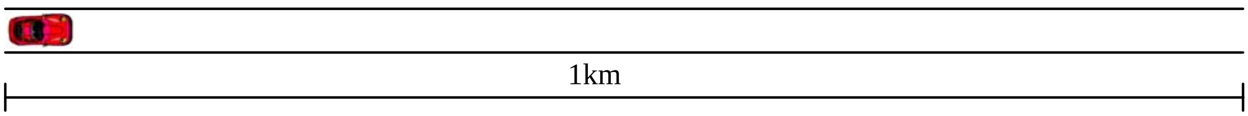

Stop Sign Control Scenario

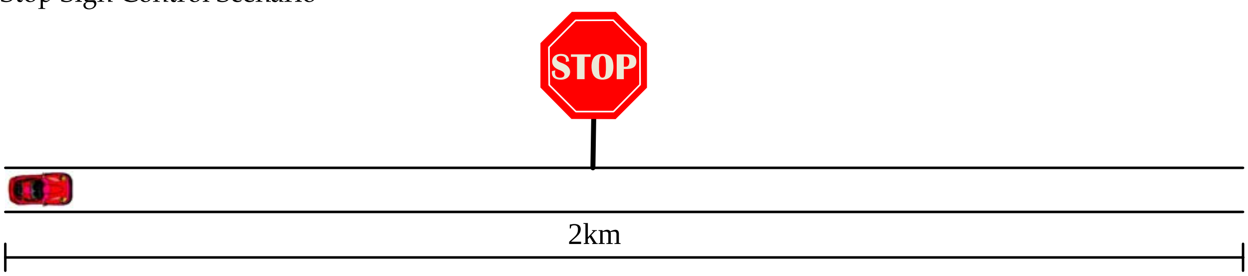

Signal Control Scenario

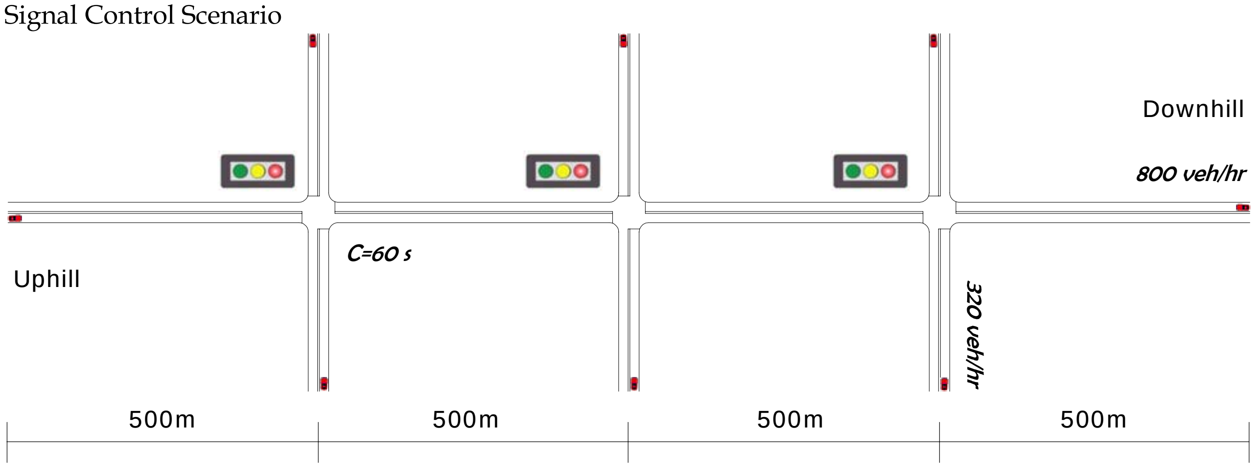

Figure A-1: Utilized Networks

Appendix B: Geometric Design Alternatives

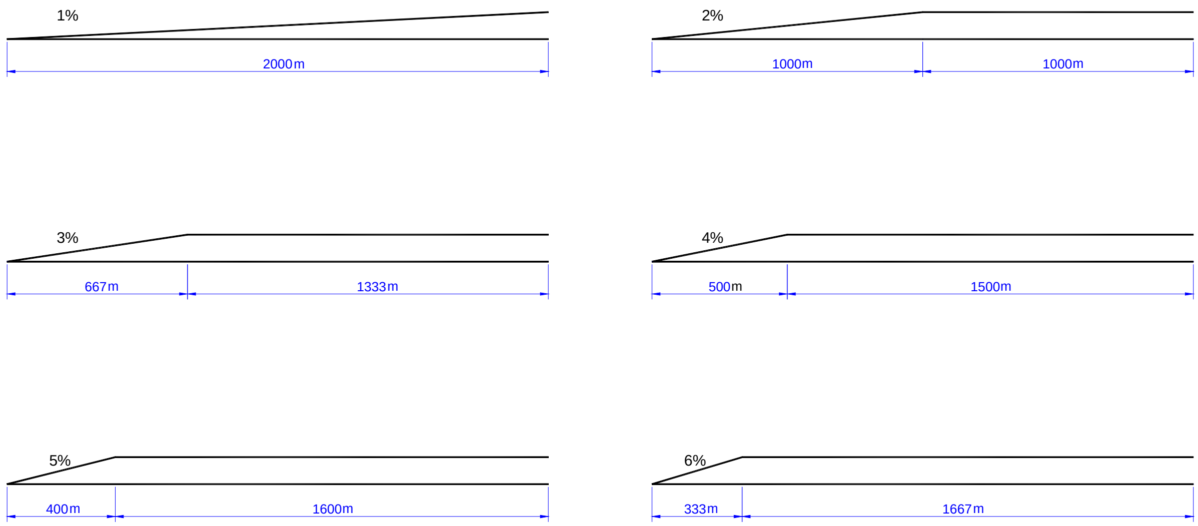

Figure B-1: Geometric Design Alternatives

Appendix C: MOE Profiles and Percent Changes

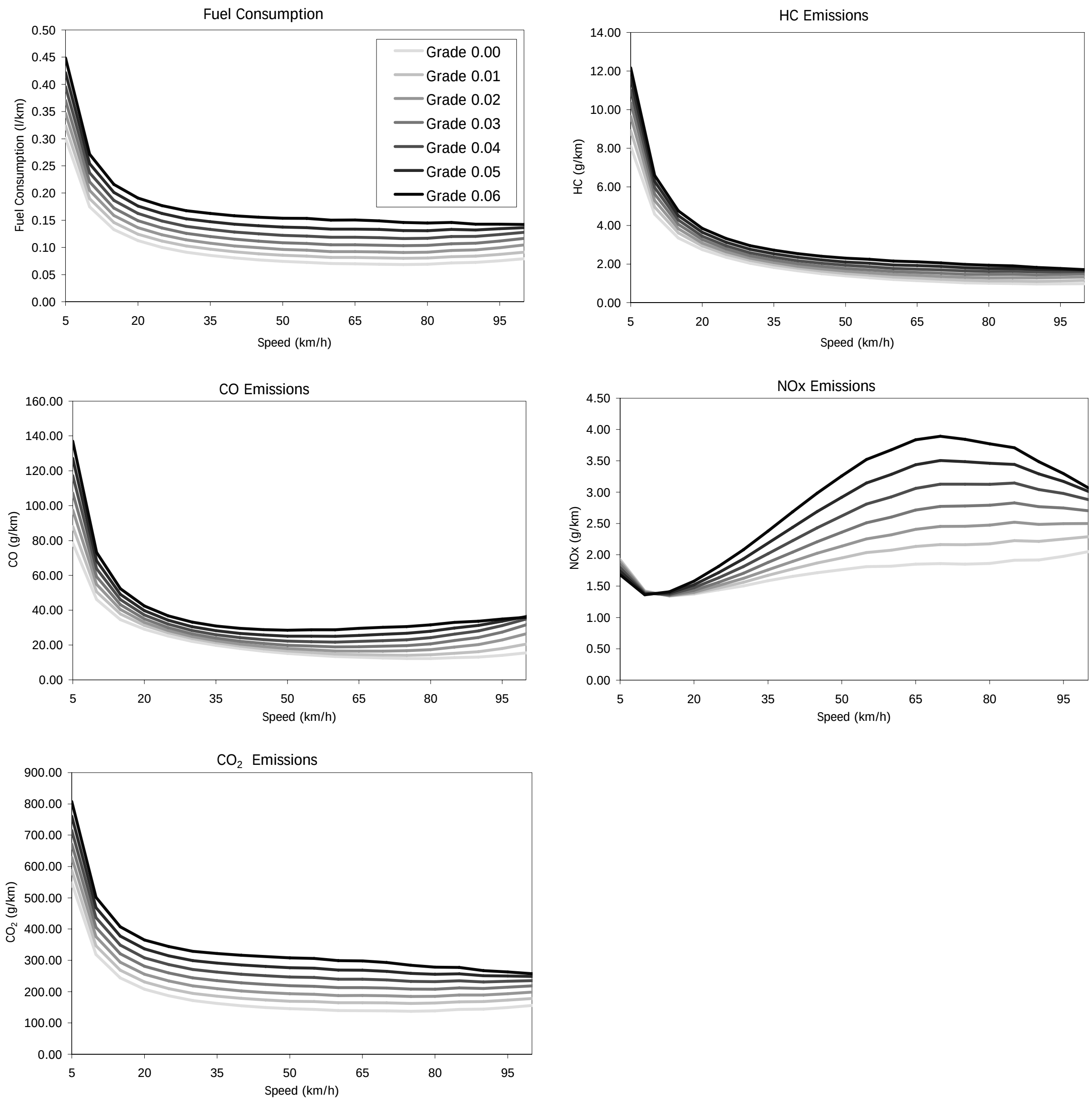

Figure C-1: MOE profiles for HEV (Uniform Speed Scenario)

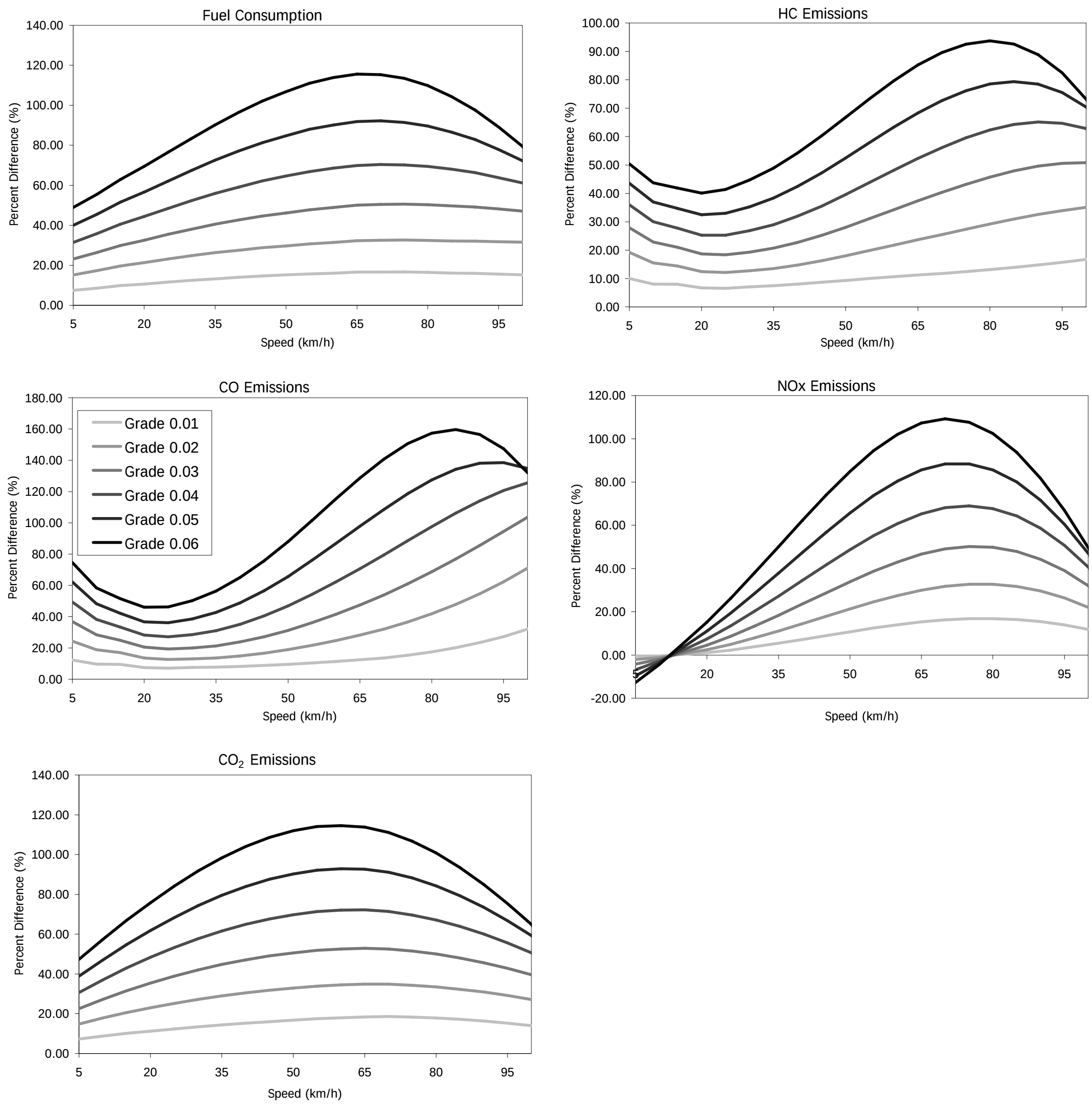

Figure C-2: Percent change in MOEs relative to 0% grade for HEV (Uniform Speed Scenario)

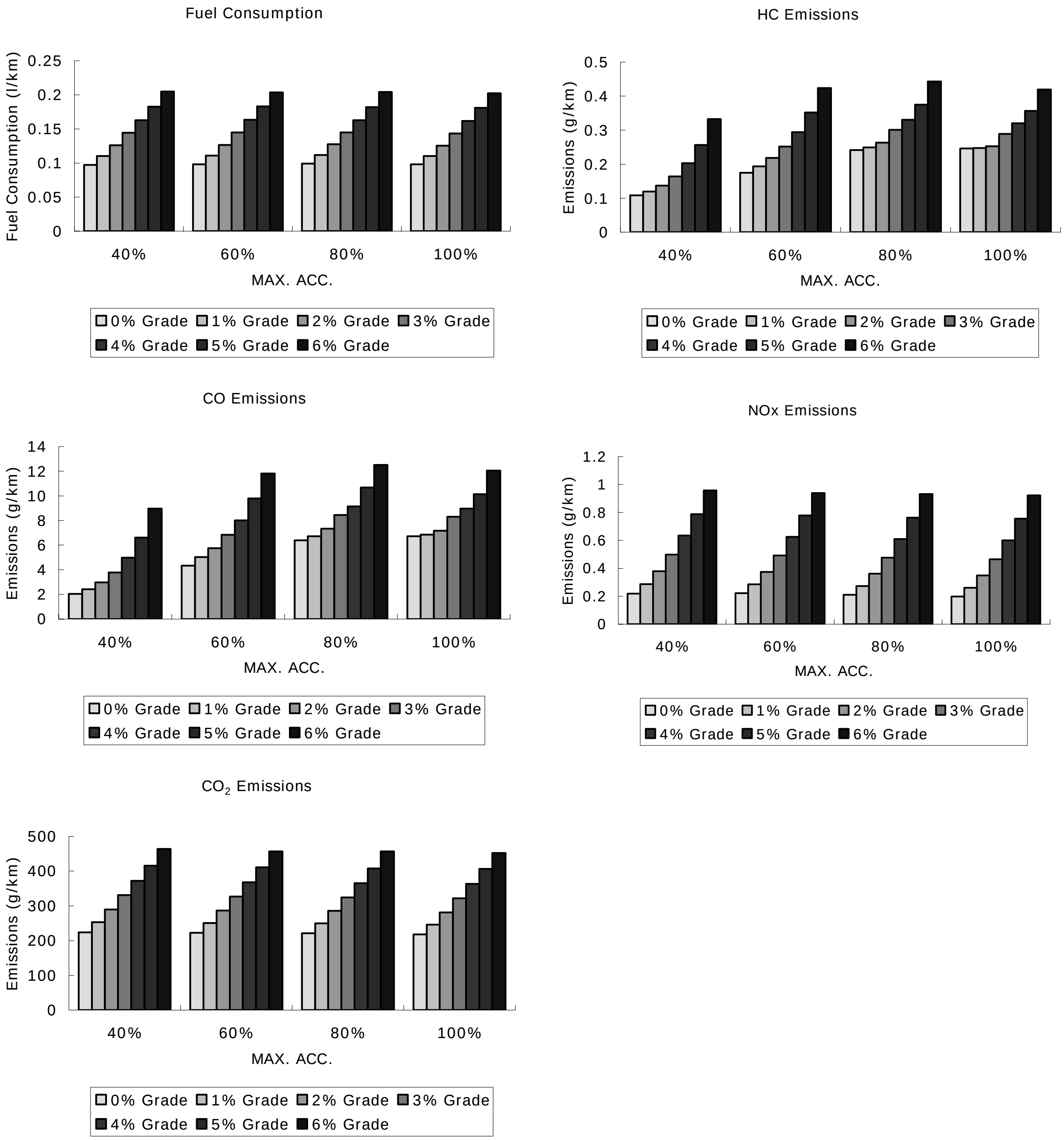

Figure C-3: MOEs as a function of roadway grade and maximum acceleration levels for normal LDV (Stop Sign Control Scenario)

Fuel Consumption

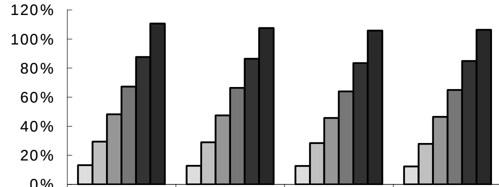

	40%	60%	80%	100%
1% Grade	13%	13%	13%	12%
2% Grade	30%	29%	28%	28%
3% Grade	48%	47%	46%	46%
4% Grade	67%	66%	64%	65%
5% Grade	88%	86%	83%	85%
6% Grade	111%	108%	106%	106%

MAX. ACC.

1% Grade 2% Grade 3% Grade 4% Grade 5% Grade 6% Grade

HC Emissions

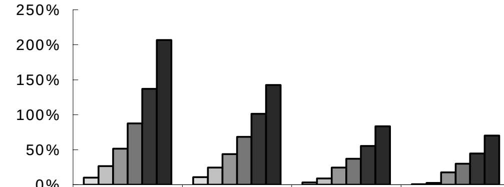

	40%	60%	80%	100%
1% Grade	10%	11%	3%	1%
2% Grade	27%	25%	9%	3%
3% Grade	51%	44%	25%	18%
4% Grade	88%	68%	37%	30%
5% Grade	137%	101%	55%	45%
6% Grade	207%	142%	84%	70%

MAX. ACC.

1% Grade 2% Grade 3% Grade 4% Grade 5% Grade 6% Grade

CO Emissions

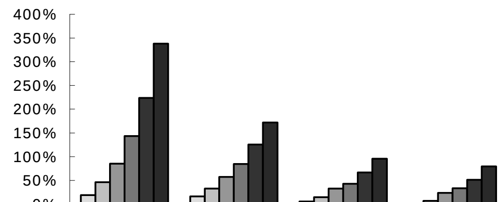

	40%	60%	80%	100%
1% Grade	19%	16%	5%	2%
2% Grade	46%	32%	15%	7%
3% Grade	85%	57%	32%	24%
4% Grade	143%	84%	43%	33%
5% Grade	223%	125%	67%	51%
6% Grade	338%	172%	95%	79%

MAX. ACC.

1% Grade 2% Grade 3% Grade 4% Grade 5% Grade 6% Grade

NOx Emissions

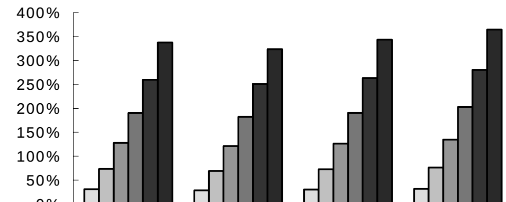

	40%	60%	80%	100%
1% Grade	31%	29%	30%	32%
2% Grade	73%	69%	73%	76%
3% Grade	128%	121%	126%	134%
4% Grade	190%	182%	191%	203%
5% Grade	260%	251%	263%	281%
6% Grade	337%	324%	344%	364%

MAX. ACC.

1% Grade 2% Grade 3% Grade 4% Grade 5% Grade 6% Grade

CO_2 Emissions

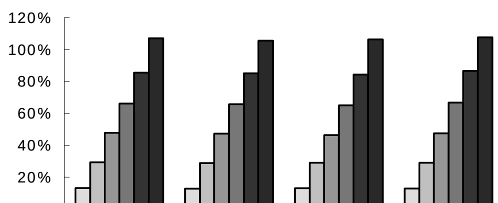

	40%	60%	80%	100%
1% Grade	13%	13%	13%	13%
2% Grade	29%	29%	29%	29%
3% Grade	48%	47%	46%	48%
4% Grade	66%	66%	65%	67%
5% Grade	86%	85%	84%	87%
6% Grade	107%	105%	106%	108%

MAX. ACC.

1% Grade 2% Grade 3% Grade 4% Grade 5% Grade 6% Grade

Figure C-4: Percent Changes in MOEs relative to 0% grade for normal LDV (Stop Sign Control Scenario)

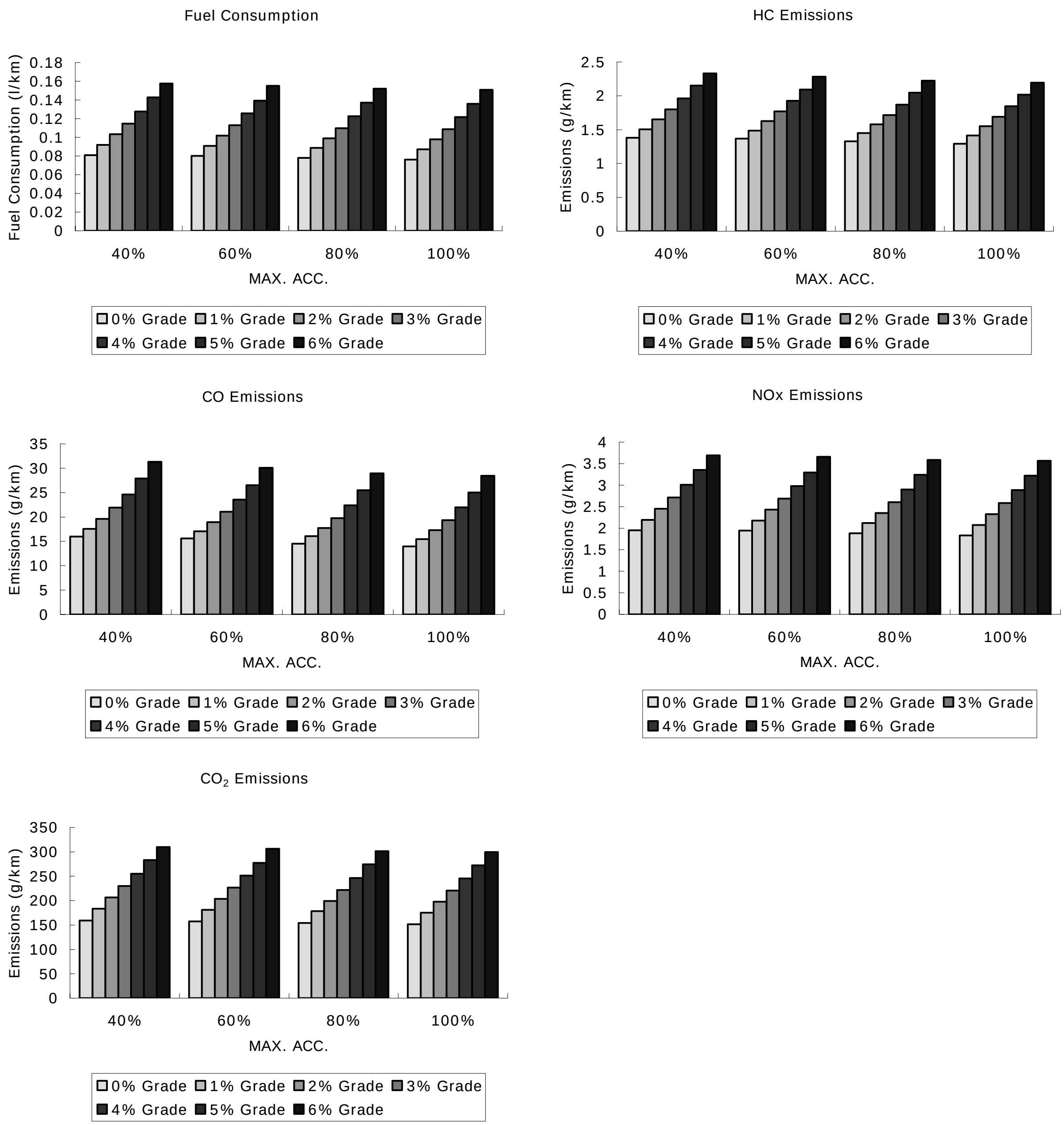

Figure C-5: MOEs as a function of roadway grade and maximum acceleration levels for HEV (Stop Sign Control Scenario)

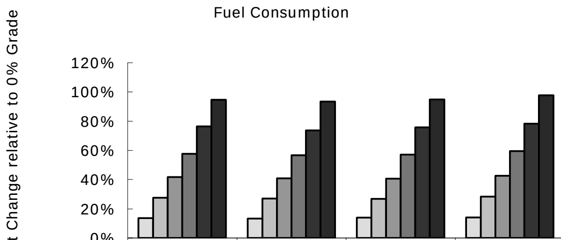

	40%	60%	80%	100%
1% Grade	14%	13%	14%	14%
2% Grade	28%	27%	27%	28%
3% Grade	42%	41%	41%	43%
4% Grade	58%	57%	57%	60%
5% Grade	76%	74%	76%	78%
6% Grade	95%	93%	95%	98%

MAX. ACC.

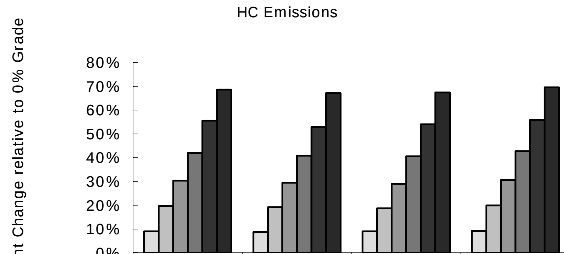

	40%	60%	80%	100%
1% Grade	9%	9%	9%	9%
2% Grade	20%	19%	19%	20%
3% Grade	30%	30%	29%	31%
4% Grade	42%	41%	41%	43%
5% Grade	56%	53%	54%	56%
6% Grade	69%	67%	67%	70%

MAX. ACC.

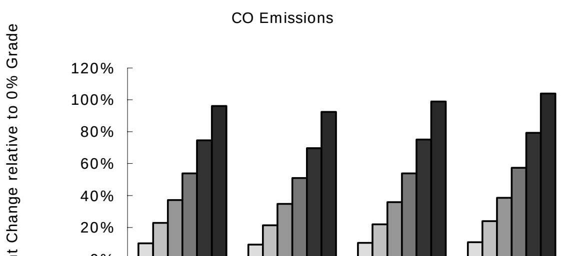

	40%	60%	80%	100%
1% Grade	10%	9%	10%	11%
2% Grade	23%	21%	22%	24%
3% Grade	37%	35%	36%	39%
4% Grade	54%	51%	54%	57%
5% Grade	75%	70%	75%	79%
6% Grade	96%	92%	99%	104%

MAX. ACC.

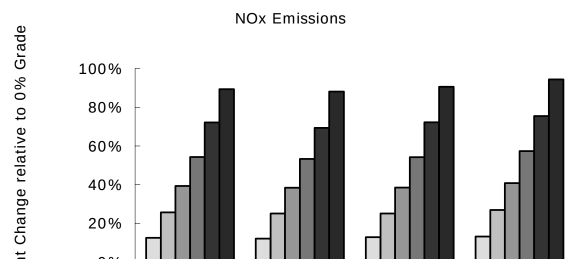

	40%	60%	80%	100%
1% Grade	12%	12%	13%	13%
2% Grade	26%	25%	25%	27%
3% Grade	39%	38%	39%	41%
4% Grade	54%	53%	54%	57%
5% Grade	72%	69%	72%	76%
6% Grade	89%	88%	91%	94%

MAX. ACC.

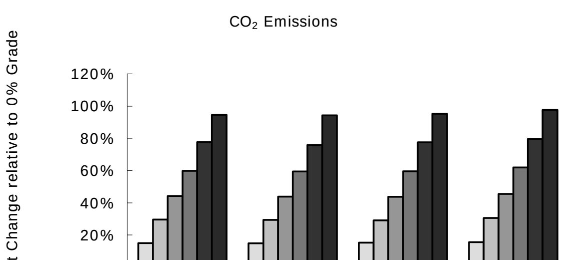

	40%	60%	80%	100%
1% Grade	15%	15%	15%	16%
2% Grade	30%	29%	29%	31%
3% Grade	44%	44%	44%	45%
4% Grade	60%	59%	60%	62%
5% Grade	78%	76%	78%	80%
6% Grade	94%	94%	95%	98%

MAX. ACC.

Figure C-6: Percent Changes in MOEs relative to 0% grade for HEV (Stop Sign Control Scenario)

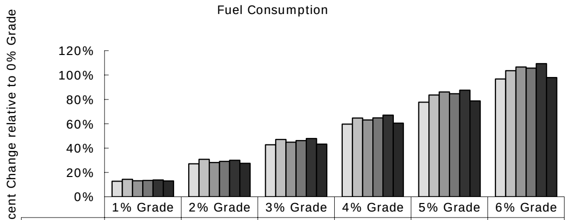

	1% Grade	2% Grade	3% Grade	4% Grade	5% Grade	6% Grade
Offset 0s	13%	27%	43%	60%	78%	97%
Offset 10s	14%	31%	47%	65%	84%	104%
Offset 20s	13%	28%	45%	63%	86%	107%
Offset 30s	14%	29%	46%	65%	85%	106%
Offset 40s	14%	30%	48%	67%	88%	109%
Offset 50s	13%	28%	43%	61%	79%	98%

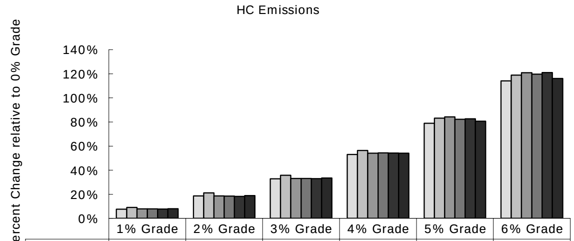

	1% Grade	2% Grade	3% Grade	4% Grade	5% Grade	6% Grade
Offset 0s	8%	19%	33%	53%	79%	114%
Offset 10s	9%	21%	36%	56%	83%	119%
Offset 20s	8%	19%	33%	54%	84%	121%
Offset 30s	8%	19%	33%	54%	82%	120%
Offset 40s	8%	18%	33%	54%	83%	121%
Offset 50s	8%	19%	33%	54%	81%	116%

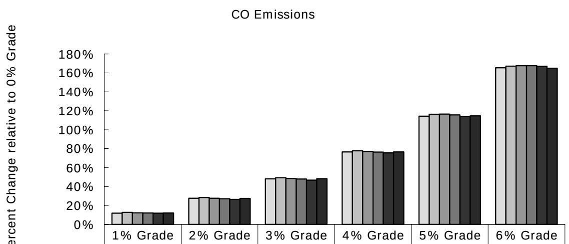

	1% Grade	2% Grade	3% Grade	4% Grade	5% Grade	6% Grade
Offset 0s	12%	28%	48%	77%	114%	165%
Offset 10s	13%	28%	49%	78%	116%	167%
Offset 20s	12%	28%	48%	77%	116%	168%
Offset 30s	12%	27%	48%	76%	116%	168%
Offset 40s	12%	26%	47%	76%	114%	167%
Offset 50s	12%	27%	48%	77%	115%	165%

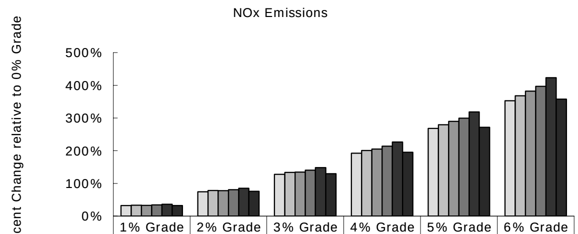

	1% Grade	2% Grade	3% Grade	4% Grade	5% Grade	6% Grade
Offset 0s	32%	75%	128%	193%	268%	353%
Offset 10s	34%	79%	134%	201%	279%	368%
Offset 20s	33%	78%	135%	205%	290%	382%
Offset 30s	34%	81%	140%	214%	300%	397%
Offset 40s	36%	85%	149%	226%	319%	424%
Offset 50s	33%	76%	130%	195%	272%	358%

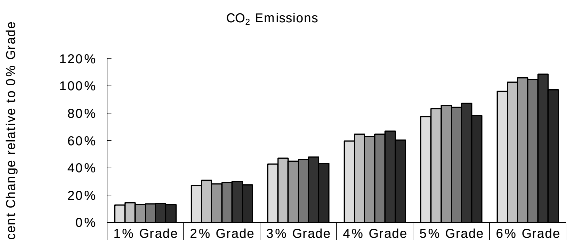

	1% Grade	2% Grade	3% Grade	4% Grade	5% Grade	6% Grade
Offset 0s	13%	27%	43%	60%	77%	96%
Offset 10s	14%	31%	47%	65%	83%	103%
Offset 20s	13%	28%	45%	63%	86%	106%
Offset 30s	14%	29%	46%	65%	84%	105%
Offset 40s	14%	30%	48%	67%	87%	109%
Offset 50s	13%	28%	43%	60%	78%	97%

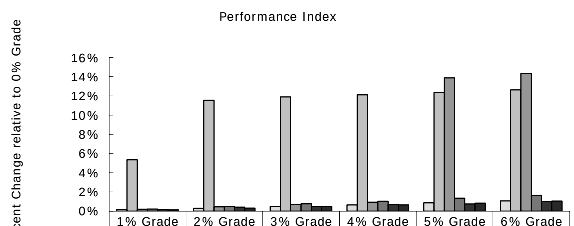

	1% Grade	2% Grade	3% Grade	4% Grade	5% Grade	6% Grade
Offset 0s	0%	0%	0%	1%	1%	1%
Offset 10s	5%	12%	12%	12%	12%	13%
Offset 20s	0%	0%	1%	1%	14%	14%
Offset 30s	0%	0%	1%	1%	1%	2%
Offset 40s	0%	0%	0%	1%	1%	1%
Offset 50s	0%	0%	0%	1%	1%	1%

Figure C-7: Percent Changes in MOEs relative to 0% grade for normal LDV (Signal Control Scenario)

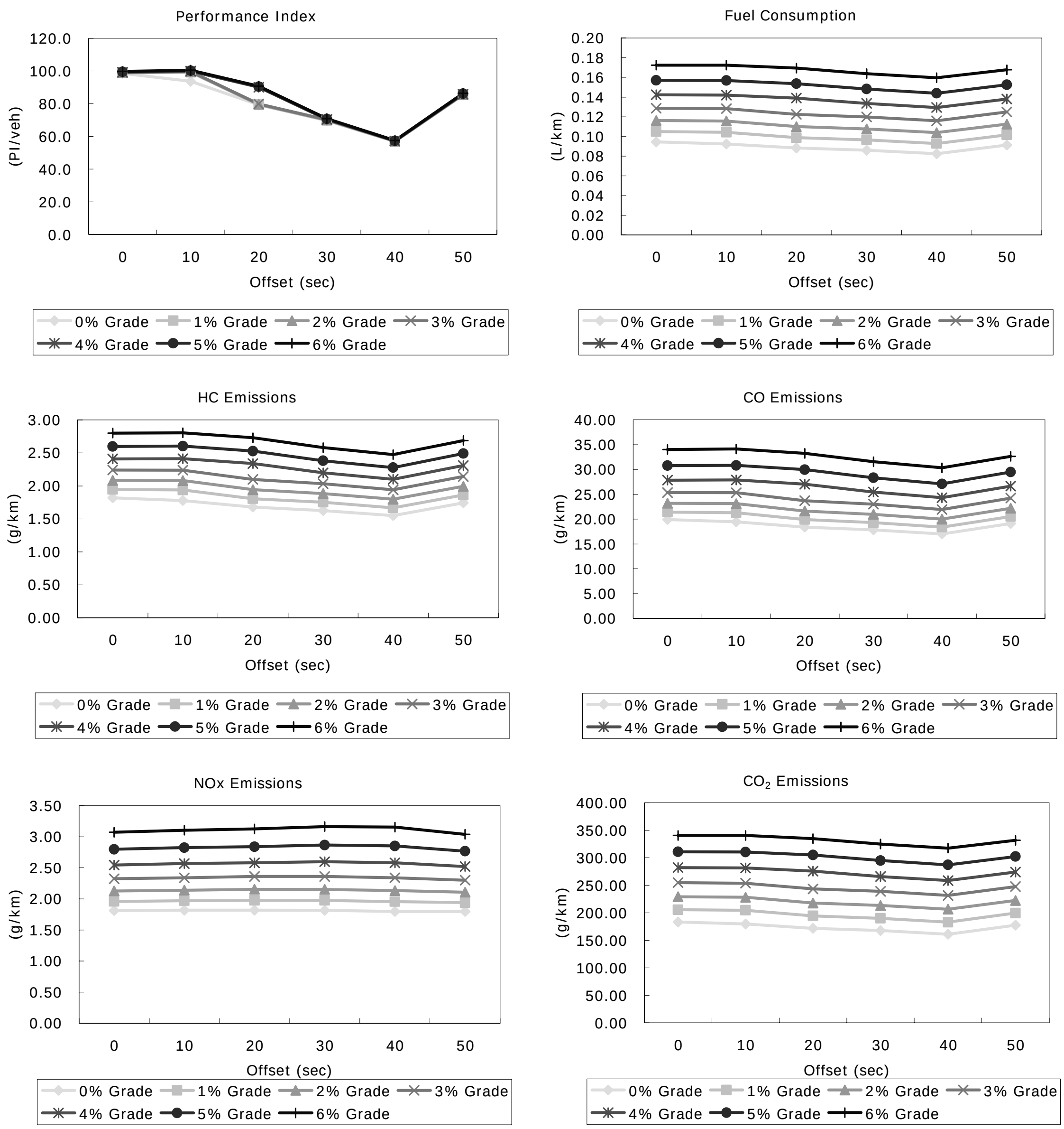

Figure C-8: PI and MOEs as a function of signal offsets for HEV

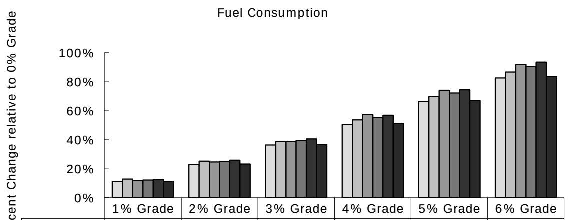

	1% Grade	2% Grade	3% Grade	4% Grade	5% Grade	6% Grade
Offset 0s	11%	23%	36%	51%	66%	83%
Offset 10s	13%	25%	39%	54%	70%	87%
Offset 20s	12%	25%	39%	57%	74%	92%
Offset 30s	12%	25%	39%	55%	72%	91%
Offset 40s	13%	26%	41%	57%	74%	94%
Offset 50s	11%	23%	37%	51%	67%	84%

Road Grade

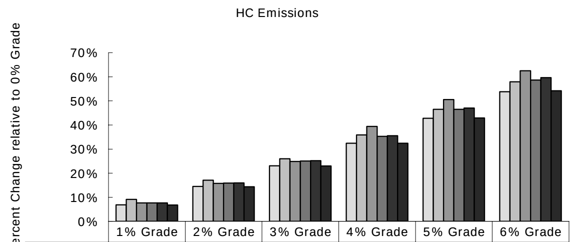

	1% Grade	2% Grade	3% Grade	4% Grade	5% Grade	6% Grade
Offset 0s	7%	14%	23%	32%	43%	54%
Offset 10s	9%	17%	26%	36%	47%	58%
Offset 20s	8%	16%	25%	39%	51%	63%
Offset 30s	8%	16%	25%	35%	47%	59%
Offset 40s	8%	16%	25%	36%	47%	60%
Offset 50s	7%	14%	23%	32%	43%	54%

Road Grade

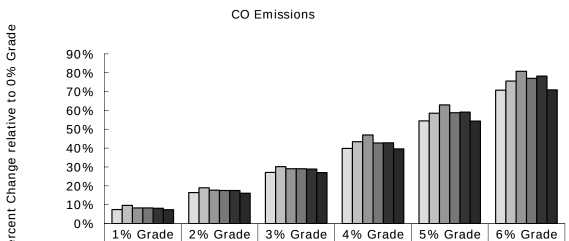

	1% Grade	2% Grade	3% Grade	4% Grade	5% Grade	6% Grade
Offset 0s	7%	16%	27%	40%	54%	71%
Offset 10s	10%	19%	30%	43%	59%	76%
Offset 20s	8%	18%	29%	47%	63%	81%
Offset 30s	8%	18%	29%	43%	59%	77%
Offset 40s	8%	18%	29%	43%	59%	78%
Offset 50s	7%	16%	27%	40%	54%	71%

Road Grade

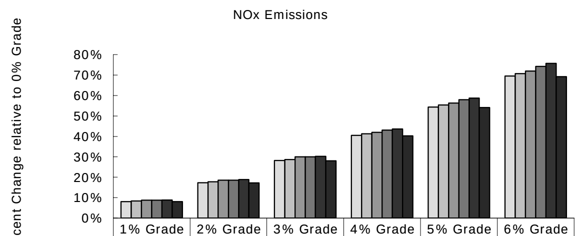

	1% Grade	2% Grade	3% Grade	4% Grade	5% Grade	6% Grade
Offset 0s	8%	17%	28%	40%	54%	70%
Offset 10s	8%	18%	29%	41%	55%	71%
Offset 20s	9%	19%	30%	42%	56%	72%
Offset 30s	9%	19%	30%	43%	58%	74%
Offset 40s	9%	19%	30%	44%	59%	76%
Offset 50s	8%	17%	28%	40%	54%	69%

Road Grade

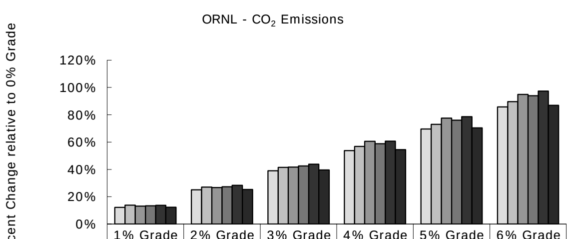

	1% Grade	2% Grade	3% Grade	4% Grade	5% Grade	6% Grade
Offset 0s	12%	25%	39%	54%	70%	86%
Offset 10s	14%	27%	41%	57%	73%	90%
Offset 20s	13%	27%	42%	61%	77%	95%
Offset 30s	13%	27%	43%	59%	76%	94%
Offset 40s	14%	28%	44%	61%	79%	97%
Offset 50s	12%	25%	40%	54%	70%	87%

Road Grade

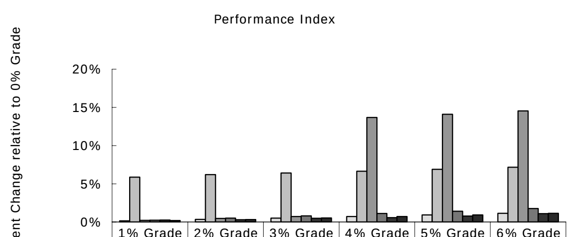

	1% Grade	2% Grade	3% Grade	4% Grade	5% Grade	6% Grade
Offset 0s	0%	0%	0%	1%	1%	1%
Offset 10s	6%	6%	6%	7%	7%	7%
Offset 20s	0%	0%	1%	14%	14%	15%
Offset 30s	0%	1%	1%	1%	1%	2%
Offset 40s	0%	0%	0%	1%	1%	1%
Offset 50s	0%	0%	1%	1%	1%	1%

Road Grade

Figure C-9: Percent Changes in MOEs relative to 0% grade for HEV (Signal Control Scenario)

Appendix D: VT-Micro and PERE Estimated vs. In-laboratory Measured Emission Rates

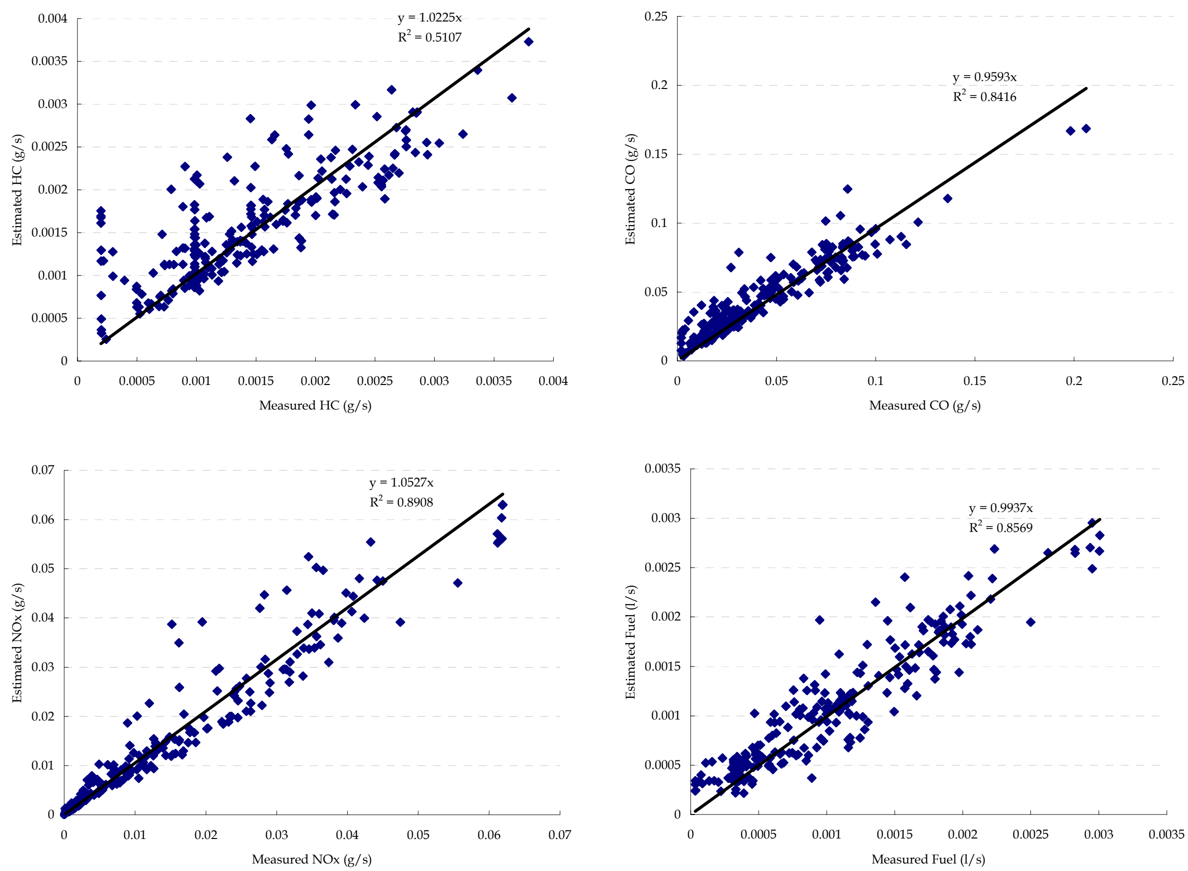

Figure D-1: VT-Micro Estimated vs. In-laboratory Measured Emission Rates for Station Wagon

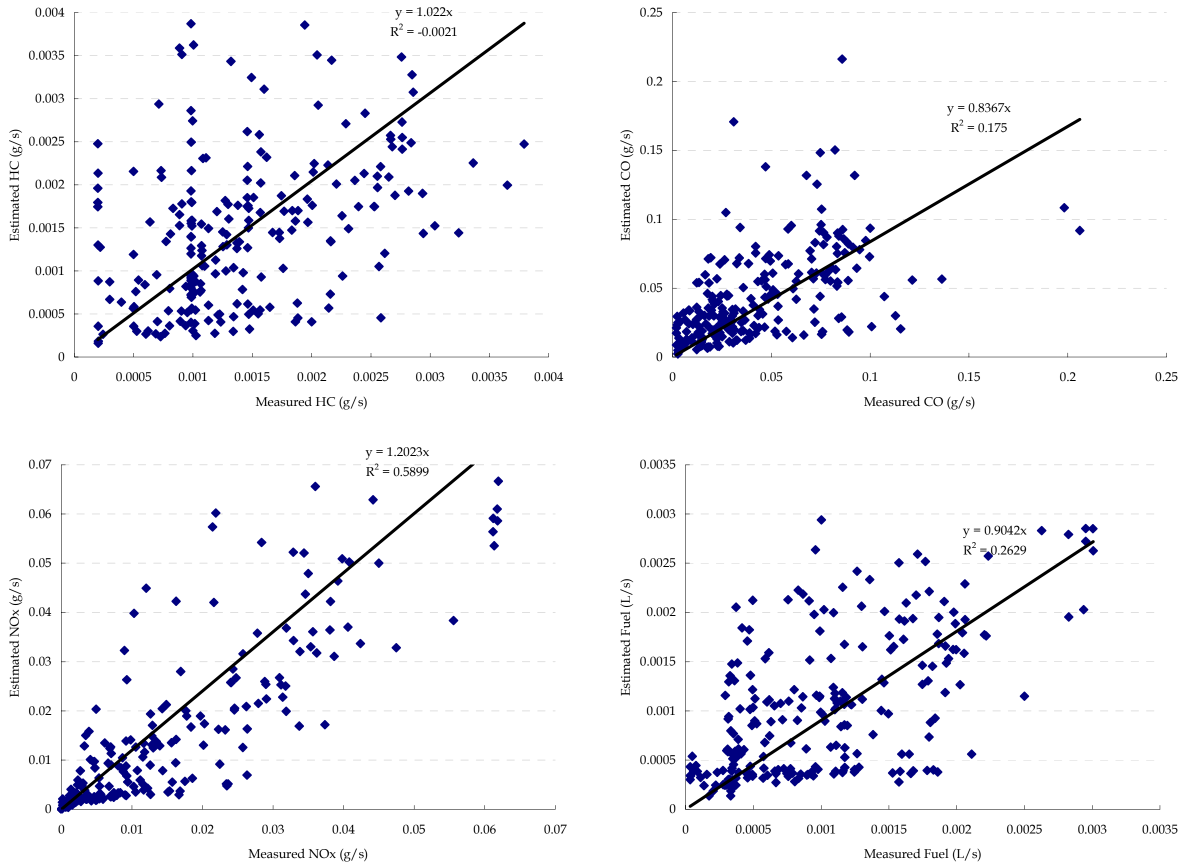

Figure D-2: PERE Estimated vs. In-laboratory Measured Emission Rates for Station Wagon

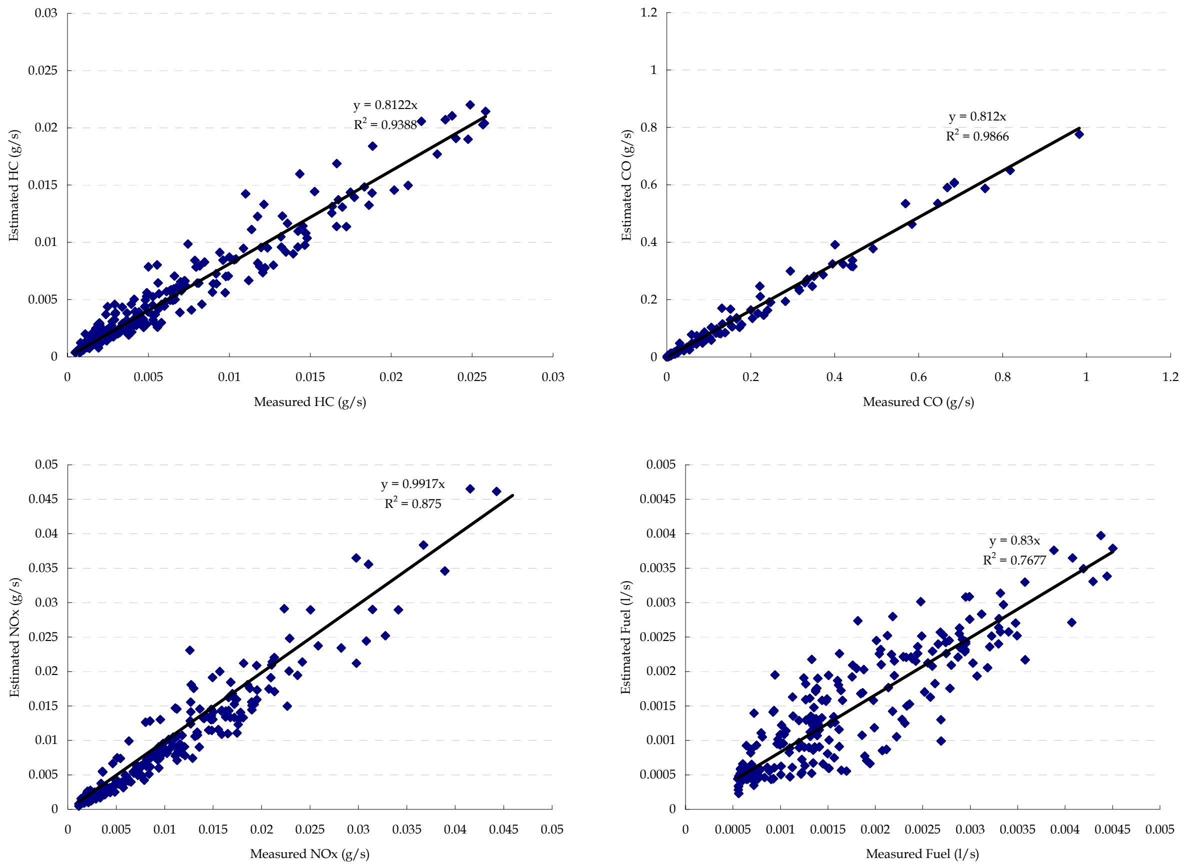

Figure D-3: VT-Micro Estimated vs. In-laboratory Measured Emission Rates for Full-Size

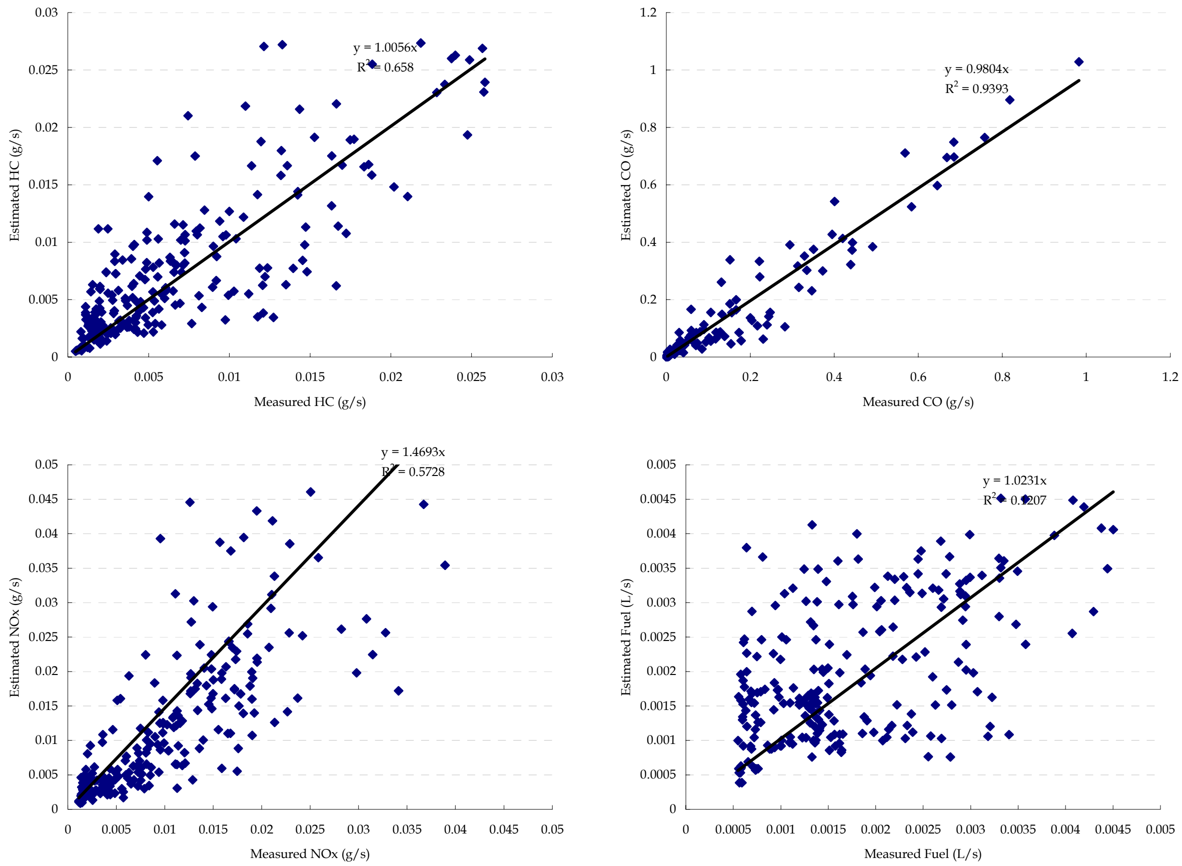

Figure D-4: PERE Estimated vs. In-laboratory Measured Emission Rates for Full-Size

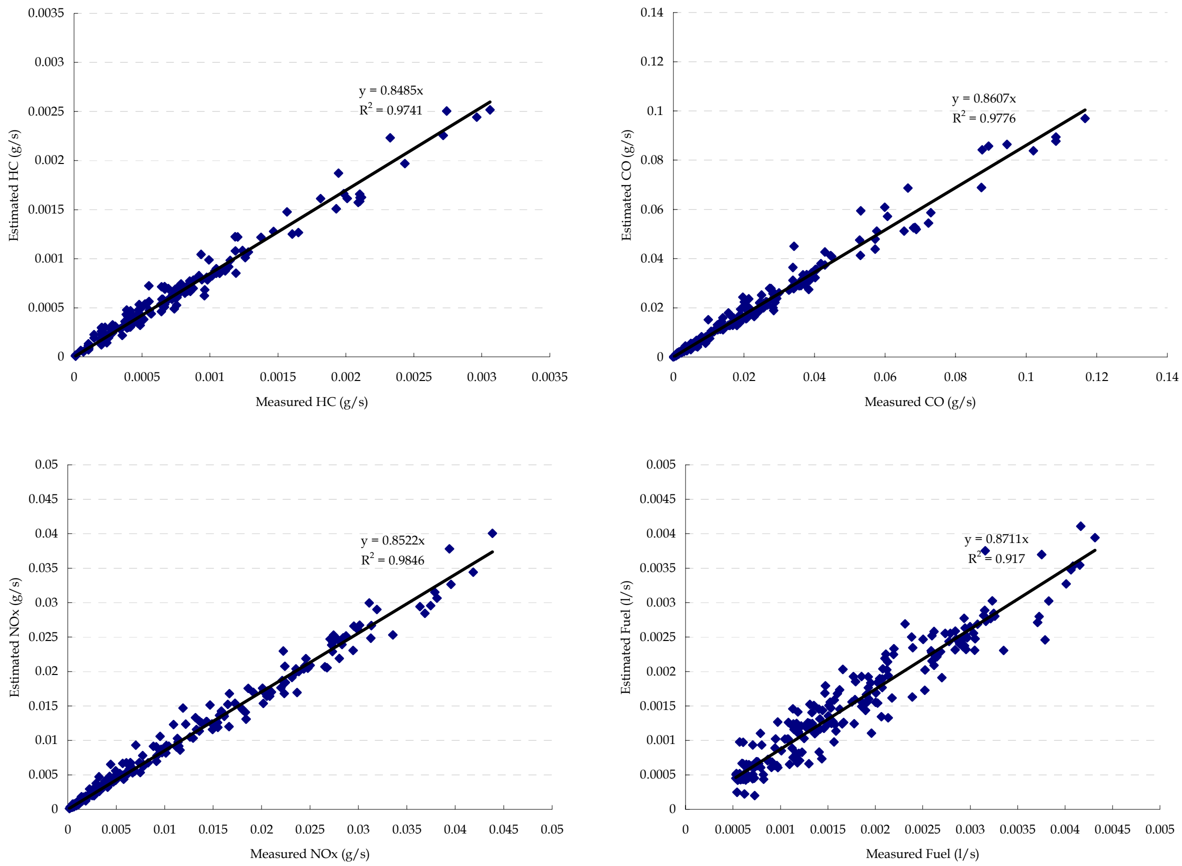

Figure D-5: VT-Micro Estimated vs. In-laboratory Measured Emission Rates for Mini Van

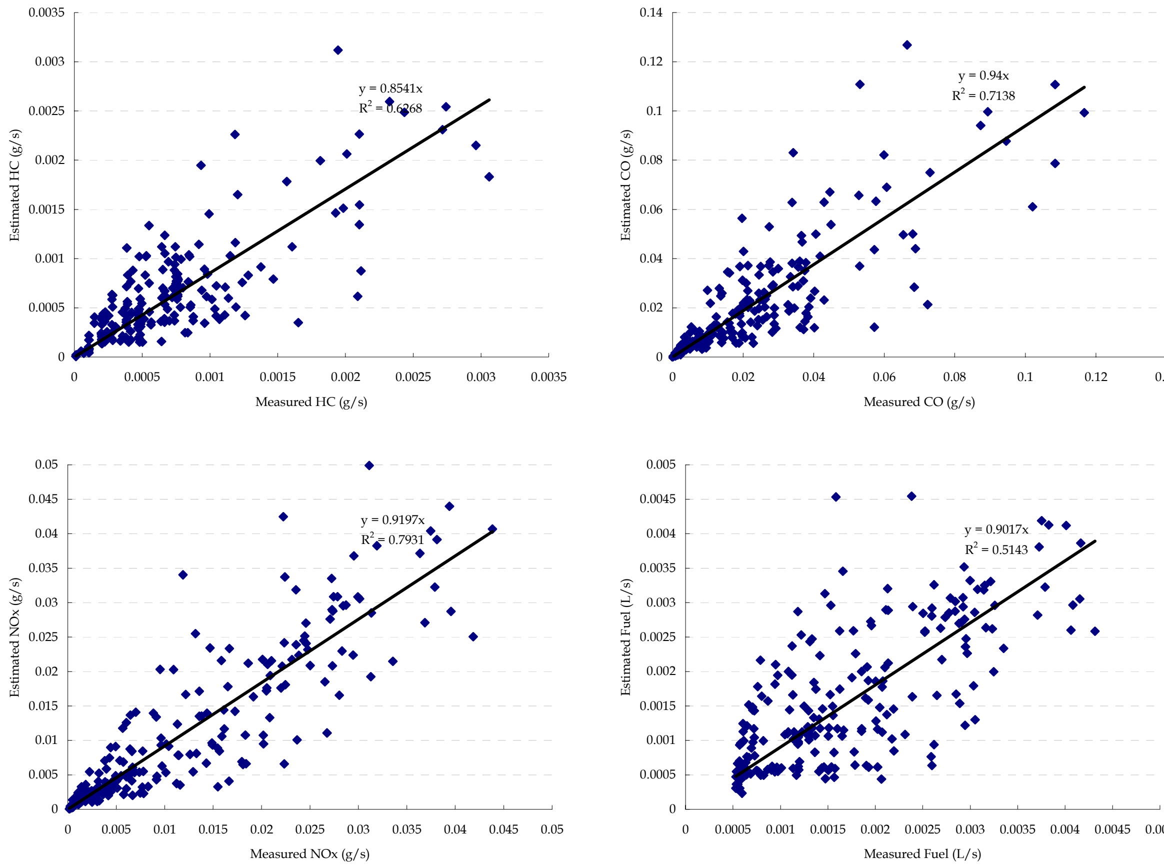

Figure D-6: PERE Estimated vs. In-laboratory Measured Emission Rates for Mini Van

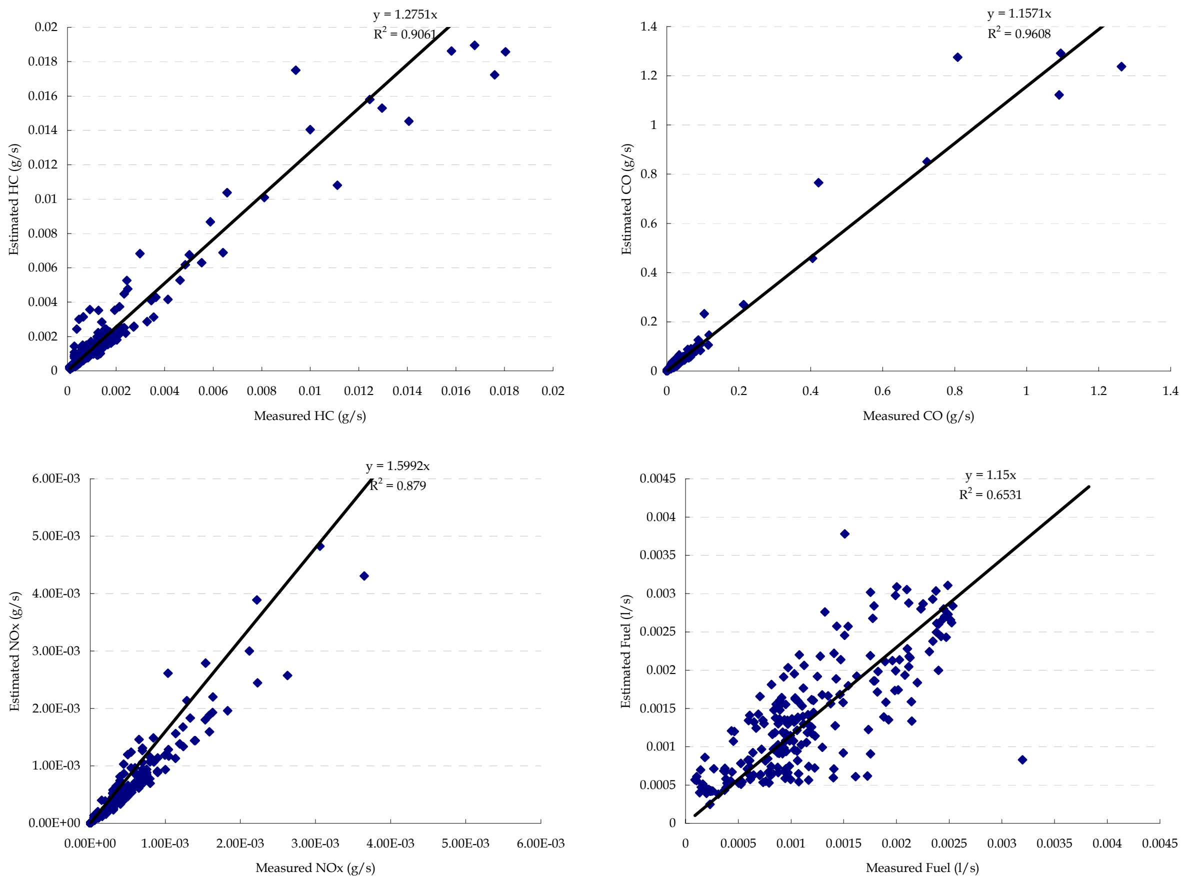

Figure D-7: VT-Micro Estimated vs. In-laboratory Measured Emission Rates for Pickup

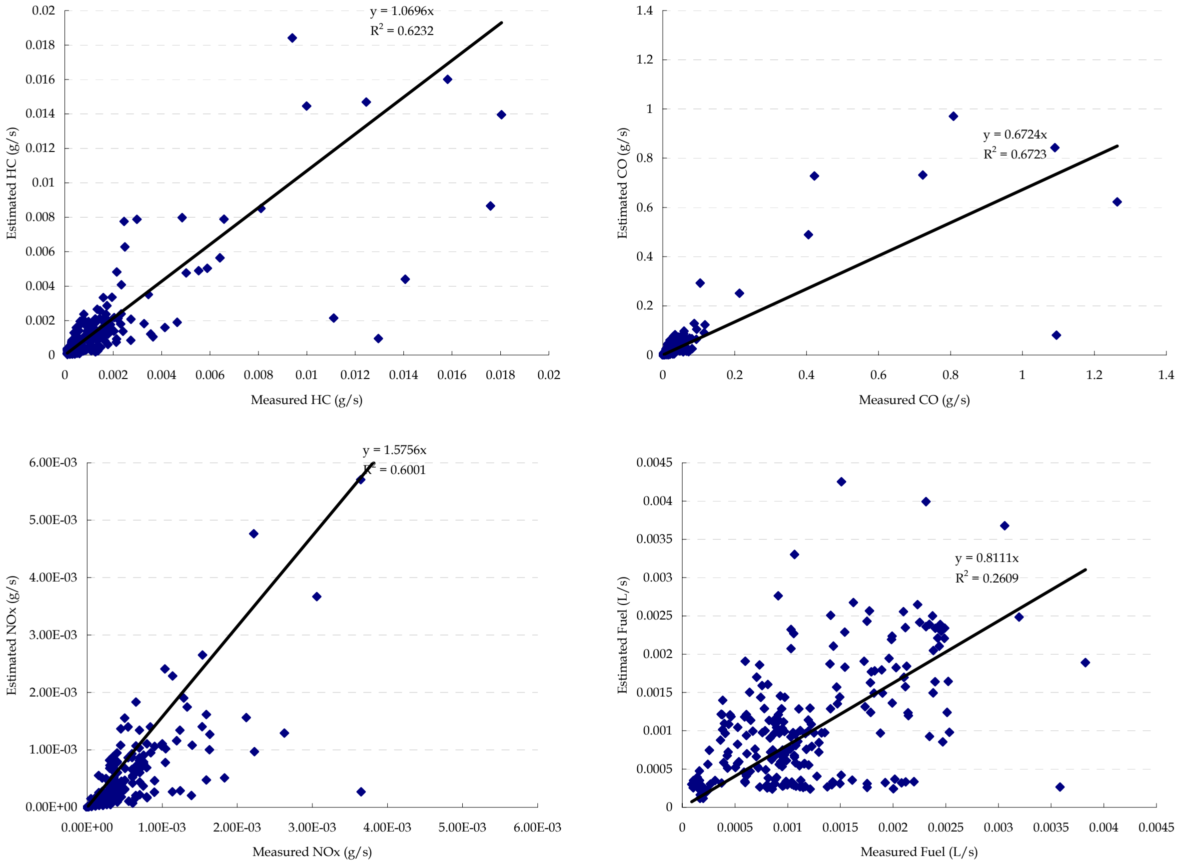

Figure D-8: PERE Estimated vs. In-laboratory Measured Emission Rates for Pickup

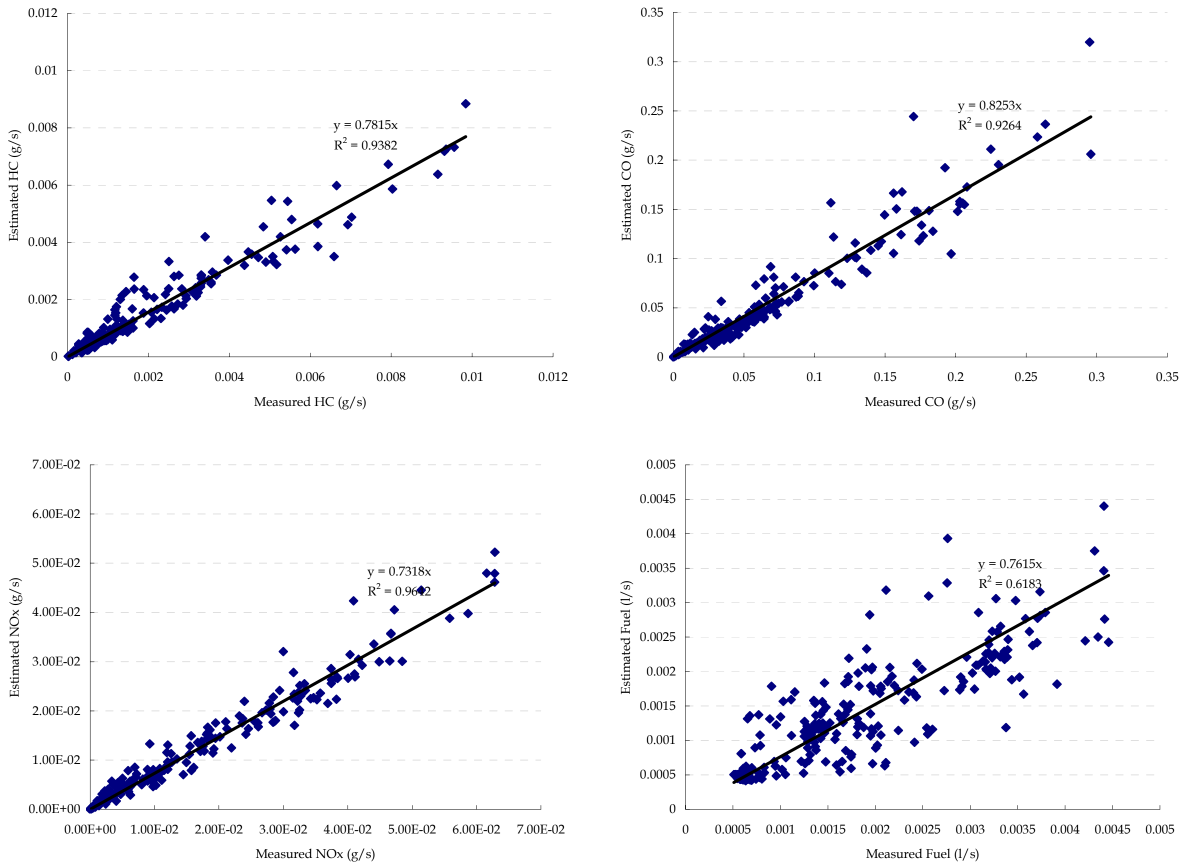

Figure D-9: VT-Micro Estimated vs. In-laboratory Measured Emission Rates for SUV

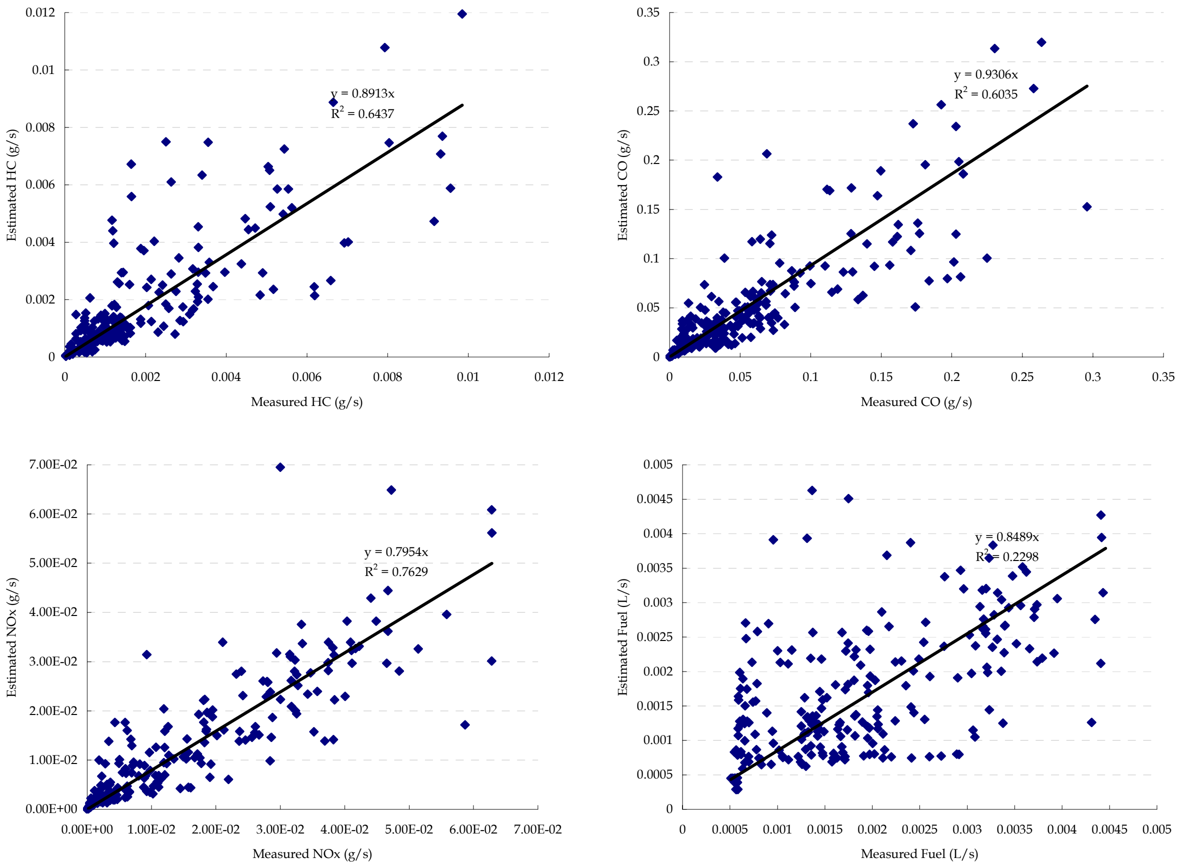

Figure D-10: PERE Estimated vs. In-laboratory Measured Emission Rates for SUV

Appendix E: In-Laboratory Measured IM240 Emission and Estimated Emission

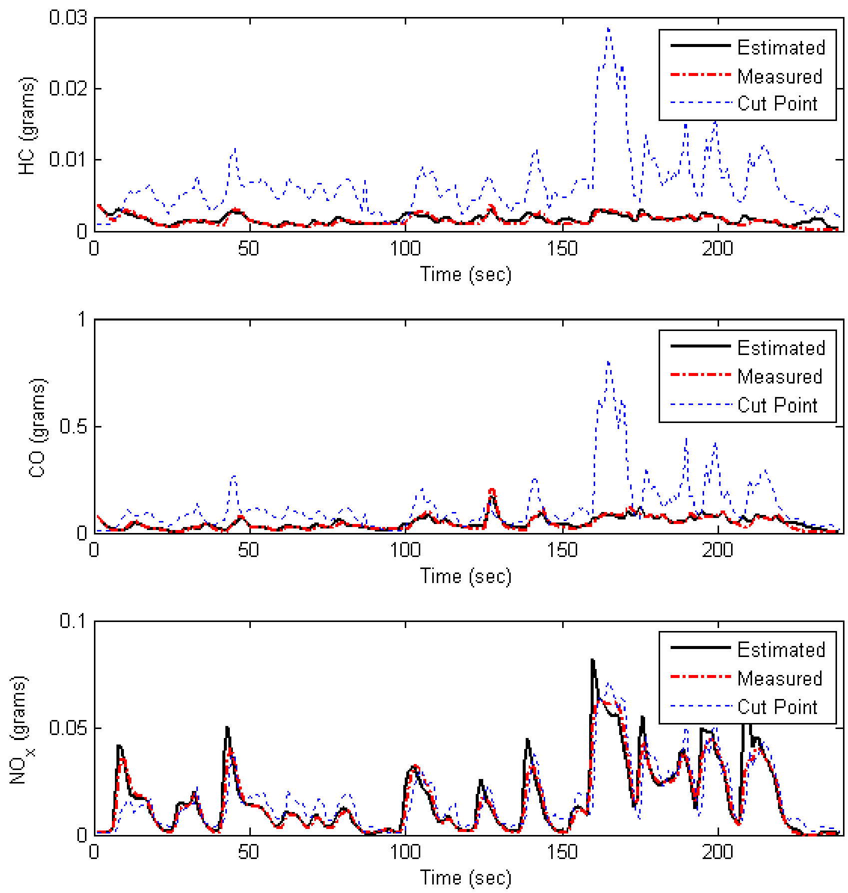

Figure E-1: In-Laboratory Measured IM240 Emission and Estimated Emission for Station Wagon

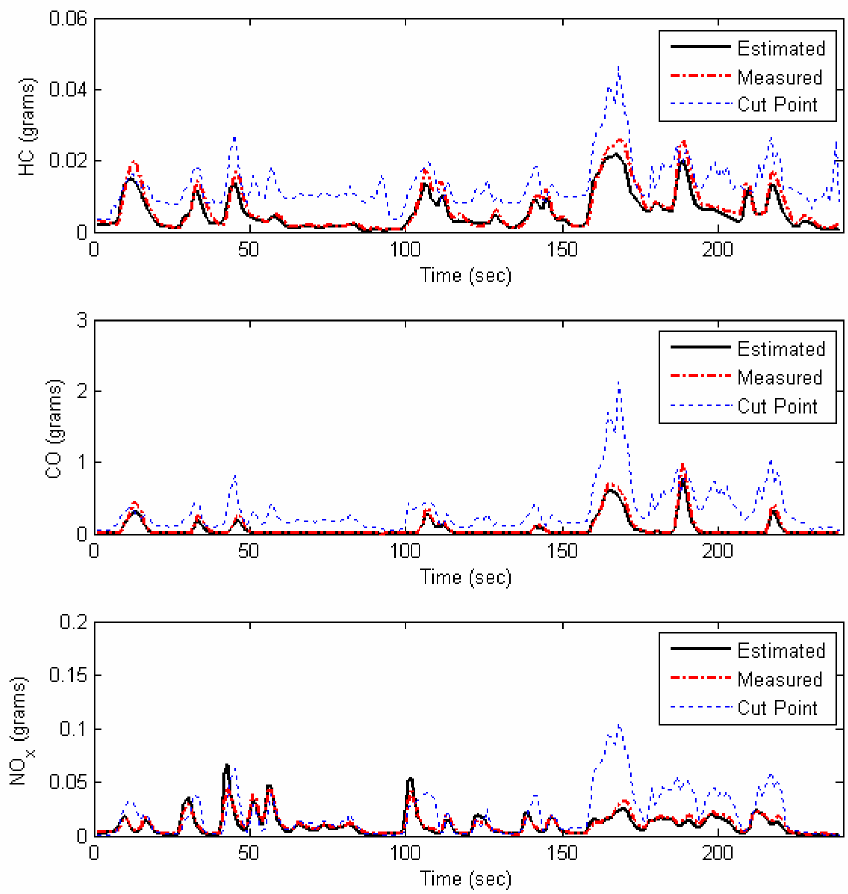

Figure E-2: In-Laboratory Measured IM240 Emission and Estimated Emission for Full-Size

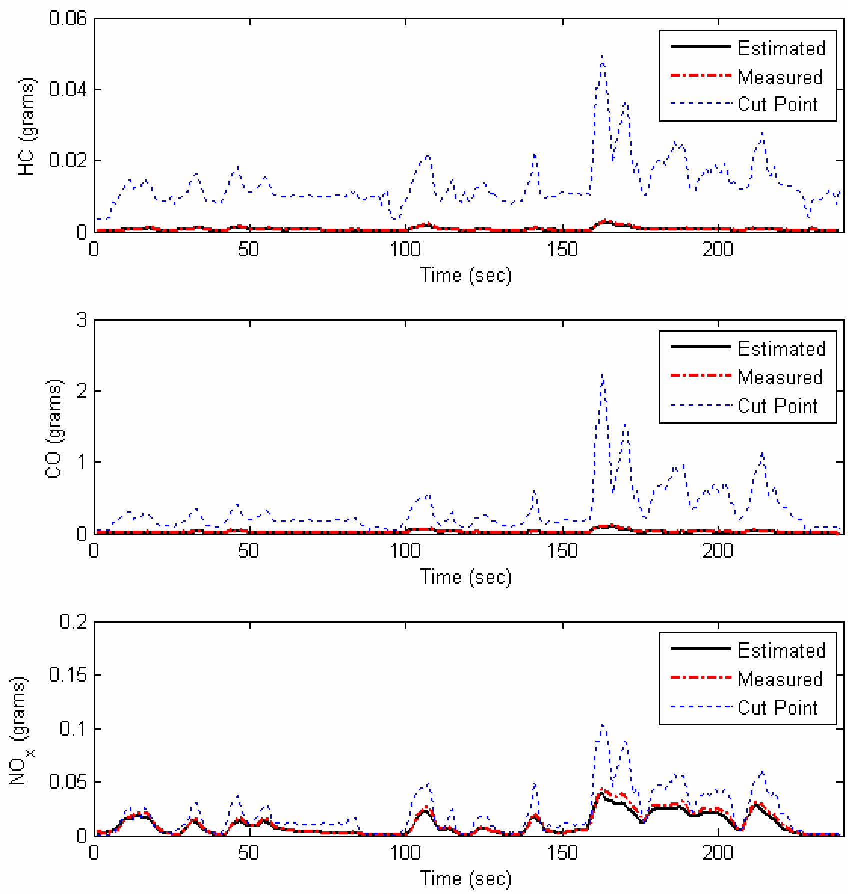

Figure E-3: In-Laboratory Measured IM240 Emission and Estimated Emission for Mini Van

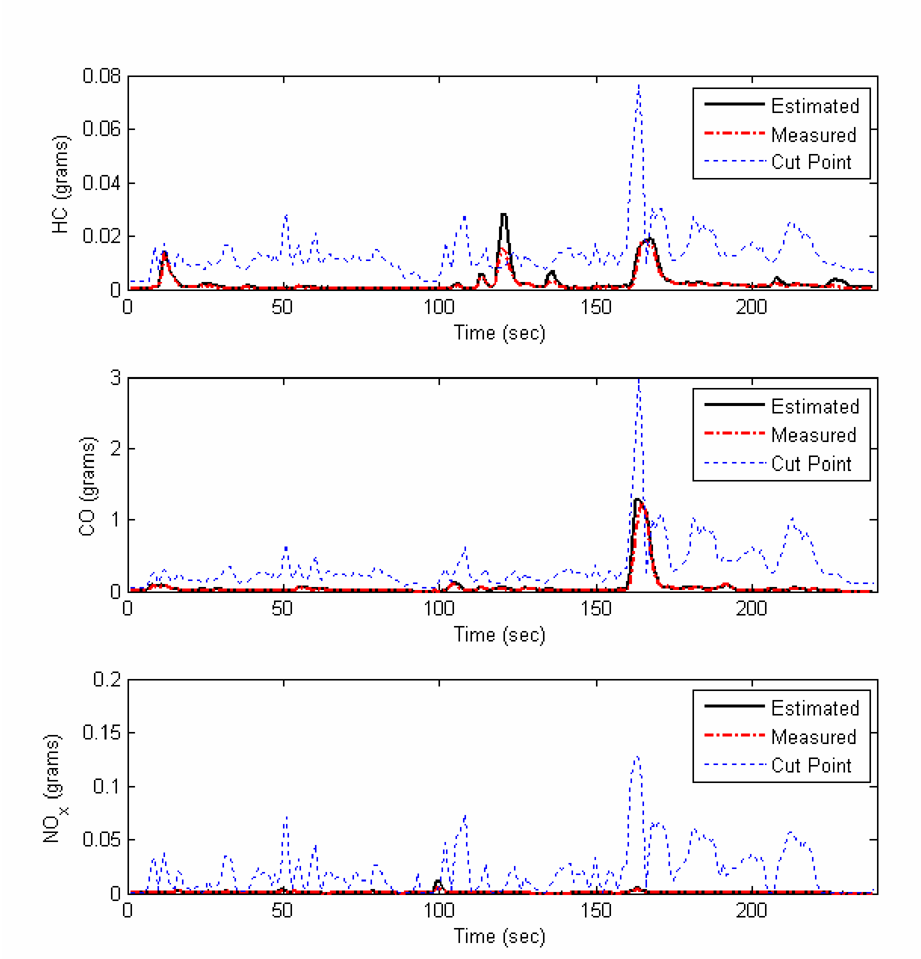

Figure E-4: In-Laboratory Measured IM240 Emission and Estimated Emission for Pickup

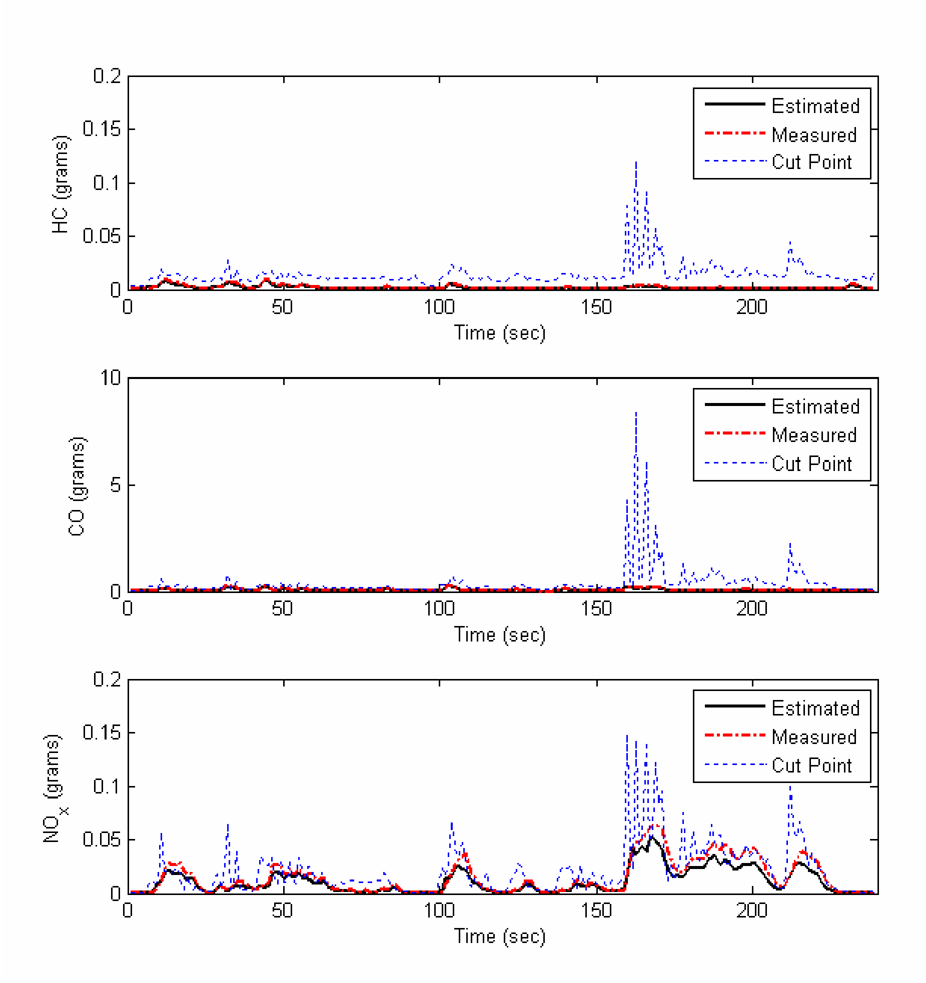

Figure E-5: In-Laboratory Measured IM240 Emission and Estimated Emission for SUV